CHAPTER 10

Male Urogenital Ducts and Cloacal Anatomy

Stanley E. Trauth[1] *and David M. Sever*[2]

10.1 INTRODUCTION

From seminiferous tubules of the testis, snakes and other squamates possess a system of efferent ducts, at least some of which function not only in the passage of sperm but also in sperm storage and as accessory sex glands. The seminiferous tubules connect to the rete testis, which passes sperm sequentially to the ductuli efferentes, the ductus epididymis, and the ductus deferens. The sexual segment of the kidney, described in chapter 11, is a male accessory sex gland that passes secretions into the ureter. The ductus deferens merges with its ipsilateral ureter in viperid snakes, whereas the ductus deferens empties posterior to its ipsilateral ureter and into its ipsilateral ampulla urogenital papilla in colubroid snakes. The above description represents a new interpretation of the alignment and termination of the urogenital ducts in viperid and colubroid snakes and will be illustrated and discussed in detail later in this chapter. Eventually, all products within the adjoined urogenital ducts exit via a single urogenital papilla or paired urogenital papillae into the cloaca. Depending on taxon, species may have ampullae ductus deferentia, ampullae ureters, and/or ampullae urogenital papillae. In this chapter, we review the literature on these structures, provide much new information, and indicate directions for future research.

[1]Department of Biological Sciences, Arkansas State University, State University, Arkansas 72467 USA
[2]Department of Biological Sciences, Southeastern Louisiana University, Hammond, Louisiana 70402 USA

10.2 PROXIMAL EFFERENT DUCTS

10.2.1 Overview

Volsøe (1944) indicates that the testes of the Common European Adder (*Vipera berus*), as well as the rest of the urogenital system, are retroperitoneal, but we have found a distinct mesorchium in the species we have examined. Posterior to the testes, the ductus deferens is supported by mesentery until reaching the dorsal surface of the kidney, where the serosae of the kidney and ductus deferens are united but distinct. Posterior to the kidney, the ductus deferens is suspended by the same mesentery as the ureter until reaching the cloacal wall.

Until recently, the ducts leading from the seminiferous tubules of snakes were called the ductuli efferentes and these connected to the ductuli epididymides, which had a proximal portion that was non-ciliated (ductuli epididymides I) and a distal portion with ciliated epithelium (ducutli epidymides II) connecting to the ductus epididymis (Volsøe 1944; Fox 1952; Saint Girons 1958; Fox 1977).

Sever (2010) demonstrated the proximal testicular ducts of the Black Swamp Snake (*Seminatrix pygaea*) were histologically and ultrastructurally similar to those of other amniotes that have been studied with these techniques, including a lizard (Akbarsha *et al.* 2007), a turtle (Holmes and Gist 2004), a crocodilian (Guerrero *et al.* 2004), birds (Aire 2007), and mammals (Hess 2002). Sever (2010) adopted the nomenclature used for these other amniotes so that the ductuli efferentes and ductuli epididymides I become known as the rete testis, and the ductuli epididymides II is called the ductuli efferentes (Table 10.1; Jones 1998).

Most of the observations below concern *Seminatrix pygaea* from Sever (2004, 2010) and results on the Cottonmouth (*Agkistrodon piscivorus*) recently published by Siegel *et al.* (2009), but we also present some new findings

Table 10.1 Nomenclature for the proximal efferent ducts of snakes since Volsøe (1944) and general characteristics of the epithelial lining

Sever (2010) name	*Jones (1998) name*	*Volsøe (1944) name*	*Epithelium*	*Absorption*	*Secretion*
Rete testis	Rete testis	Ductuli efferentes Ductuli epididymides I	Simple squamous/ cuboidal, non-ciliated	Yes	Yes
Ductuli efferentes	Ductuli efferentes	Ductuli epididymides II	Simple cuboidal, ciliated and non-ciliated cells	Yes	Yes
Ductus epididymis	Ductus epididymis	Ductus epididymis	Non-ciliated, pseudostratified	Yes	Yes
Ductus deferens	Ductus epididymis	Ductus deferens	Non-ciliated, pseudostratifed	Yes	Yes/No

on *A. piscivorus*. Light micrographs of the proximal testicular ducts of the two species are illustrated in Figs. 10.1-10.2, and ultrastructure is shown in Figs. 10.3-10.10.

Distal ends of seminiferous tubules as well as the anterior testicular ducts and the adrenal gland are encased in a modification of the serosa on the dorsal surface of the testis called the epididymal sheath (Siegel *et al.* 2009). Intratesticular portions of the rete testis branch off the seminiferous tubules within the capsule of the testis (Fig. 10.1A-C), whereas extratesticular portions extend into the epididymal sheath (Figs. 10.1E, 10.2A,C,D). In *Agkistrodon piscivorus*, some rete tubules do not have intratesticular portions as their seminiferous tubules extend into the epididymal sheath (Fig. 10.2B-D). The ductuli efferentes are entirely extratesticular within the epididymal sheath (Figs. 10.1A,D,E, 10.2A-C).

Rete testis branch off along the entire border of the testis, although the ductus epididymis extends only along the posterior two-thirds of the testis in *Agkistrodon piscivorus* and *Seminatrix pygaea*. The proximal portions of the rete testis widen after branching off the seminiferous tubules (Fig. 10.1C), and divide into smaller branches before passing into the ductuli efferentes. The ductuli efferentes are small, highly branched and convoluted (Figs. 10.1D,E, 10.2B,C).

The rete testis lacks ciliated epithelium whereas the ductuli efferentes possess both ciliated and non-ciliated cells, making the two regions easy to distinguish, even with light microscopy. Indeed, the ductuli efferentes are the only ducts in the male snake reproductive tract with ciliated cells (Table 10.1).

The rete testis, ductuli efferentes, and ductus epididymis of *Agkistrodon piscivorus* and *Seminatrix pygaea* generally give positive histochemical reactions for neutral carbohydrates (periodic-acid/Schiff's reagent: PAS positive) and proteins (bromphenol blue positive), although the carbohydrate reaction in the ductus epididymis is not as intense as in other regions in *S. pygaea* (Fig. 10.1E,F). PAS positive granules are conspicuous in the ductuli efferentes of *A. piscivorous* throughout the year (Siegel *et al.* 2009).

10.2.2 Ultrastructure of Proximal Testicular Ducts

In *Seminatrix pygaea*, the cuboidal epithelial cells of the rete testis have large, indented euchromatic nuclei, and cells are separated by narrow intercellular canaliculi which are labrinythine apically (Fig. 10.3). Short microvilli are present, and mitochondria are elongate and electron dense. Numerous small vesicles occur along the luminal border and a flocculent material occurs in the supranuclear area of most epithelial cells. Although some vesicles may be involved in absorption, Sever (2010) found evidence that exocytosis is also occurring by an apocrine process. Chromatin material becomes more condensed in spring and summer, when active spermatogenesis is occurring, with spermiation commencing in July (Gribbins *et al.* 2005).

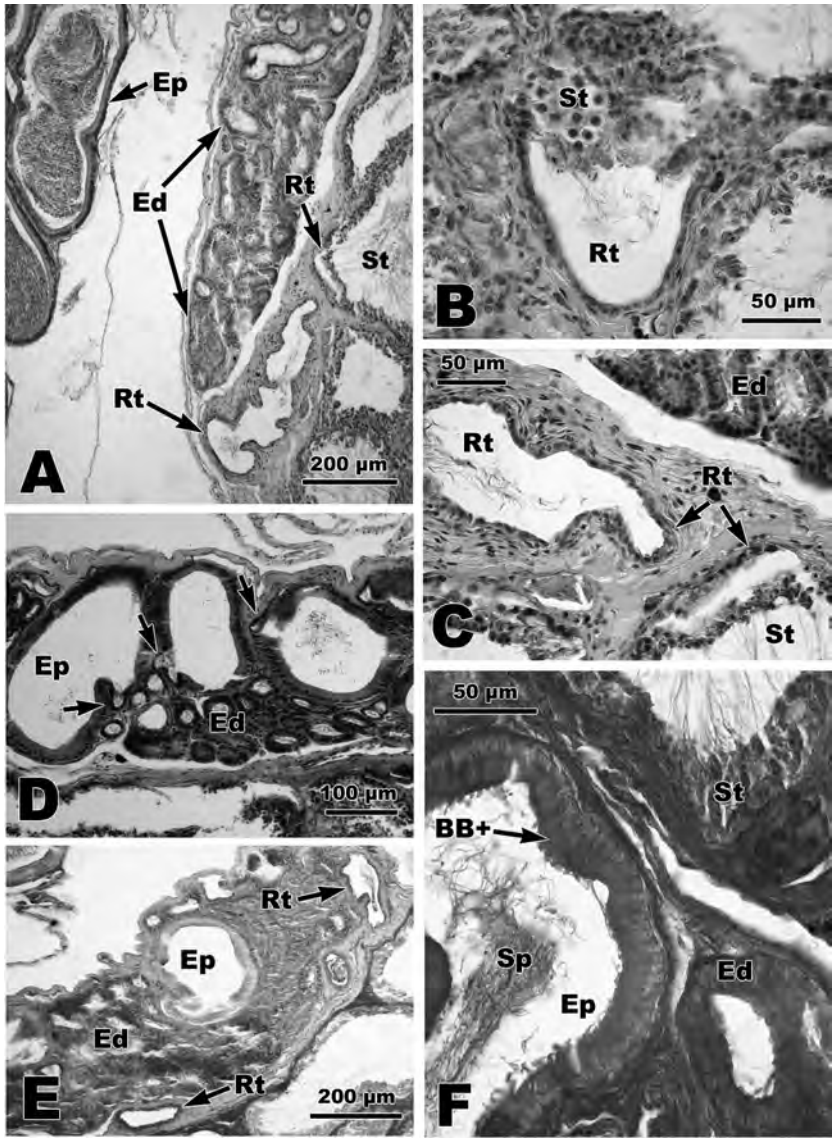

Fig. 10.1 Light micrographs of proximal testicular ducts of *Seminatrix pygaea.* **A.** Overview of relationships among seminiferous tubules, rete testis, ductuli efferentes, and ductus epididymis. **B,C.** Intratesticular rete testis evaginating from seminiferous tubules. **D.** Ductuli efferentes merging with ductus epididymis in extratesticular epididymal sheath (arrows). A-D stained with hematoxylin and eosin. **E.** PAS/AB histochemistry of extratesticular rete testis, ductuli efferentes, and ductus epididymis. PAS positive reactions indicating neutral carbohydrates are illustrated by intensity of the red stain. **F.** Bromphenol blue histochemistry of ductuli efferentes and ductus epididymis. Positive (BB+) reactions indicating proteins are illustrated by the intensity of the blue stain. Ed, ductuli efferentes; Ep, ductus epididymis; Rt, rete testis; Sp, sperm; St, seminiferous tubules.

Color image of this figure appears in the color plate section at the end of the book.

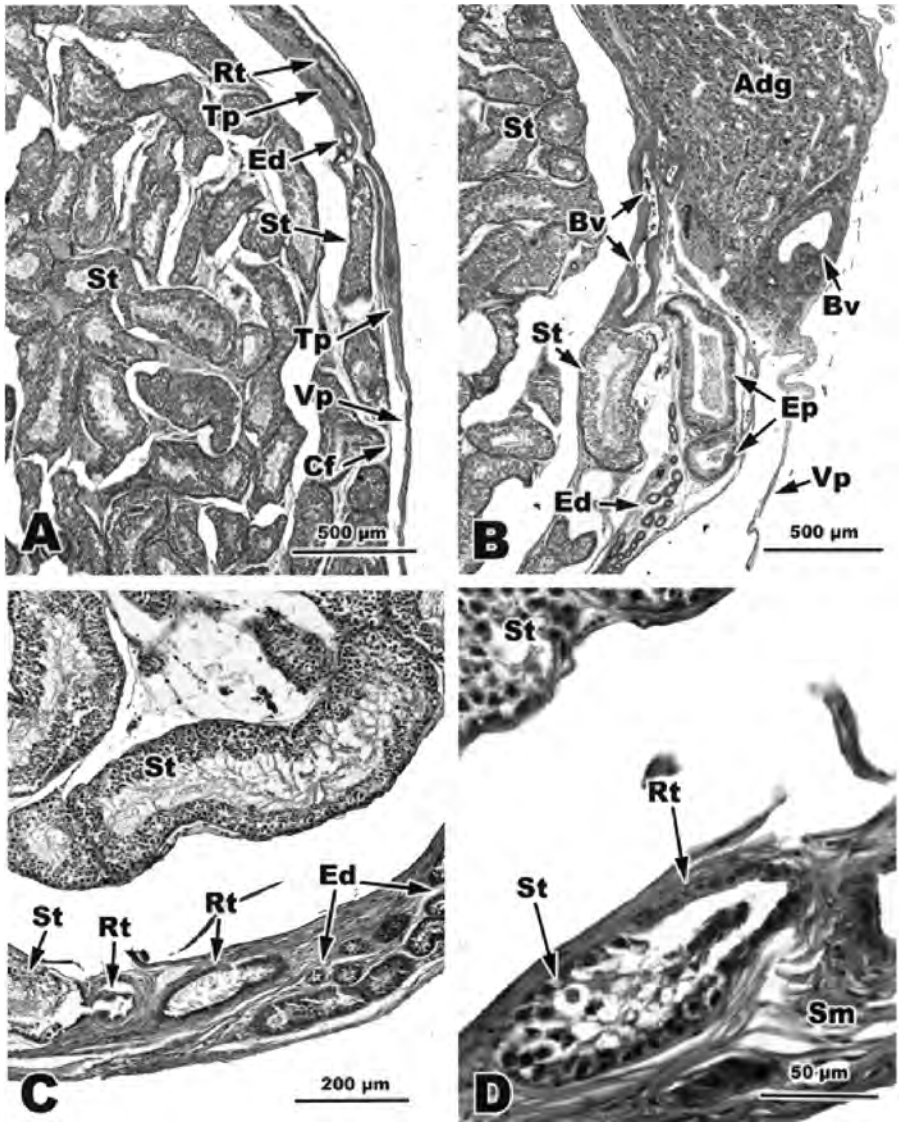

Fig. 10.2 Light micrographs of proximal testicular ducts of *Agkistrodon piscivorus*, stained with hematoxylin and eosin. **A.** Overview of relationships among seminiferous tubules, rete testis, ductuli efferentes, and ductus epididymis. **B.** Extratesticular seminiferous tubules in the epididymal sheath with ductuli efferentes, ductus epididymis, and adrenal gland. **C,D.** Extratesticular rete testis evaginating from seminferous tubule. Adg, adrenal gland; Bv, blood vessel; Cf, collagen fibers; Ed, ductuli efferentes; Ep, ductus epididymis; Rt, rete testis; Sm, smooth muscle; St, seminiferous tubule; Tp, tunica propria; Vp, visceral pleuroperitoneum.

Color image of this figure appears in the color plate section at the end of the book.

The ductuli efferentes have both ciliated and secretory cells (Figs. 10.4, 10.5). Lumina are narrower than in the rete testis, and cilia seem to fill the space (Fig. 10.5). The supranuclear flocculent material is conspicuous in many secretory cells, and apocrine blebs cleave off into the lumen (see Sever 2010). Like the rete testis, intercellular canaliculi are narrow.

At the base of microvilli, coated pits form larger vesicles, endosomes (Fig. 10.6). Electron-dense lysosomes occur in the supra-nuclear regions, and the rough endoplasmic reticulum is well-developed. Seasonal variation again includes an increase of chromatin material in spring and summer, and also an increase in lysosomal activity.

The ductus epididymis is pseudostratified with non-ciliated, columnar principal cells and scattered basal cells (Fig. 10.7). Some of the columnar principal cells are wider than others, but a distinct "narrow cell" as in mammals was not recognized by Sever (2010), because all of the columnar cells seem similar in cytology. Microvilli are short and the elongate "stereocilia" observed in mammals are absent (Figs. 10.7, 10.10). The cytoplasm of the principal cells is characterized by basal, oval nuclei with peripheral chromatin and nucleoli, numerous mitochondria (especially basally), narrow intercellular canaliculi, enlarged cisternae of endoplasmic reticulum, numerous electron-dense primary lysosomes (especially apically), conspicuous apocrine blebs, and an abundance of small vesicles (Figs. 10.7-10.10). The basal cells do not appear metabolically active, and contain only a few scattered mitochondria.

The flocculent material seen in the ductuli efferentes is not as abundant in the ductus epididymis, but the supranuclear Golgi complexes bud off vesicles which contain a product similar in density to the flocculent material. The vesicles empty their contents in the apical cytoplasm to form the apocrine blebs (Fig. 10.10). Definite coated vesicles have not yet been reported, but, as noted above, lysosomes are common, and Sever (2010) illustrated vesicular inclusions in sparsely granulated membranous structures associated with rough endoplasmic reticulum. The only seasonal variation noted in *Seminatrix pygaea* is an increase in chromatic material in the nuclei and increased granular material in the lumina of post-breeding individuals from summer.

10.3 DUCTUS DEFERENS AND AMPULLA DUCTUS DEFERENTIS

10.3.1 Ductus Deferens

Review. In squamate reptiles, the ductus deferens is usually described as rather uniform in structure along its length and is the acknowledged organ of sperm storage (Fox 1952). Most anatomical studies on the ductus deferentia of squamates have been limited to gross morphology and light microscopy. The exceptions are ultrastructure studies by Sever (2004) on the snake *Seminatrix pygaea* and by Akbarsha *et al.* (2005) on the Fan-throated Lizard (*Sitana ponticeriana*), and several electron micrographs of the ductus

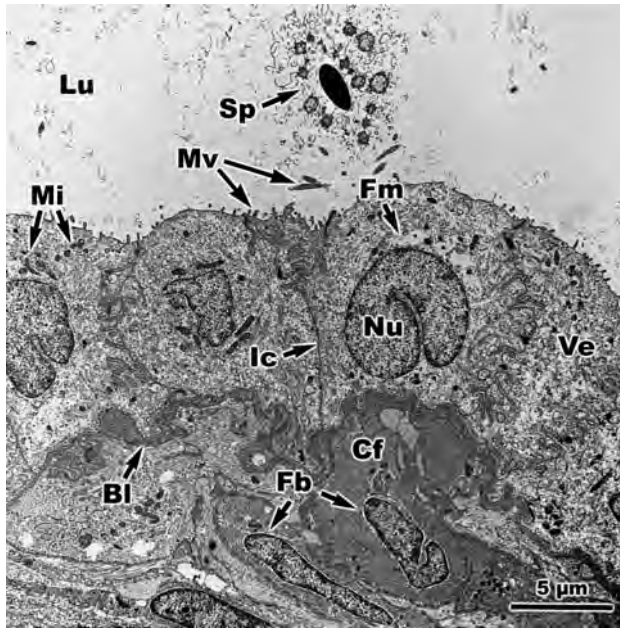

Fig. 10.3 Transmission electron micrograph of the rete testis of *Seminatrix pygaea.* Bl, basal lamina; Cf, collagen fibers; Fb, fibroblast nuclei; Fm, flocculent material; Ic, intercellular canaliculi; Lu, lumen; Mi, mitochondria; Mv, microvilli; Nu, nucleus; Sp, sperm; Ve, vesicles.

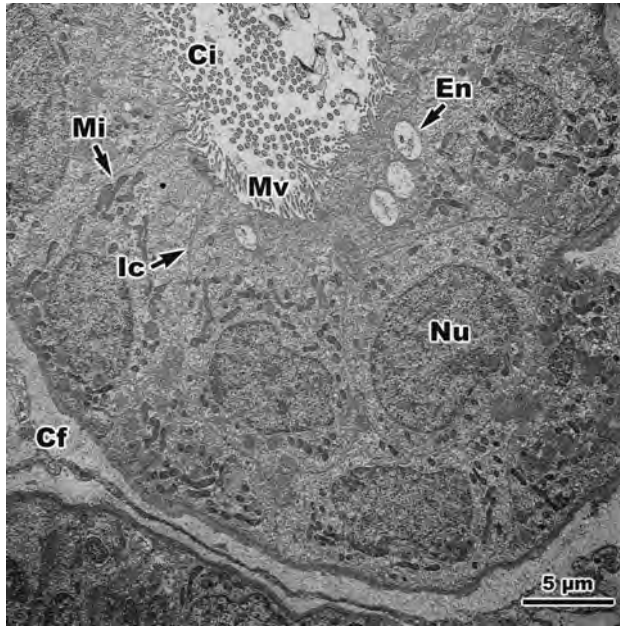

Fig. 10.4 Transmission electron micrograph of the ductuli efferentes of *Seminatrix pygaea*. Cf, collagen fibers; Ci, cilia; En, endocytic vacuole; Ic, intercellular canaliculi; Mi, mitochondria; Mv, microvilli.

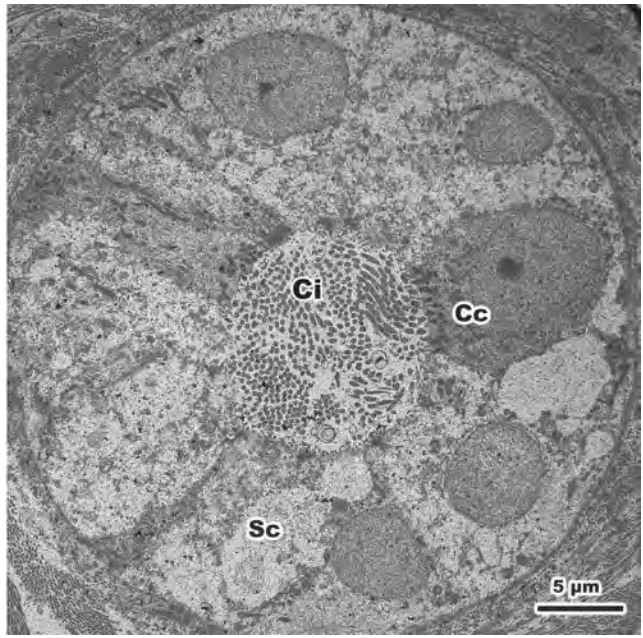

Fig. 10.5 Transmission electron micrograph of the ductuli efferentes of *Agkistrodon piscivorus*. Cc, ciliated cell; Ci, cilia; Sc, secretory cell.

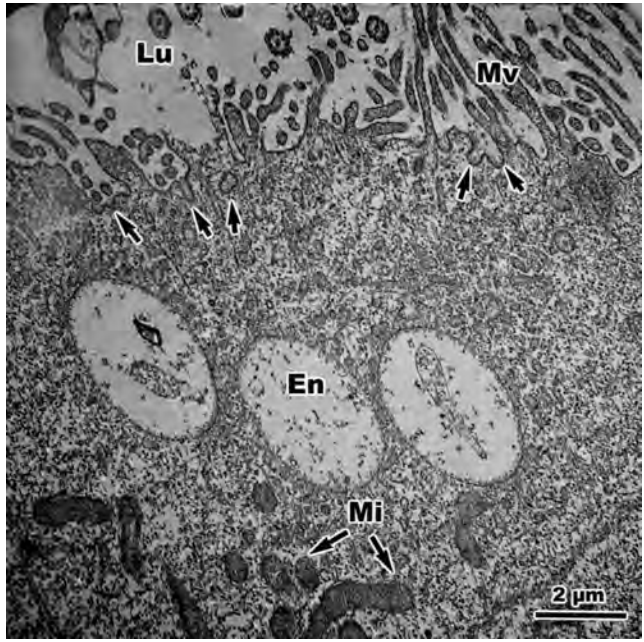

Fig. 10.6 Transmission electron micrograph of the apical cytoplasm of the ductuli efferentes of *Seminatrix pygaea*. Unlabeled arrows indicate coated vesicles. En, endocytic vacuoles; Lu, lumen; Mi, mitochondria; MV, microvilli.

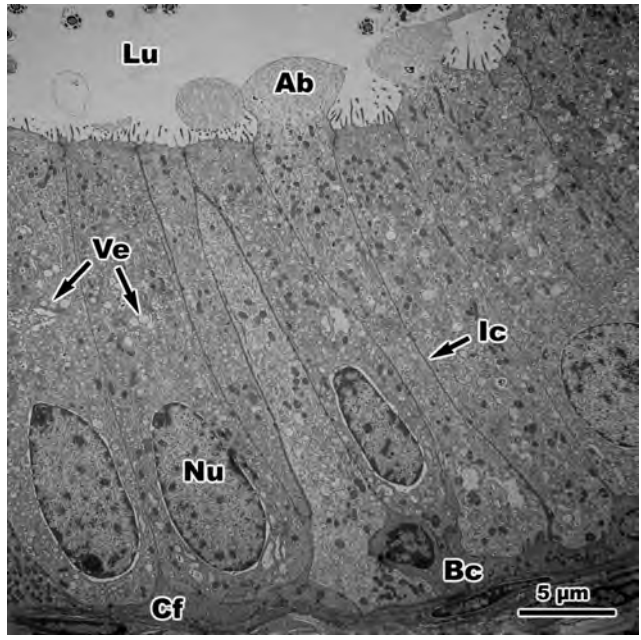

Fig. 10.7 Transmission electron micrograph of the ductus epididymis of *Seminatrix pygaea.* Ab, apocrine bleb; Bc, basal cell; Cf, collagen fibers; Ic, intercellular canaliculi; Lu, lumen; Nu, nucleus; Ve, vesicles.

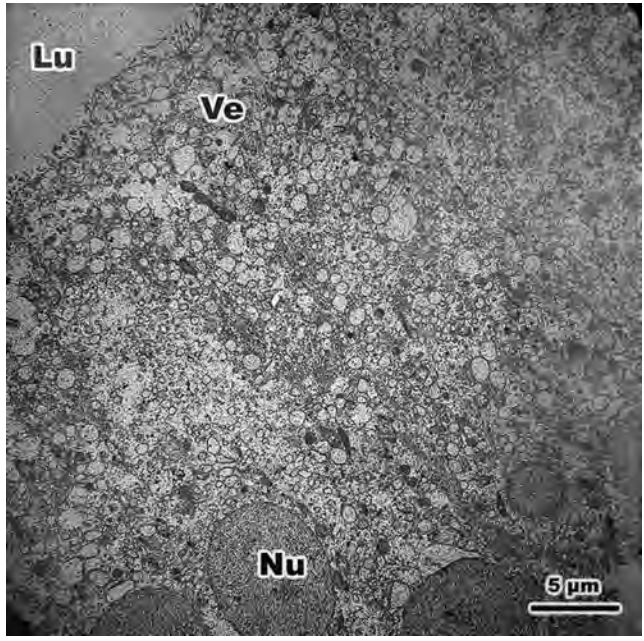

Fig. 10.8 Transmission electron micrograph of the apical cytoplasm of the ductus epididymis of *Agkistrodon piscivorus.* Lu, lumen; Nu, nucleus; Ve, vesicles.

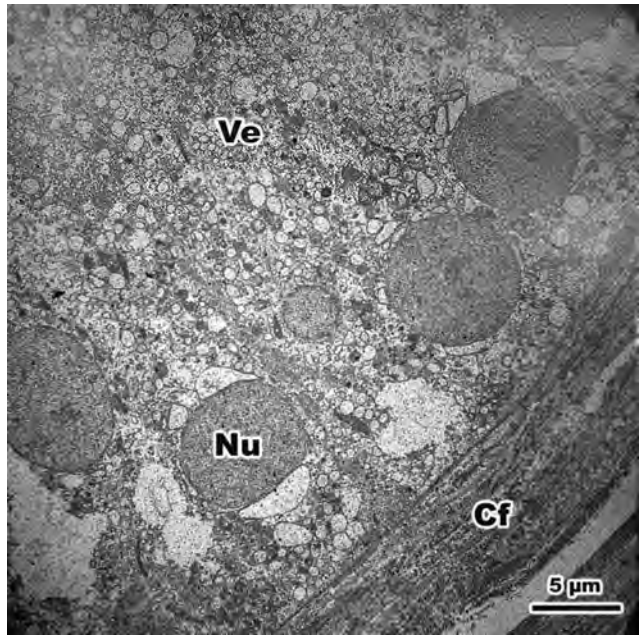

Fig. 10.9 Transmission electron micrograph of the basal cytoplasm of the ductus epididymis of *Agkistrodon piscivorus*. Cf, collagen fibers; Nu, nucleus; Ve, vesicles.

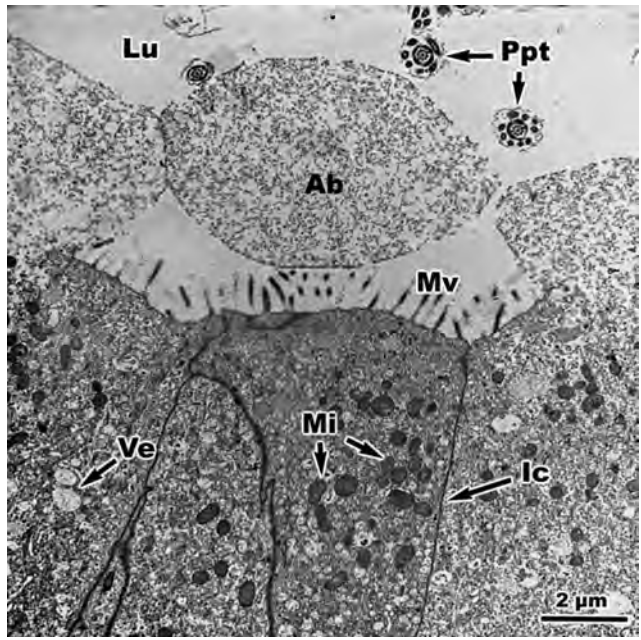

Fig. 10.10 Transmission electron micrograph of the apical cytoplasm of the ductus epididymis of *Seminatrix pygaea.* Ap, apocrine bleb; Ic, intercellular canaliculus; Lu, lumen; Mi, mitochondria; Mv, microvilli; Ppt, principal piece of the tail; Ve, vesicles.

deferens of *Agkistrodon piscivorus* illustrated by Siegel *et al.* (2009). With light microscopy, neither Volsøe (1944) in *Vipera* nor Fox (1952) in *Thamnophis* sp. reported secretory activity in the ductus deferens. Sever (2004) found that the ductus deferens of *S. pygaea* reacted negatively to histochemical tests for carbohydrates and proteins, but Siegel *et al.* (2009) found some positive reactions with these tests for *A. piscivorus*, as indicated below.

The ductus deferens is formed into short tight loops (not coils) as it passes caudally. The demarcation between epididymis and ductus deferens is gradual, with the lumen of the ductus becoming wider, and the epithelium becoming lower. Like the epididymis, the ductus deferens is pseudostratified (Figs. 10.11, 10.12). The epithelium of the principal cells varies from cuboidal to low columnar, and the rather scant cytoplasm is basophilic. As in the epididymis, apocrine blebs are present (Fig. 10.11B). Golgi bodies, rough endoplasmic reticulum, and vesicles are numerous in the cytoplasm (Figs. 10.10C, 10.12A,B).

Sever (2004) in *Seminatrix pygaea* and Siegel *et al.* (2009) in *Agkistrodon piscivorus* reported presence of copious sperm in the ductus deferentia of specimens collected throughout the year. Secretory material associated with the sperm mass in *A. piscivorus* is eosinophilic, bromphenol blue positive (for proteins), and PAS positive (for neutral carbohydrates). These reactions are most intense in areas around the border of the sperm mass that lack sperm, and the secretory material is globular (Siegel *et al.* 2009). Scattered reactions to alcian blue (glycosaminoglycans) occur around the sperm mass in specimens collected in all seasons, and numerous vacuoles are found between the apical cytoplasm and the luminal secretory material in some specimens. Like *S. pygaea*, much of the cytoplasm of the ductus deferens seems non-reactive to histochemical tests in *A. piscivorus*, but in all seasons PAS positive, alcian blue positive, and bromophenol blue positive material is located in the apical cytoplasm. Transmission electron microscopy reveals the presence of secretory vacuoles containing a diffuse material, characteristic of carbohydrates (Fig. 10.13).

New observations. We examined the distal urogenital tracts of several North American colubroid species and provide new micro-anatomical information below on the ductus deferens of adult snakes. Among the representative snakes investigated, we report on the histological and ultrastructural features of the following species: Northern Scarletsnake (*Cemophora coccinea copei*), Western Diamond-backed Rattlesnake (*Crotalus atrox*), Prairie Ringneck Snake (*Diadophis punctatus arnyi*), Western Mudsnake (*Farancia abacura reinwardtii*), Texas Ratsnake (*Pantherophis obsoletus*), Western Pygmy Rattlesnake (*Sistrurus miliarius streckeri*), and the Eastern Gartersnake (*Thamnophis sirtalis sirtalis*). Segments of the urogenital tracts in each species were extracted from a region between 5-10 mm anterior to the cloacal cavity.

We found ductal morphologies in two of these snakes congruent with our previous descriptions above for *Seminatrix pygaea*. Among the species whose ductal morphology was most similar to the ductus deferens of

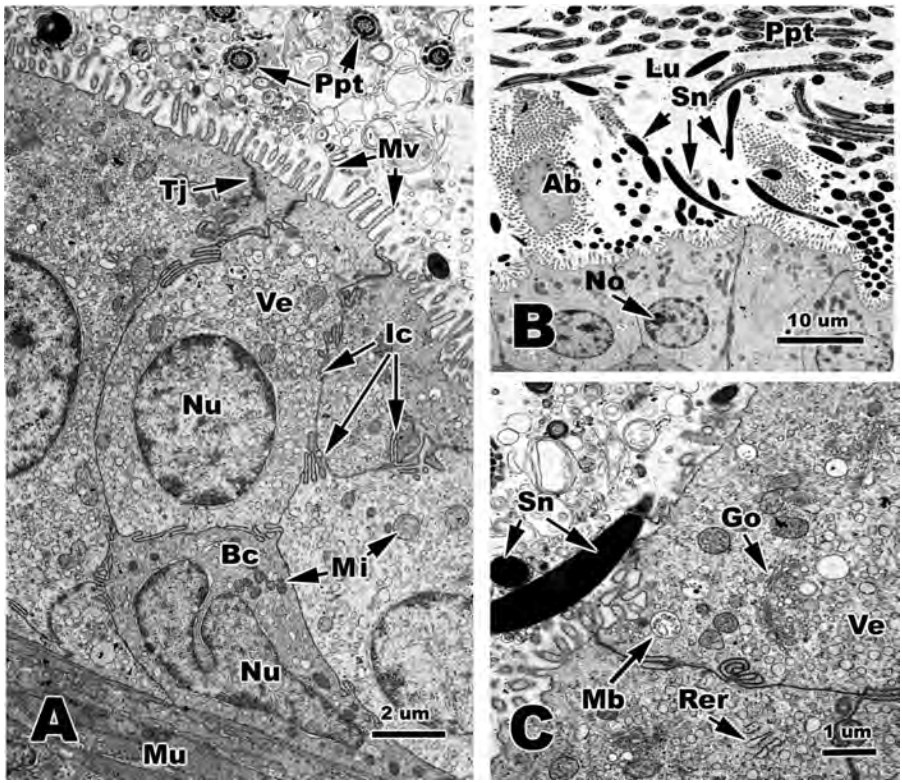

Fig. 10.11 Transmission electron micrographs of the ductus deferens of *Seminatrix pygaea*. **A.** Overview of epithelium. **B,C.** Apical cytoplasm. Ab, apocrine bleb; Bc, basal cell; Go, Golgi bodies; Ic, intercellular canaliculi; Lu, lumen; Mb, multivesicular body; Mi, mitochondria; Mu, muscularis; Mv, microvilli; No, nucleolus; Nu, nucleus; Ppt, principal piece of the tail; Rer, rough endoplasmic reticulum; Sn, sperm nuclei; Tj, tight junction; Ve, vesicles.

S. pygaea was the micro-anatomy found in *Diadophis punctatus arnyi*, which exhibits a pseudostratified, columnar epithelium consisting of a mixture of tall-to-medium height principal cells, narrow cells, and low basal cells (Fig. 10.14D). The epithelial cell cytoplasms exhibit a combination of basophilic and eosinophilic staining properties in *D. punctatus arnyi*. *Sistrurus miliarius streckeri* also possesses a ductal pseudostratification, but, in addition, revealed patches of simple columnar cells (Fig. 10.14F).

Crotalus atrox has a low columnar epithelium (Fig. 10.14G,H) different from that of *Sistrurus miliarius* and more similar to the ductus deferens of *Cemophora coccinea copei* and *Thamnophis sirtalis sirtalis*, which represent the simplest form anatomically and histologically. In the latter two species, the duct is highly looped, greatly distended, and exhibits a thin epithelium with short or flattened cells similar to that illustrated by Fox (1952) in the Coast Gartersnake (*T. elegans terrestris*). The low columnar cells of the epithelial lining stain basophilically in both *C. coccinea copei* and *T. s. sirtalis* (Fig. 10.14A-C) as well as in *C. atrox* (Fig. 10.14G,H). One notable difference

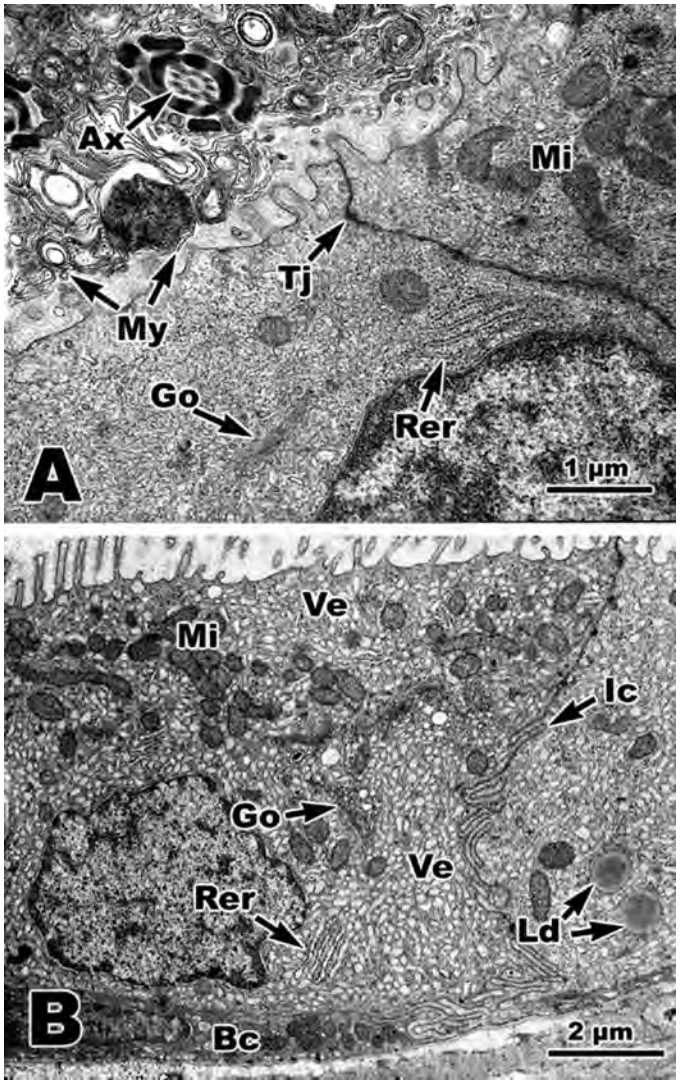

Fig. 10.12 Transmission electron micrographs of the ductus deferens of *Seminatrix pygaea.* **A.** Apical cytoplasm. **B.** Epithelium with numerous vesicles. Ax, axoneme; Bc, basal cell; Go, Golgi bodies; Ic, intercellular canaliculus; Ld, lipid droplets; Mi, mitochondria; My, myelinic figures; Rer, rough endoplasmic reticulum; Tj, tight junction; Ve, vesicles.

is in the thickness of the ductal muscularis, which is greater in diameter in *T. s. sirtalis* than in *C. coccinea copei* (Fig. 10.14A-C). Not illustrated is the relatively thick ductal muscularis in *C. atrox*, which is similar to the relative thickness of the ductal wall of minute typhlopids (Fox 1965). Basophilic ductal epithelia also occur in both viperids, *C. atrox* and *S. miliarius streckeri* (Fig. 10.14F-H). We found an eosinophilic epithelium in *Farancia abacura*

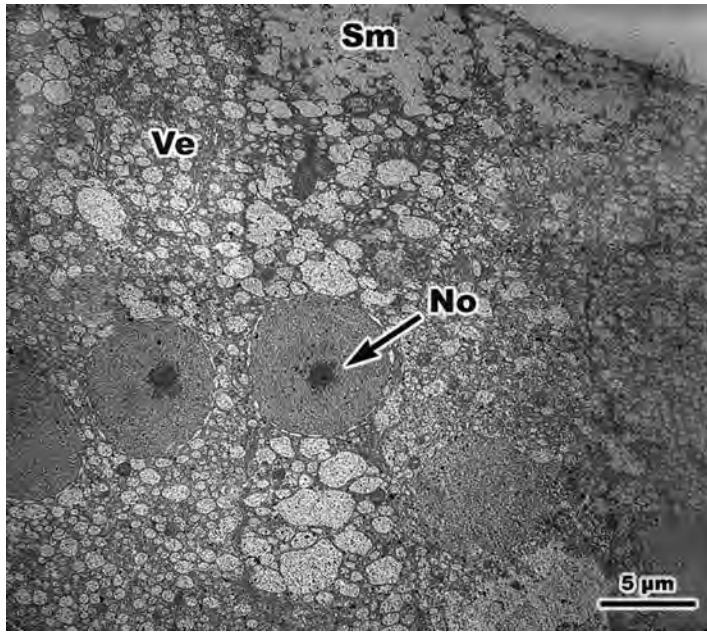

Fig. 10.13 Transmission electron micrograph of the ductus deferens of *Agkistrodon piscivorus.* No, nucleolus; Sm, secretory material; Ve, vesicles.

reinwardtii, and the epithelium has large intercellular spaces along the basal lamina of the ductal epithelium (Fig. 10.14E).

The secretory nature of the ductus deferens displayed in Fig. 10.14 is unclear, primarily because we utilized no specific histological staining tests for carbohydrates and proteins in these species. We suspect, however, that some secretory activity may occur in *Diadophis punctatus arnyi* and *Farancia abacura reinwardtii* based upon the eosinophilic staining properties of their ductal epithelia using general cytological stains.

The ductus deferens of *Pantherophis obsoletus* provided an opportunity to investigate, in some detail, both the ductal morphology and secretory activity of a colubrine species. The ductal secretory activity of a reproductively active individual is illustrated in Fig. 10.15. Large apocrine cytoplasmic blebs dominate the ductal epithelial lining in this species. These cytoplasmic blebs exhibit eosinophilia (Fig. 10.15A) and ultrastructurally appear to be either passively released by cleaving the apical region of cells or are pinched off *en masse* as membrane-bound globular blebs (Fig. 10.15B). These apocrine blebs are similar to those noted in the ductus epididymis and ductus deferens of *Seminatrix pygaea* (Figs. 10.7-10.11). The secretory epithelium of *P. obsoletus* exhibits a low columnar epithelium and lacks stereocilia. The apical cytoplasm as well as the apical blebs found in *P. obsoletus* contain secretory vacuoles (Fig. 10.15B) similar to the description of those found in the viperid, *Agkistrodon piscivorus* (Fig. 10.13).

10.3.2 Ampulla Ductus Deferentis

Review. In many mammals, the distal end of the ductus deferens differs histologically from more proximal portions and is called the ampulla. In contrast to the rest of the ductus deferens, the epithelium of the ampulla is deeply folded, and tortuous out-pocketings that arise between the folds extend into the surrounding muscularis and possess secretory cells (Setchell *et al.* 1994). The mammalian ampulla is morphologically similar to the seminal vesicles (Riva *et al.* 1982) and has been variously implicated in maturation, nourishment, storage, and phagocytosis of sperm (Cooper and Hamilton 1977; Bergerson *et al.* 1994). Among squamates, the occurrence of an ampulla has been documented histologically in two species of lizards, the Oriental Garden Lizard (*Calotes versicolor*; Akbarsha and Meeran 1995) and *Sitana ponticeriana* (Akbarsha *et al.* 2005), and two species of snake, *Seminatrix pygaea* (Sever 2004) and *Agkistrodon piscivorus* (Siegel *et al.* 2009).

Sever (2004) found that the distal end of the ductus deferens of the snake *Seminatrix pygaea* differs from more proximal portions of the genital tract by possessing a highly fluctuated epithelium. As noted above, *S. pygaea* stores sperm throughout the ductus deferens during the entire year, and this includes the ampullary portion. Largely on the basis of negative histochemical tests, Sever (2004) reported that the epithelium of the ampulla of *S. pygaea* is not secretory but noted that the numerous small apical vesicles could function in fluid absorption. In addition to the highly folded epithelium, clusters of sperm nuclei are more intimately associated with the apical ampullary epithelium than elsewhere in the ductus deferens, but no evidence of phagocytosis of sperm was found. In contrast, the ampulla of mammals is glandular and phagocytic. Sever (2004) concluded that the only character shared by *S. pygaea* and mammals is the folded epithelium.

Akbarsha *et al.* (2005) subsequently conducted an ultrastructural study on the ampulla of *Sitana ponticeriana* (Agamidae). The ampulla of *S. ponticeriana* is differentiated into storage and glandular portions. The epithelium of the storage portion is like that in the ductal portion of the ductus deferens, although wider in diameter. The cells of the ductus deferens and storage region of the ampulla consist of principal cells (involved in endocytosis and phagocytosis of dead sperm), dark cells (characterized by numerous coated apical pits and membrane bound vesicles in the cytoplasm), and basal cells (which appear inactive). The principal cells of the storage region are broader than tall. The glandular portion consists of dark and light principal cells and foamy cells, all of which are tall and form villous folds. All three types are secretory, with the products likely different from one another. No evidence of phagocytic activity was found in the glandular portion.

Akbarsha *et al.* (2005) suggested that the ampulla of agamid lizards is a composite gland of the ampulla ductus deferentis and seminal vesicles of mammals. They proposed that within the Squamata, the ampulla differs

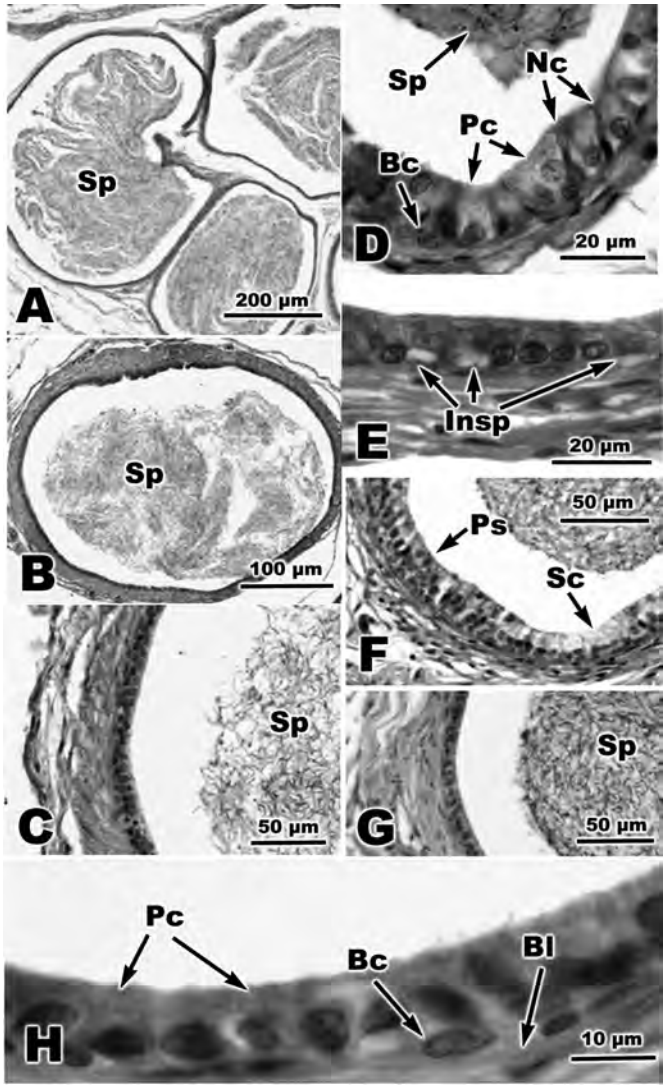

Fig.10.14 Light micrographs of the distal region of the ductus deferens and its secretory epithelium in representative male North American colubroid snakes, stained with hematoxylin and eosin. **A.** *Cemophora coccinea copei*, transverse section revealing a convoluted region of the ductus deferens, which are packed with spermatozoa (Sp). The secretory epithelium is reduced and rests upon a thin ductal wall. **B.** *Thamnophis sirtalis sirtalis*, transverse section of the ductus deferens reveals a thickened muscular wall; a mass of spermatozoa lies within its lumen. **C.** Higher magnification of C showing a thin layer of low columnar cells. **D.** *Diadophis punctatus arnyi*, portion of secretory epithelium showing principal cells (Pc), narrow cells (Nc), and basal cells (Bc). **E.** *Farancia abacura reinwardtii*, portion of the wall of the ductus deferens revealing low columnar cells. Intercellular spaces (Insp) interspersed along basal lamina. **F.** *Sistrurus miliarius streckeri*, showing regional variation of the ductus deferens with area of simple columnar cells (Sc) versus region of pseudostratified columnar cells (Ps).

Fig. 10.14 Contd. ...

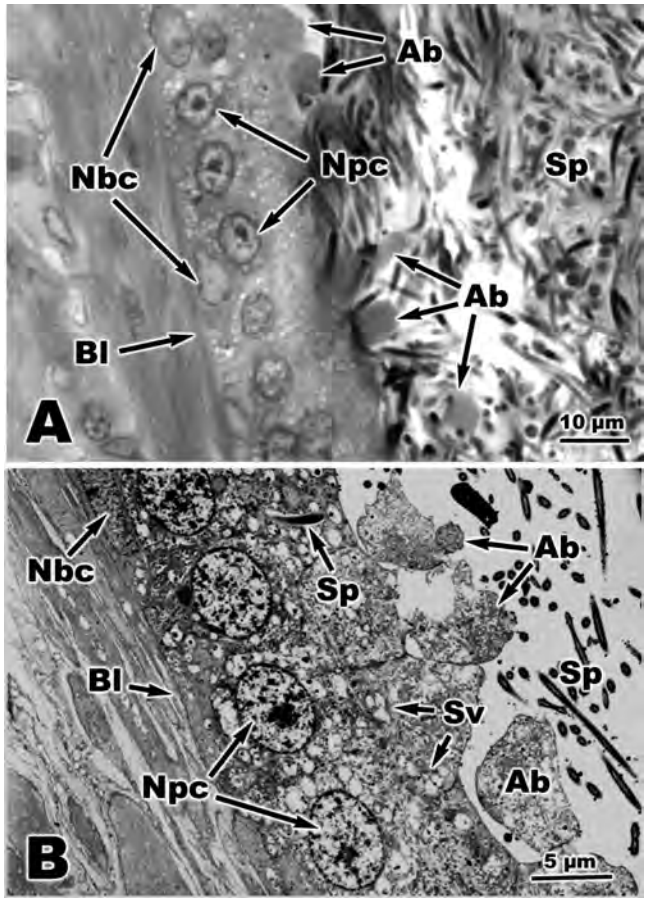

Fig. 10.15 The ductus deferens and its secretory epithelium in *Pantherophis obsoletus*. **A.** Light micrograph of the low columnar epithelium revealing numerous cytoplasmic apocrine blebs (Ab) lying adjacent to epithelial cells and within the ductal lumen. Principal cells with their oval-shaped nuclei (Npc) outnumber basal cells which exhibit oblong nuclei (Nbc). Spermatozoa are crowded along the epithelial lining. Ladd multiple stain of plastic-embedded tissue. **B.** Transmission electron micrograph of epithelium shown in A. Apocrine blebs can be seen detaching from the apical surfaces of the principal cells. Numerous secretory vacuoles (Sv) can be seen at several levels within these cells. Note sperm embedded within cytoplasm of principal cell. Ab, apocrine bleb; Bl, basal lamina; Nbc, nuclei of basal cell; Npc, nuclei of principal cell; Sp, sperm; Sv, secretory vacuoles.

Color image of this figure appears in the color plate section at the end of the book.

... Fig. 10.14 Contd.

G. *Crotalus atrox*, low simple columnar epithelium rests upon a thickened ductal wall (similar to B). **H.** Higher magnification of G. Epithelium greatly reduced in height as in A; basal cells (Bc) reside along the basal lamina (Bl). Narrow cells, which are common in D, were not observed. Bc, basal cells; Bl, basal lamina; Insp, intercellular space; Nc, narrow cells; Pc, principal cells; Ps, pseudostratified; Sc, simple columnar; Sp, sperm.

Color image of this figure appears in the color plate section at the end of the book.

in structure and function. Akbarsha *et al.* (2005) found additional cell types (dark and foamy cells) in the ampulla of *Sitana ponticeriana* not noted by Sever (2004) in *Seminatrix pygaea*. More importantly, three cell types in the lizard were secretory in the glandular portion of the ampulla, and no secretory activity was reported for *S. pygaea.*

Siegel *et al.* (2009) reported that the ampulla of *Agkistrodon piscivorus* is composed of a portion suspended in the posterior part of the pleuroperitoneal coelom alongside the ureter and a segment that passes through the cloacal walls to join with the ureter. Externally, the coelomic ampulla is discerned by a straightening of the loops from the ductus deferens. Internally, the ampulla is characterized by irregular folded epithelial walls until the final intramural portion when the epithelium becomes regular again as the junction with the ureter is approached. Sperm occur in the ampulla of *A. piscivorus* throughout the year, although sperm are scant in October and November specimens.

Siegel *et al.* (2009) reported that the cytoplasm of the anterior portion of the ampulla of *Agkistron piscivorus* is characterized by numerous vacuoles, and the vacuoles also occur between the apices of the epithelial cells and the secretory material encasing the sperm mass. Throughout the year, luminal material is eosinophilic and intensely PAS positive, and small PAS positive granules are scattered throughout the epithelium. Positive reactions with alcian blue and with bromphenol blue are also observed in the cytoplasm and luminal material, but these reactions are not as strong and pervasive as those for PAS. Siegel *et al.* (2009) present electron micrographs that show the presence of apical secretory vacuoles containing a diffuse substance and a dense matrix containing sperm in the lumen.

Thus, in one snake, *Seminatrix pygaea*, no secretory activity is reported for the ampulla (Sever 2004), whereas in another, *Agkistrodon piscivorus*, ample evidence for production of a carbohydrate secretion exists (Siegel *et al.* 2009). It is likely, as in the proximal testicular ducts, that the numerous vesicles in the ampullary cytoplasm of *S. pygaea* do not merely function in endocytosis of luminal fluids. Instead the vesicles may be indicative of a constitutive secretory pathway in which the secretory product is not stored in granules but is continually produced and released through these vesicles. Still, the absence of positive histochemical tests indicate that the ampulla of *S. pygaea* may have less secretory activity than that found in *A. piscivorus*, and some of the species described below.

New observations. We report below on new histological and ultrastructural information pertaining to the ampulla ductus deferentis in several adult North American colubrine snakes; these include the following species (Figs. 10.16-10.19): *Cemophora coccinea copei*, Southern Black Racer (*Coluber constrictor priapus*), Speckled Kingsnake (*Lampropeltis holbrooki*), Mississippi Green Watersnake (*Nerodia cyclopion*), Rough Greensnake (*Opheodrys aestivus*), *Pantherophis obsoletus*, Midland Brownsnake (*Storeria dekayi wrightorum*), Flat-headed Snake (*Tantilla gracilis*), and Rough Earthsnake (*Virginia striatula*).

As in *Seminatrix pygaea*, diagnostic morphological characteristics of the ampulla found in seven of the eight snake species listed above are the highly fluctuating epithelium (Fig. 10.16) and a greatly enlarged ampullary diameter (a diameter which is greater than that of the associated ductus deferens). We found that the complexity of the epithelial folding of the ampulla varies sharply among the species examined. For example, a simple set of 4-6 low, non-villous folds occur in the ampulla of *Storeria dekayi wrightorum* (Fig. 10.17A), whereas *Nerodia cyclopion* possessed the most complex arrangement of ampullary folds (Fig. 10.16G). In *S. dekayi*, the region possessing the ampullary folds is restricted to a very narrow segment of the ampulla (less that 100 μm in total length), and this portion of the ductal region appears rudimentary in overall structure. For instance, this ampulla contains poorly developed ampullary crypts between the folds. In addition, a low pseudostratified, columnar epithelium lines the ampullary crypts and the entire ampullary luminal lining.

The comparative micro-anatomy of the internal ampullary wall (including folds, irregular projections, and crypts) between two species, *Coluber constrictor priapus* and *Opheodrys aestivus* (Fig. 10.16C,F), reveals a great similarity in ampullary duct morphology. This condition represents a higher level of anatomical complexity over that seen in *Storeria dekayi wrightorum*. In the ampulla of these two species, the ductal epithelium exhibits mostly low villous or non-villous folds, which are separated by weakly-defined ampullary crypts (Fig. 10.17B). These folds are generally less numerous and reduced in hillock height when compared to the folds found by Sever (2004) in *Seminatrix pygaea*. The low pseudostratified columnar epithelium of *C. constrictor priapus* did, however, show some evidence of secretory activity as the apical portions of these hillock cells are eosinophilic when stained with hematoxylin and eosin.

A comparison of another pair of species, *Tantilla gracilis* and *Virginia striatula*, shows near identical ductal morphologies with one another (Fig. 10.16D,E). Both species possess relatively tall epithelial hillocks or projections and well developed ampullary crypts. None of the crypts houses any sperm aggregates, although some sperm appear captured within apical cells (Fig. 10.17D). The apical ampullary epithelia (Fig. 10.17D,E) of these two species are more similar to that of *Seminatrix pygaea* than to the micro-anatomies of either *Coluber constrictor priapus* or *Opheodrys aestivus*. Unlike the longitudinally-directed ampullary duct morphology of *V. striatula* (and all the other species mentioned thus far), the ampulla of *T. gracilis* appears as a looped cluster of ducts, and they contain oblong plate-like esosinophilic masses within their lumina (Fig. 10.16D).

A third level of micro-anatomical ampullary complexity occurs in *Cemophora coccinea copei* (Fig. 10.16A). In this species, the ampullary apical epithelium exhibits mostly tall to medium-sized hillocks (irregular epithelial projections) that are festooned (Fig. 10.17F), an indication of possible endocytic activity. Apical cell nuclei, however, appear to be undergoing pyknosis, and cytoplasmic fragmentation occurs, resulting in

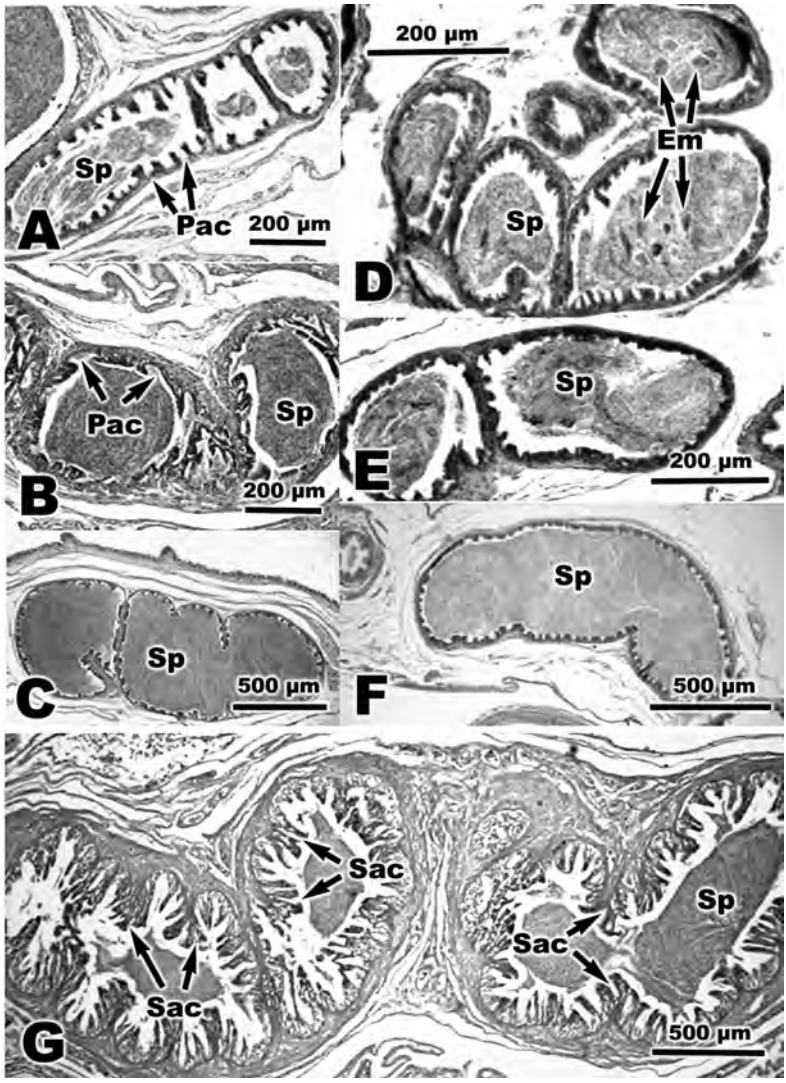

Fig. 10.16 Light micrographs of the ampulla ductus deferentis in adult male North American colubrine snakes, stained with hematoxylin and eosin. All histosections contain densely packed masses of spermatozoa. **A.** *Cemophora coccinea* copei, ampullary epithelial folds exhibit a repetitively festooned appearance with primary ampullary crypts (Pac). **B.** *Lampropeltis holbrooki.* **C.** *Coluber constrictor priapus,* expansive ampullary duct with reduced folds and crypts. **D.** *Tantilla gracilis*, showing multiple loops of the ampulla ductus deferentis. Dense eosinophilic masses (Em) are embedded among spermatozoa. **E.** *Virginia striatula*, with ampulla ductus deferentis similar to morphology found in D. **F.** *Opheodrys aestivus*, ampullary epithelium similar to morphology found in C**. G.** *Nerodia cyclopion*, ampullary epithelial lining highly convoluted and highly branched exhibiting primary and secondary (Sac) ampullary crypts. Em, eosinophilic masses; Pac, primary ampullary crypts; Sac, secondary ampullary crypts; Sp, sperm.

Color image of this figure appears in the color plate section at the end of the book.

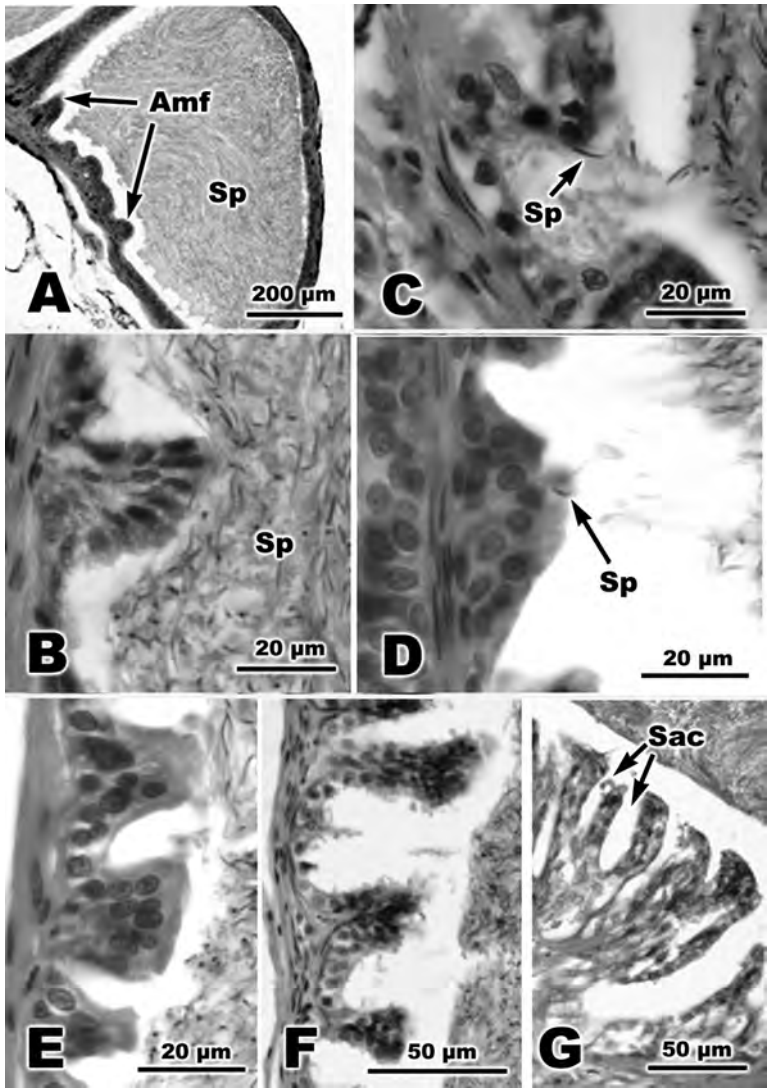

Fig. 10.17 Light micrographs of the ductal epithelium of the ampulla ductus deferentis in adult male colubrine snakes (B-G histosections from Fig. 10.16), stained with hematoxylin and eosin. **A.** *Storeria dekayi*, ductal epithelium has low to flattened columnar cell arrangement with few villous internal ampullary folds (Amf). **B.** *Coluber constrictor priapus*, ductal epithelium elevated, but without festooned appearance. **C.** *Lampropeltis holbrooki*, ampullary crypt exhibiting sperm cell (Sp) embedded within epithelial cell. **D.** *Virginia striatula*, portion of ductal epithelium exhibiting pyramidal-shaped cell layers flanked by narrow ampullary crypts. Note sperm cell embedded with epithelial cell (similar to C). **E.** *Tantilla gracilis*, the ductal epithelium comprised truncated cell clusters residing between narrow ampullary crypts. **F.** *Cemophora coccinea copei*, laterally expanded ampullary crypts lie between tall columns of the ductal epithelium. **G.** *Nerodia cyclopion*, tentacle-like branching pattern of the ductal epithelium showing secondary ampullary crypt. Amf, ampullary folds; Sac, secondary ampullary crypts; Sp, sperm.

Color image of this figure appears in the color plate section at the end of the book.

cell surfaces which lack uniformity (i.e., exhibited uneven boundaries). A basophilia characterizes these distal hillock cell layers, and one could also argue that some exocytic secretory pathway is actively taking place.

The fourth level of ampullary complexity occurs in *Lampropeltis holbrooki* (Fig. 10.16B). In this species, the ampullary folds are wider and taller than in any of the previous species; thus, the ampullary crypts are also enlarged. The ductal wall in *L. holbrooki* (Fig. 10.16B) is thicker than in any of the previous species. Unlike the ampullary crypts of the storage region in *Seminatrix pygaea*, few sperm are found within crypts, although sperm are embedded into cells along the apical hillocks (Fig. 10.17C).

The most complex ampullary micro-anatomy is found in *Nerodia cyclopion*. The entire ampullary lining has numerous large primary ampullary folds (Fig. 10.16G), which form a repetitive cup-like pattern along the ampullary ductal wall. Interspersed along the primary ampullary folds are individual as well as unique, tentacle-like arrangements of secondary ampullary folds, the latter characterized by secondary ampullary crypts (Fig. 10.17G). The apical epithelial cell regions of the secondary ampullary folds shows a mild basophilia, but not as intense as that in the apical cell clusters of *Cemophora coccinea copei* and *Lampropeltis holbrooki*. No spermatozoa are apparent within any of the primary or secondary ampullary crypts in *N. cyclopion*.

As was the case with our examination of the ductus deferens of snakes aforementioned, we were able to examine the ampulla ductus deferentis of *Pantherophis obsoletus* in greater micro-anatomical detail than other snake species. The ampulla of *P. obsoletus* represents another degree of complexity (differing from all other species) by exhibiting a gland-like appearance. The ampulla consists of a lobate cluster of ducts (Fig. 10.18A) along with a multitude of blind outpocketings or pouches that terminate as ampullary crypts. These ampullary crypts also differ from the other species examined by containing dense aggregates of sperm cells whose nuclei occur in bundles within the crypts (Fig. 10.18B). Transmission electron microscopy reveals, however, that the sperm heads are not embedded into the epithelial cell lining of the crypts (Fig. 10.19). This same observation was mentioned by Sever (2004) for *Seminatrix pygaea*. Cytologically, principal cells within crypts contain scattered patches of rough endoplasmic reticulum and mitochondria along the apical surfaces of their nuclei (Fig. 10.19); also, no secretory vacuoles are evident within these cells. A comparison with epithelial cells of the ductus deferens (Fig. 10.15) shows striking differences. Secretory vacuoles that dominate cytoplasmic volume in the secretory epithelium of the ductus deferens are absent from the ampullary epithelium. Although the ductal epithelium within crypts remains pseudostratified columnar throughout most of the ampulla, the irregular height of the principal cells within crypts as well as the presence of apocrine blebs within the luminal region of the crypts point to the possibility of secretory activity.

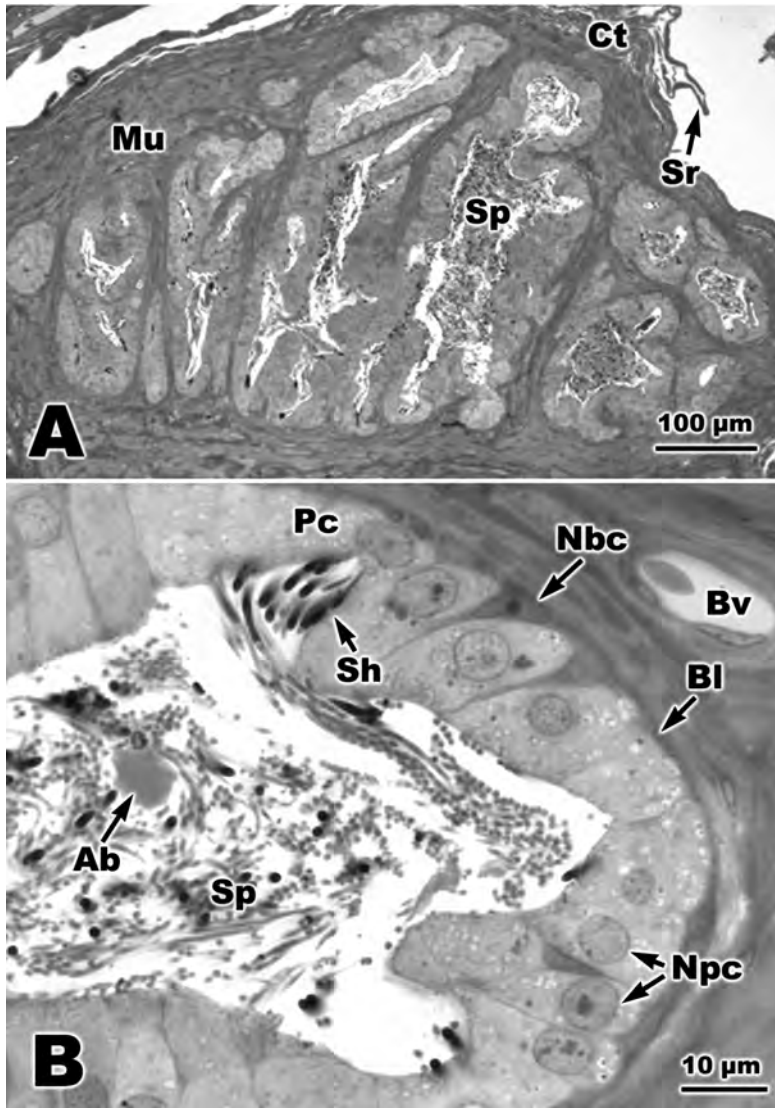

Fig. 10.18 Light micrographs of the ampulla ductus deferentis of an adult *Pantherophis obsoletus*, stained with the Ladd multiple stain. **A.** Section through several coils of the ampulla revealing a tall-to-irregular columnar epithelium; spermatozoa fill the lumina of the coils. The body of the ampulla is surrounded by a muscularis (Mu) and a connective tissue sheath (Ct). A serosa lines the external surface of the ampulla. **B.** Higher magnification of a crypt with the irregular columnar epithelium shown in A. A cluster of sperm heads (Sh) can be seen lying within a depressed space between principal cells (Pc), which contain mostly round nuclei (Npc). A basal cell and its nucleus (Nbc) appear tightly squeezed between two principal cells. Ab, apocrine bleb; Bl, basal lamina; Bv, blood vessel; Ct, connective tissue; Mu, muscularis; Nbc, nuclei of basal cells; Npc, nuclei of principal cells; Pc, principal cell; Sh, sperm heads; Sp, sperm; Sr, serosa.

Color image of this figure appears in the color plate section at the end of the book.

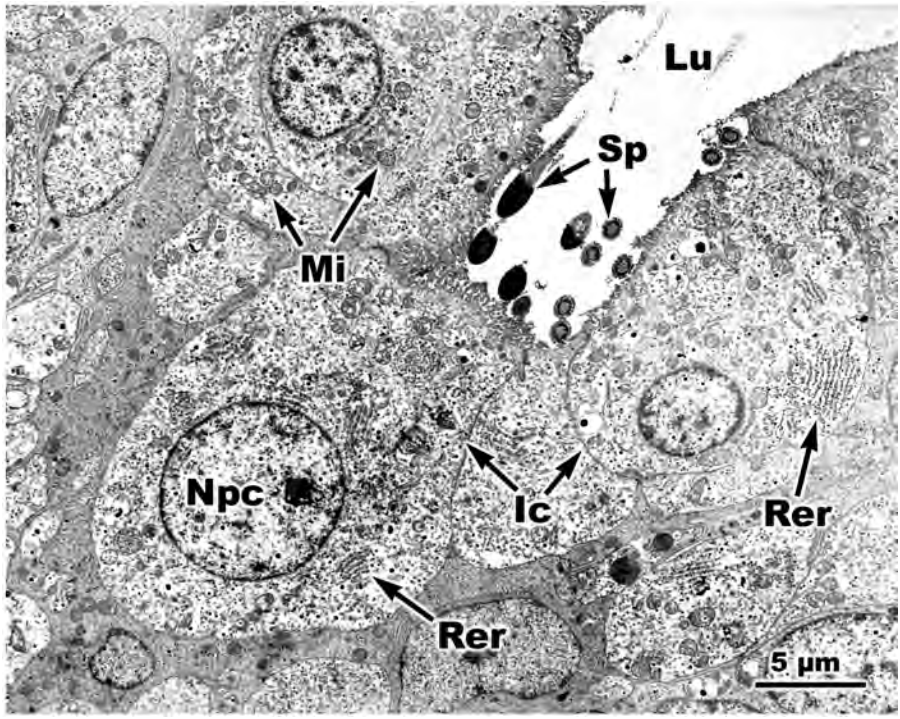

Fig. 10.19 Transmission electron micrograph of an epithelial crypt of the ampulla ductus deferentis (shown in Fig. 10.18) of *Pantherophis obsoletus*. The borders of several principal cells surround a cluster of spermatozoa. Ic, intercellular canaliculi; Lu, lumen; Mi, mitochondria; Npc, nucleus of principal cell; Rer, rough endoplasmic reticulum; Sp, sperm.

10.3.3. Ampulla Urogenital Papilla and Ampulla Ureter

Review. In this section, we recognize the significance of a unique anatomical illustration provided by Martin Saint Ange (1854). We have redrawn it in Fig. 10.20 in order to help clarify our explanations below about snake distal urogenital tract anatomy. Depicted within this figure (two-headed arrow) is a cutaway internal view of the distal expansion of the ureter of a colubrine snake in which Martin Saint Ange inserted tracts of both the ureter proper (as the small anterior tube) and the internal ductus deferens (the small posterior tube) configured from its lateral position. Henceforth, we shall refer to this expanded portion housing the two urogenital ducts as the ampulla urogenital papilla, a new terminology applied to this urogenital region of male colubrine snakes.

Much uncertainty has prevailed in the snake literature dealing with the distal reproductive anatomy of males, especially in reference to the lower urogenital tracts (e.g., see Sever 2004). A clear understanding of distal urogenital tract morphology has been hampered primarily by arguments and descriptions by Volsøe (1944), who equated the distal urogenital tract morphology (and terminology) he had employed for *Vipera*,

a viperid species, with that of the tract morphology of a colubrine, the Grass Snake (*Tropidonotus* = *Natrix natrix*) as illustrated by Martin Saint Ange (Fig. 10.20B). In fact, both anatomies are descriptively correct and illustrate two fundamentally different and distinct distal urogenital duct morphologies found in males. Volsøe (1944) added additional obfuscations to understanding this region by denying the presence of an ampulla ductus deferentis (discussed previously) and by explaining away other pertinent incongruities in tract morphologies as anatomical misinterpretations by previous authors. In the following, we provide new descriptive as well as comparative morphological information regarding the micro-anatomy of the ampulla urogenital papilla, which is morphologically similar in all colubrine snakes investigated thus far. We, then, compare this micro-anatomy to its functional anatomical counterpart, the ampulla ureter, which is found in all viperid snakes (see section 10.3.4). We also provide ultrastructural evidence for secretory activity of the epithelium in both the ampulla urogenital papilla and the ampulla ureter.

New observations. The ampulla urogenital papilla (pl., ampullae urogenital papillae) is one of two small complimentary blind pouches, each representing the terminal repository of products released by the male urogenital tracts in North American colubrine snakes. The two pouches increase in volume as they advance posteriorly and reach their maximum diameters within the urogenital papilla. Each normally receives urinary and reproductive products, which include nitrogenous wastes (uric acid), sperm, and the epithelial secretions from the linings of the ureter and ductus deferens. Their overall sizes are similar to one another. They become greatly inflated by the presence of sperm or uric acid, but this increased volume is not sufficient to consider them important in sperm or uric acid storage. The expanded length of an individual pouch varies according to snake body size. We measured the distance from the anteriormost edge to the level of their orifices on the urogenital papilla. For example, the longest ampulla urogenital papilla, occurs in the Eastern Coachwhip, *Coluber flagellum flagellum* (5.50 mm) and smallest is in *Diadophis punctatus arnyi* (0.60 mm). The following are other total lengths measured (in decreasing order of size in mm): Eastern Hog-nosed Snake, *Heterodon platirhinos* (5.02), *Farancia abacura reinwardtii* (4.29), *Pantherophis obsoletus* (3.85), *C. constrictor priapus* (3.66), *Thamnophis sirtalis sirtalis* (2.86), Red Milksnake, *Lampropeltis triangulum syspila* (2.76), *L. holbrooki* (2.55), *Cemophora coccinea copei* (2.45), *Opheodrys aestivus* (2.36), *Nerodia cyclopion* (2.19), Orange-striped Ribbonsnake, *T. proximus proximus* (1.93), *Tantilla gracilis* (1.20), *Sonora semiannulata* (1.14), *Virginia striatula* (1.09), Graham's Crayfish Snake, *Regina grahamii* (0.99), *Storeria dekayi wrightorum* (0.99), Smooth Earthsnake, *V. valeriae* (0.83), and Western Wormsnake, *Carphophis vermis* (0.70).

Although macroscopic images and SEM images (external ampullary folds) reveal the general region occupied by the ampulla urogenital papilla (Figs. 10.20E, 10.21), this structure is best delineated microscopically through transverse serial histosections beginning at the level of the anteriormost

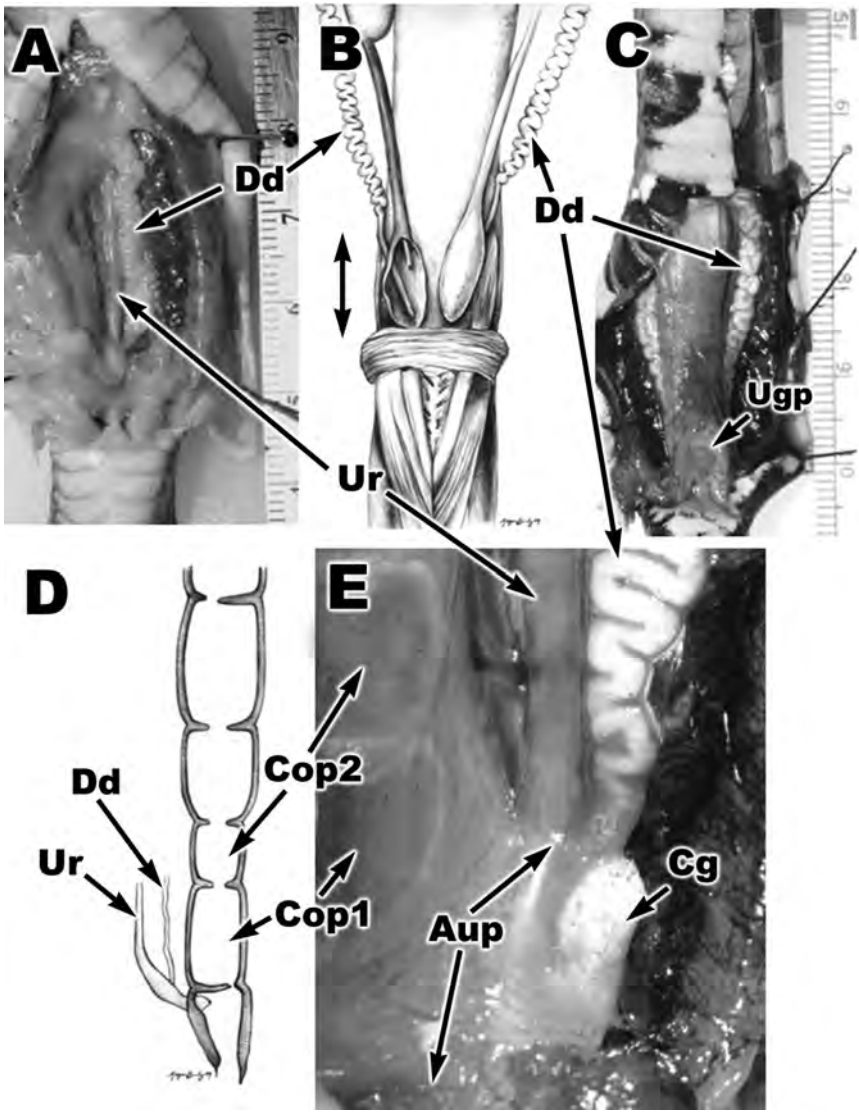

Fig. 10.20 Composite illustration of the distal urogenital anatomy of adult male North American colubrine snakes matched to anatomical diagrams (**B** and **D**) redrawn from Martin Saint Ange (1854) and Volsøe (1944), respectively. Two-headed arrow in B encompasses an entire ampulla urogenital papilla. Ventral views of *Lampropeltis calligaster, Nerodia fasciata confluens*, and *Thamnophis proximus proximus* (**A**, **C**, and **E**) reveal positional relationships among the anatomical structures. Aup, ampulla urogenital papilla; Cg, cloacal gland; Cop1, first coprodaeal chamber; Cop2, second coprodaeal chamber; Dd, ductus deferens; Ugp, urogenital papilla (Ugp); Ur, ureter. **B** is adapted from Martin Saint Ange, G.-J. 1854. J.-B. Balliére, Libraire de l'Académe Impériale de Médecine, Paris, Plate X, Fig. 2. **D** is adapted from Volsøe, H. 1944. Spolia Zoologica Musei Hauniensis V. Skrifter, Universitetets Zoologiske Museum, København, Text Fig. 10.

Color image of this figure appears in the color plate section at the end of the book.

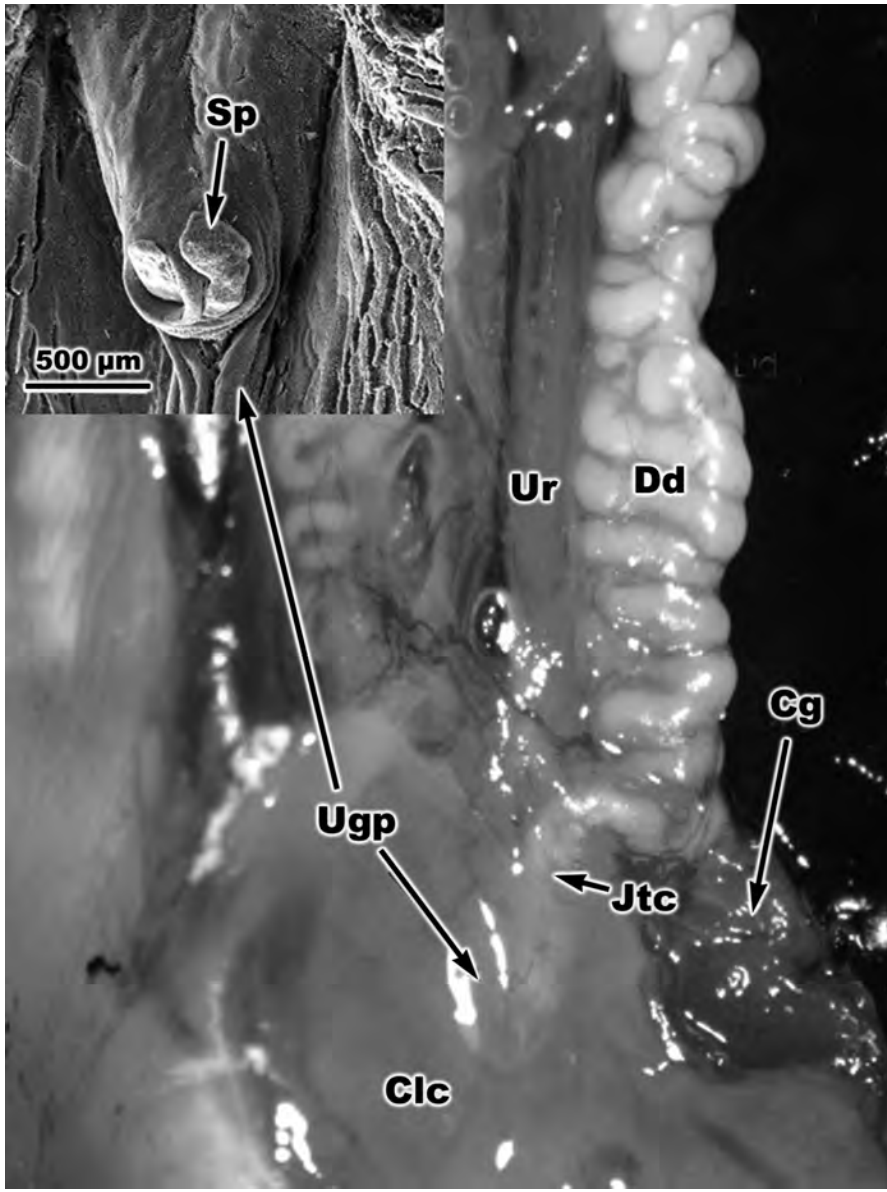

Fig. 10.21 Macroscopic view of the distal urogenital anatomy of a male *Opheodrys aestivus*, a North American colubrine snake, showing urogenital ducts and associated structures. Scanning electron micrograph (inset) reveals sperm extruding from the urogenital papilla in this species. Clc, cloacal chamber; Cg, cloacal gland; Dd, ductus deferens; Jtc, ductus deferens merging with ampulla urogenital papilla; Sp, sperm; Ugp, urogenital papilla; Ur, ureter.

Color image of this figure appears in the color plate section at the end of the book.

limit of the cloacal gland and then proceeding posteriorly toward the orifices of the urogenital papilla. We have chosen a representative colubrine, *Thamnophis proximus proximus* (same specimen measured above), for our descriptive treatment of this structure (Figs. 10.22, 10.23, 10.24).

In Fig. 10.22A, the ureters and the ductus deferentia can be seen in a horizontal plane with each ductus deferens being located lateral to its respective ureter. Both sets of ducts are positioned dorsal to the coprodaeal chamber. At the level viewed in Figs. 10.22B to 10.22D, each ductus deferens changes position as it begins a gradual progression in a ventromedial direction so as to eventually lie nearly ventral to their respective ureter (as shown in Fig. 10.22D-F). Immediately following the plane level of Fig. 10.22D, the anteriormost region of one ampulla urogenital papilla can be seen as a small pouch breaking through the dorsal wall of the muscularis of one ureter (Fig. 10.22E,F). Eventually, both ampullae can be seen in this area, and they continue to enlarge and push the ureters downward until they reside in a near midventral position beneath their respective ampullary cavities (Fig. 10.23A). Soon thereafter, a ureter can be seen opening directly into the cavity of its ampulla (Fig. 10.23B); eventually, both ureters open into the ampullary cavities (Fig. 10.24A). The ductus deferentia move toward the ventral surface of the ampullary cavities and empty into them at a point nearly identical to where the ureters open (Fig. 10.24A,B). The ampullary cavities now expand into the cloacal cavity, leaving a bulging, outward curved depression on the surface topography of the anterior dorsal recess. These bulges are best seen using SEM and are the external ampullary folds (Fig. 10.32). Eventually, the ampullae reach maximum width in the plane level of the orifices of the urogenital papilla (Fig. 10.24D). Posterior to the plane of the orifices, the ampullae quickly disappear.

The degree of folding and the relative thickness of the epithelial lining of the ampulla urogenital papilla, as observed within the urogenital papilla, are highly variable among the different species of snakes (Fig. 10.25). One of the simplest design morphologies can be seen in *Cemophora coccinea copei* (Fig. 10.25A), which exhibits a relatively smooth, unfurrowed epithelial lining when the ampullae are packed with sperm (as in Fig. 10.25A). A thin incomplete midsagittal ampullary wall separates the two ampullary cavities and, thus, allows their contents to combine at the apical region near the common urogenital orifice, which this species possesses. The thin lips of the urogenital papilla are also apparent here. This peculiar bellows configuration found in *C. coccinea copei* was not observed in other species. A low, pseudostratified columnar epithelium lines the two ampullary cavities.

The midsagittal partition separating the two ampullary cavities is complete in *Sonora semiannulata* (Fig. 10.25B) as well as the remaining species examined. This species exhibits thickened ampullary walls, but they still retain a smooth, unfurrowed epithelial surface similar to that of *Cemophora coccinea copei*. The columnar epithelium is 4-5 cell layers in thickness.

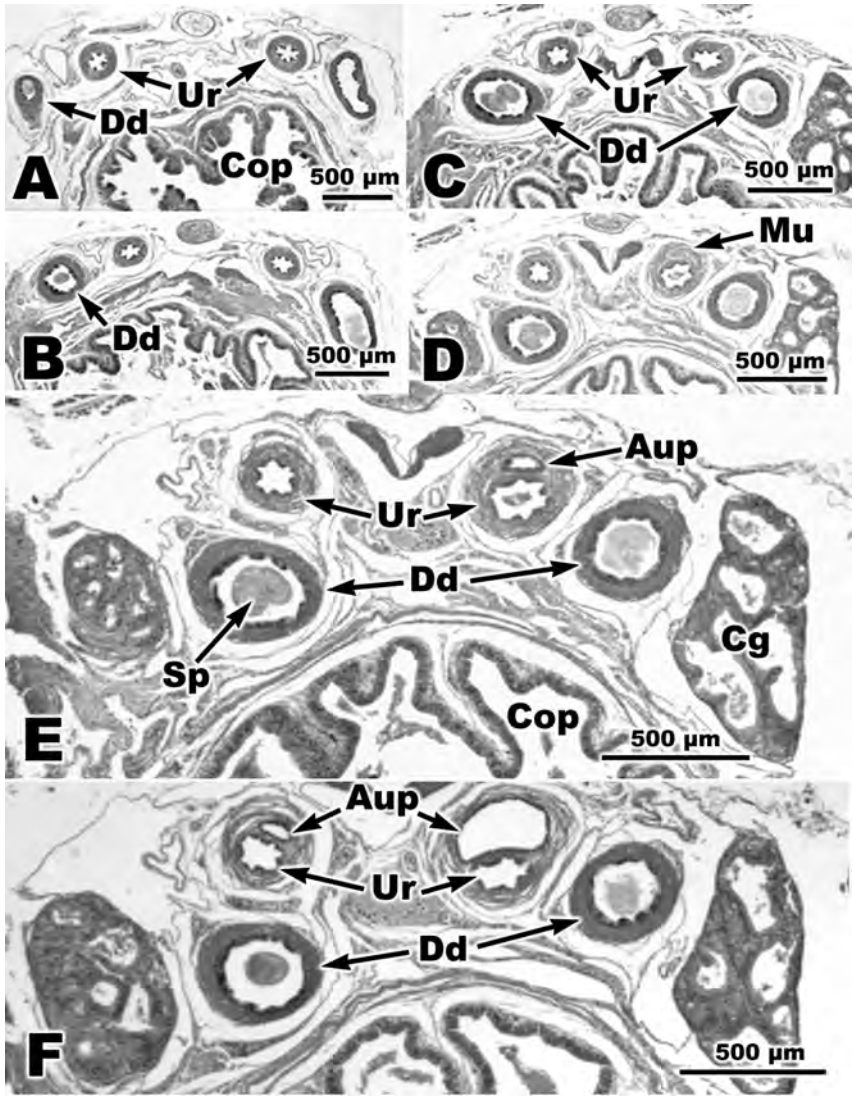

Fig. 10.22 Light micrographs of anterior-to-posterior serial histosections (Figs. 10.22-10.24) of approximately 5.0 mm of urogenital tissue revealing distal urogenital ducts and the anterior cloacal anatomy of *Thamnophis proximus proximus*, stained with hematoxylin and eosin. **A.** Anteriormost section showing the relationship between the ureter (Ur), the ductus deferens (Dd), which is situated laterally, and the first coprodaeal chamber (Cop). **B.** Section posterior to A showing gradual enlargement and medial displacement of the left ductus deferens **C.** Section revealing the near pairing of each ureter and its respective ductus deferens. **D.** Dorsomedial enlargement of the ureter muscularis indicates the anteriormost extension of the ampulla urogenital papilla (Aup); the ductus deferens now resides ventral to the left ureter. **E.** The ampulla urogenital papilla appears as a small pouch dorsal to its ipsilateral ureter. **F.** Bilateral ampullae rapidly expand their anatomical position dorsal to their respective ureters. Aup, ampulla urogenital papilla; Cg, cloacal gland; Cop, coprodaeal chamber; Dd, ductus deferens; Mu, muscularis; Sp, sperm; Ur, ureter.

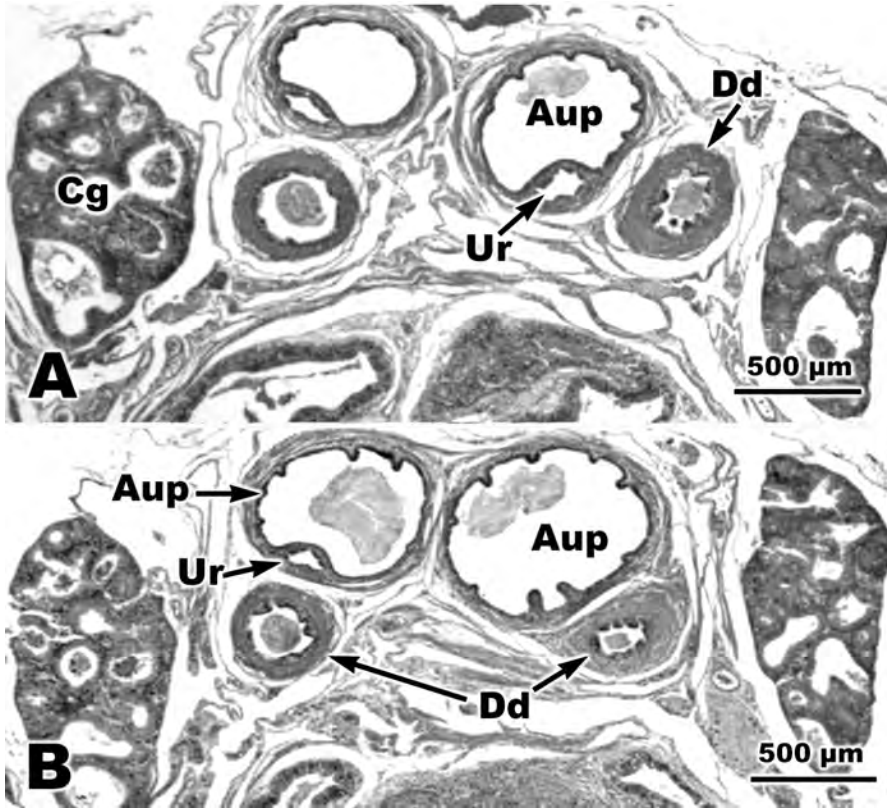

Fig. 10.23 *Thamnophis p. proximus*, continuation of Fig. 10.22. **A.** The ampullae urogenital papillae extend, displace, and constrict the ureters. **B.** The right ureter opens into its ipsilateral ampulla. Aup, ampulla urogenital papilla; Cg, cloacal gland; Dd, ductus deferens; Ur, ureter.

The epithelial lining of the ampullary cavities, as seen in *Farancia abacura reinwardtii* (Fig. 10.25C), is variable in thickness and consists of a mixture of simple columnar and low pseudostratified columnar. Little folding of the ampullary wall is evident. Although this species possesses two distinct urogenital papillae, the ampullary cavities show a thin midventral wall, a partition just prior to the orifices. This ventral partition broadens to become part of the posterior papillary ridge in this species.

In *Diadophis punctatus arnyi* (Fig. 10.25D), the ampullary walls are laterally indented near the level of the orifices by the presence of spherical muscle masses within the lamina propria. These muscle masses are not evident in other species examined. The low pseudostratified columnar epithelial lining varies little throughout the ampullary cavities, but the lining itself shows some simple folds.

The ampullary cavities of *Carphophis vermis* (Fig. 10.25E) are unusual in several anatomical features. Both cavities exhibit additional partitions of the internal ampullary walls. In addition, these well-defined internally

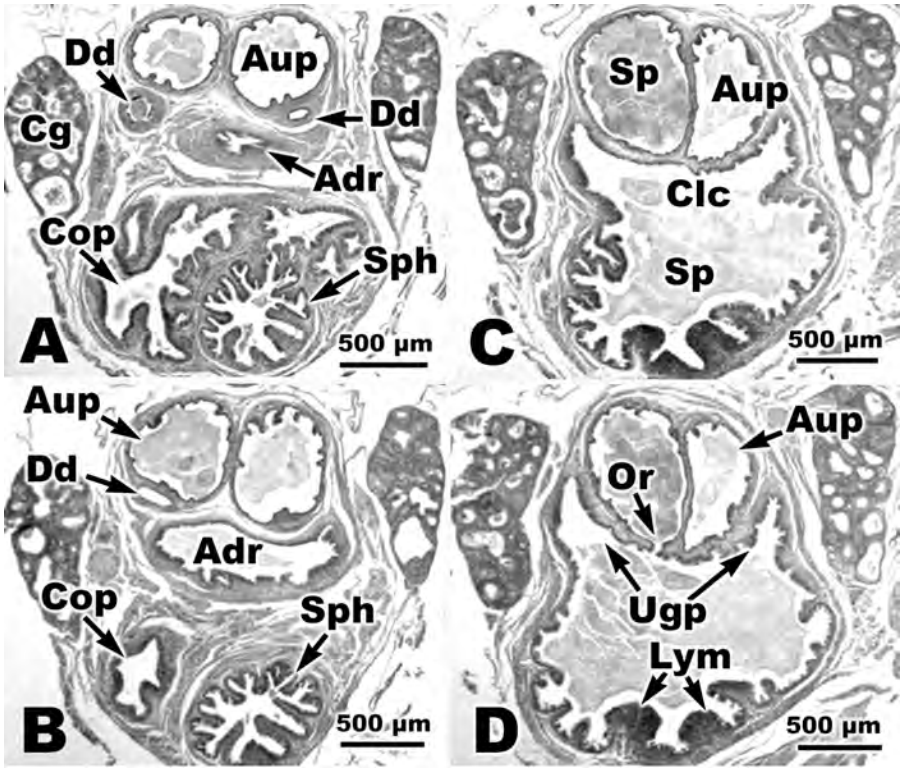

Fig. 10.24 *Thamnophis p. proximus*, continuation of Fig. 10.23. **A.** Spermatozoa fill the greatly enlarged ampullae urogenital papillae. The anterior dorsal recess (Adr) now appears beneath the ampullae urogenital papillae. The coprodaeal chamber is now flanked by the posterior coprodaeal sphincter (Sph), which separates the coprodaeum from the cloacal chamber (Clc). **B.** As the ampullae and the dorsal recess continue to enlarge, the ductus deferens on both sides near the point of confluence with the ampullae. The coprodaeal chamber becomes a blind pouch lateral to the posterior sphincter. **C.** The dorsal recess merges with the cloacal cavity to become an expanded anterior region of the cloaca proper. **D.** Sperm exit through the left orifice (Or) of the urogenital papilla (Ugp). Enlarged lymphoid tissue masses reside in the ventral wall of the cloacal cavity. Adr, anterior dorsal recess; Aup, ampulla urogenital papilla; Cg, cloacal gland; Clc, cloacal chamber; Cop, coprodaeal chamber; Lym, lymphoid masses; Or, orifice; Sp, sperm; Sph, sphincter muscle; Ugp, urogenital papilla.

thickened wall partitions escort each ductus deferens from a dorsal position to a ventral position at a point near its opening with each orifice of the urogenital papilla. A more complex version of this structural microanatomy dealing with the ductus deferens is found in *Regina grahamii* (Fig. 10.25I). The ampullary epithelium remains low, pseudostratified columnar. The tall stature of the urogenital papilla (the extent to which it projects into the cloacal cavity) of *C. vermis* can also be observed in Fig. 10.25E.

In the species examined in Fig. 10.25A-E, the ampullary lining can be characterized as being relative smooth and unfurrowed. In *Lampropeltis holbrooki* (Fig. 10.25F), as well as the three species to be discussed hereafter,

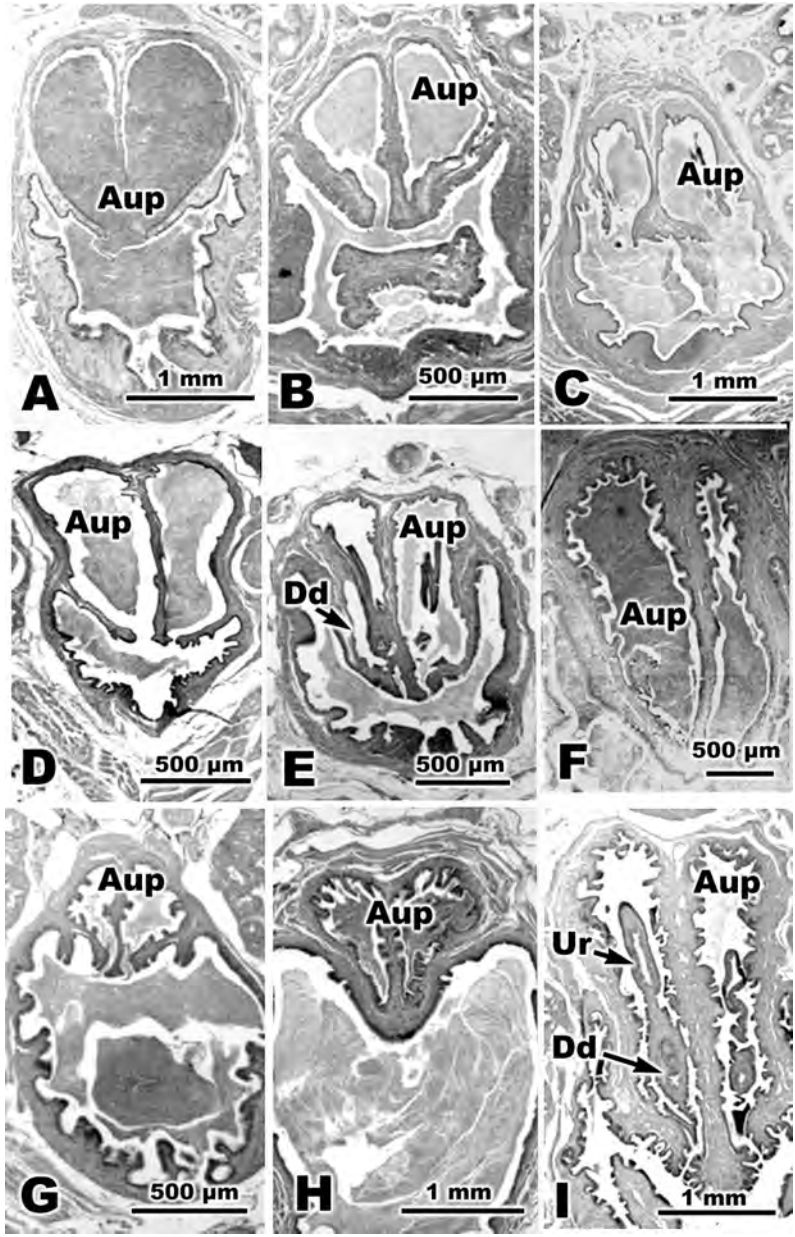

Fig. 10.25 Light micrographs of the ampulla urogenital papilla (Aup) and urogenital papillae in representative species of male North American colubrine snakes, stained with hematoxylin and eosin. All, except H, show the release of sperm through one (A) or two (B-I) urogenital orifices. Species are ranked from A though I according to the degree of folding of the epithelial lining of the Aup (see explanation in text). **A.** *Cemophora coccinea copei*. **B.** *Sonora semiannulata*. **C.** *Farancia abacura reinwardtii*. **D.** *Diadophis punctatus arnyi*. **E.** *Carphophis vermis*. **F.** *Lampropeltis holbrooki*. **G.** *Storeria dekayi wrightorum*. **H.** *Opheodrys aestivus*. **I.** *Regina grahamii*. Aup, ampulla urogenital papilla; Dd, ductus deferens; Ur, ureter.

an extensive folding of the internal ampullary wall is evident. A thickened midsagittal ampullary wall partition as well as relatively thick lateral ampullary walls characterizes the ampulla urogenital papillae in these species. Surface patches of low and tall pseudostratified columnar epithelial regions line the ampullary cavities in *L. holbrooki*.

Both *Storeria dekayi wrightorum* and *Opheodrys aestivus* possess similar ampullary cavities, each being greatly folded internally on all walls of the ampulla urogenital papilla. Two differences, observed in *O. aestivus* and not in *S. d. wrightorum*, are the spherical bulging of the dorsal ampullary cavities and the presence of primarily simple columnar epithelium, whereas *S. dekayi wrightorum* exhibits a low-to-tall pseudostratified columnar epithelium. Possibly the most strikingly unusual micro-structuring within the ampulla urogenital papilla is found in *Regina grahamii* (Fig. 10.25I). In this species, both ampullary cavities exhibit extensive internal surface folding, and the folding is so profound that additional small subcavities appear along most of the ampullary walls. Furthermore, each ureter and ductus deferens becomes enveloped by a thin longitudinally directed, vertical tissue column. The ureter resides in a dorsal position, whereas the ductus deferens resides in a ventral position. Both sets of urogenital ducts dump their products into their respective ampullary cavities at approximately the same plane level with the ureter opening slightly prior to the ductus deferens. Only *Carphophis vermis* and *Pantherophis obsoletus* (see below) examined thus far exhibit a similar urogenital micro-anatomy.

We focused, here again, some detailed histochemical and ultrastructural attention on the ampulla urogenital papilla and the associated urogenital ducts of *Pantherophis obsoletus*. In a histochemical analysis, we found that the lining of the ampulla urogenital papilla and the ureter in this species is highly secretory (Fig. 10.26). The epithelial lining of both structures is PAS positive, a strong indication of the presence of neutral carbohydrates (Fig. 10.26C,F). Upon using alcian blue to test for glycosaminoglycans, we found a strong positive reaction in the epithelial lining of the ampulla urogenital papilla (Fig. 10.26D,E). As noted by Sever (2004) for *Seminatrix pygaea*, the ductus deferens did not react positively with either PAS or with alcian blue. On the other hand, in the region of the merging of the ductus deferens and the ampulla urogenital papilla, a strong PAS positive stain occurs (Fig. 10.26F) within an enclosed sperm aggregate (Fig. 10.26F), indicating that the epithelial secretions within the ampulla possibly move up into the ductus deferens some distance.

The secretory nature of the epithelial lining of the ampulla urogenital papilla of *Pantherophis obsoletus* is further supported by ultrastructural studies. We first noted that in preparation for TEM, the pseudostratified columnar epithelium of both the ampulla and the ureter tested positive for carbohydrates using Ladd multiple stain (Fig. 10.27A,B) on plastic-embedded sections. The supranuclear surfaces of these cells were enriched by secretory material in cytoplasmic vesicles that stain dark red. Upon investigation by TEM, we found numerous secretory vesicles exhibiting a

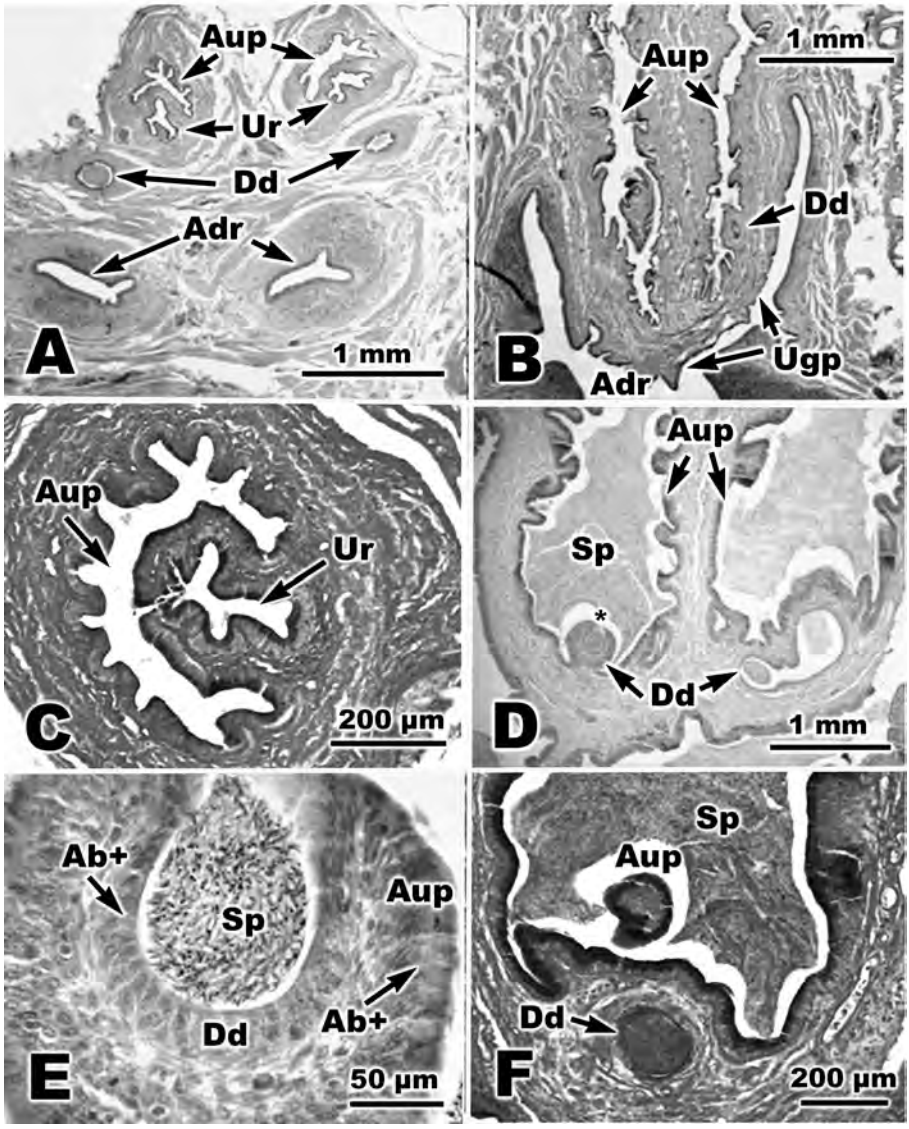

Fig. 10.26 Light micrographs (transverse histosections) of the distal urogenital anatomy of *Pantherophis obsoletus* revealing relationships among the ureter, ductus deferens, and the ampulla urogenital papilla as well as the staining properties of their secretory epithelia. **A.** Section showing urogenital anatomy prior to the merging of the ureter and the ampulla urogenital papilla. Paired extensions of the dorsal recess lie beneath the ampulla urogenital papilla-ureter-ductus deferens complexes. **B.** Section through the urogenital papilla (ventral half) in a non-reproductive adult showing the near merging of the ductus deferens with the ampulla urogenital papilla. Paired extensions of the dorsal recess surround the urogenital papilla. A and B both stained with hematoxylin and eosin. **C.** Section showing the merging of the ureter with the ampulla urogenital papilla. The epithelia of both structures exhibit a strong

Fig. 10.26 Contd. ...

variety of differing electron densities within this surface region. Some of these products appear to be released by the process of exocytosis, whereas others are possibly retained within the cells to perform cell maintenance duties. We also observed what could be phagocytosis of sperm within the epithelial lining (Fig. 10.27B).

10.3.4. Ampulla Ureter

Review. The ampulla ureter is the expanded distal segment of the ureter in male viperid snakes (Volsøe 1944). It is the functional equivalent to the ampulla urogenital papilla of colubrine snakes discussed previously. In Fig. 10.28, we have redrawn an illustration of the ampulla ureter as depicted by Volsøe (1944) and juxtaposed it with a macroscopic view of this structure from the Southern Copperhead (*Agkistrodon contortrix*) in order to better illuminate the morphology of this structure. Below, we also provide new urogenital information on the micro-anatomy of the ampulla ureter in two crotaline species, *Sistrurus miliarius* and *A. contortrix*, using light and electron microscopy.

New observations. The following Figs. 10.28-10.31 illustrate the anatomical design of the ampulla ureter and show the basic differences between this structure and the ampulla urogenital papilla of colubrine species as previously seen in Figs. 10.20-10.27. For example, the distal urogenital ducts of the colubrine species (*Thamnophis proximus proximus*) and a crotaline species (*Sistrurus miliarius streckeri*) are essentially identical at the histological planes shown in Fig. 10.22A and Fig. 10.29A, respectively.

The relative sizes (diameters) of the ureter and the ductus deferens in each species are equally similar to one another. Following a posterior histological progression, the ductus deferens does not enlarge in *Sistrurus milarius streckeri* as it does in *Thamnophis proximus proximus* (Fig. 10.22E), but instead becomes smaller than the ureter as each ductus deferens moves medially (Fig. 10.29B,C). What becomes strikingly apparent in *S. m. streckeri* in Fig. 10.29E is the enlargement of the ureters through a thickening of

... Fig. 10.26 Contd.

PAS positive stain. **D.** Section through the urogenital papilla (ventral half) in a reproductive adult showing the near merging of the ductus deferens with the ampulla urogenital papilla (see asterisk). Note the secretory epithelium of the each ampulla urogenital papilla has reacted positively with alcian blue stain (pH = 2.5-2.8). **E.** Higher magnification of region designated by the asterisk in D. The epithelial surface of the ductus deferens shows a slight positive reaction with alcian blue compared to the more intense (darker blue) reaction seen on the epithelial surface of the ampulla urogenital papilli. **F.** Ventral regions of an ampulla urogenital papilla (similar to view in D) reveals a strong PAS positive stain in the epithelium as evidenced by the intensity of the red stain. Ab+, alcian blue positive reaction; Adr, anterior dorsal recess; Aup, ampulla urogenital papilla; Dd, ductus deferens; Sp, sperm; Ugp, urogenital papilla; Ur, ureter.

Color image of this figure appears in the color plate section at the end of the book.

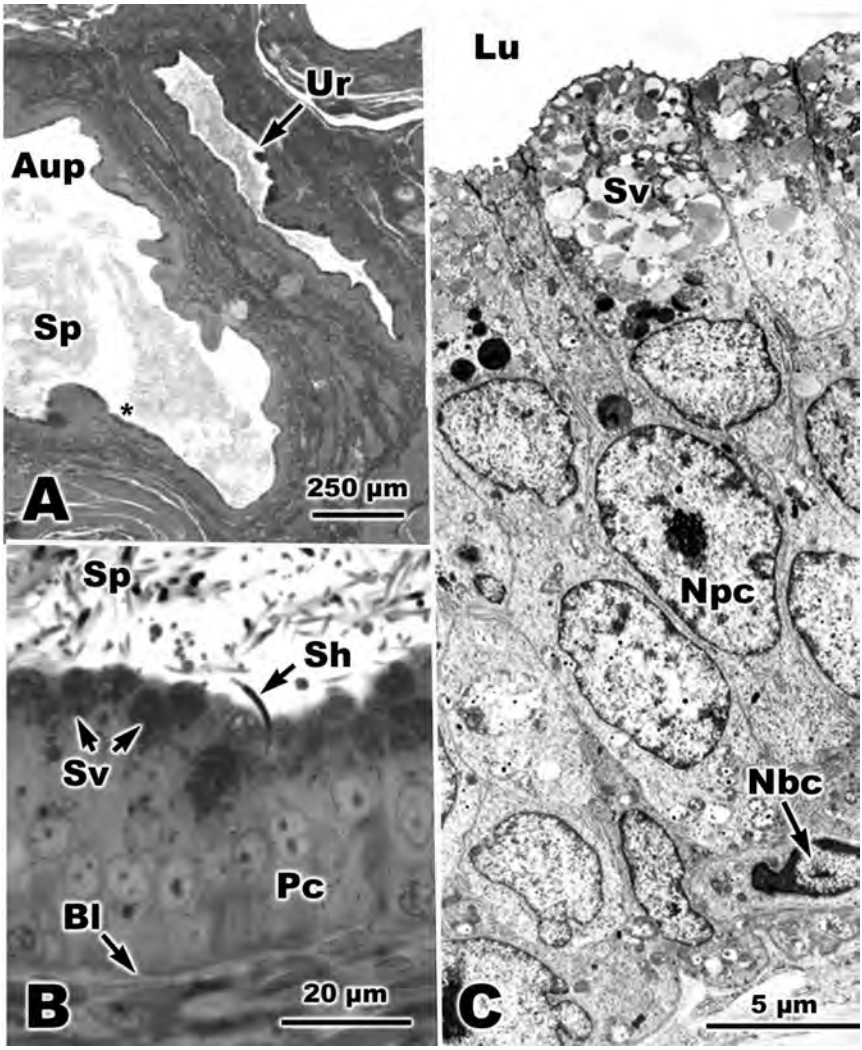

Fig. 10.27 Light and transmission electron micrographs revealing the secretory epithelium of the ampulla urogenital papilla of an adult male *Pantherophis obsoletus*. **A.** Plastic thick section (ca. 1 µm) showing the relative position of the ampulla urogenital papilla and the ureter (see Fig. 10.38A and C for comparison). Sperm are scattered within the lumina of both structures. Asterisk indicates the approximate region shown at higher magnification in B. **B.** Section through the pseudostratified columnar epithelium of the ampulla urogenital papilla as shown in A revealing intense staining of apical secretory vesicles. Sperm are abundant near epithelial surface including a sperm cell whose head is embedded within epithelium. A and B stained with Ladd multiple stain. **C.** Transmission electron micrograph showing a portion of the secretory epithelium. Note clusters of clear and opaque secretory vacuoles near the surface of the epithelial cells. Aup, ampulla urogenital papilla; Bl, basal lamina; Lu, lumen; Nbc, nucleus of basal cell; Npc, nucleus of principal cell; Pc, principal cells; Sh, sperm head; Sp, sperm; Sv, secretory vacuoles; Ur, ureter.

Color image of this figure appears in the color plate section at the end of the book.

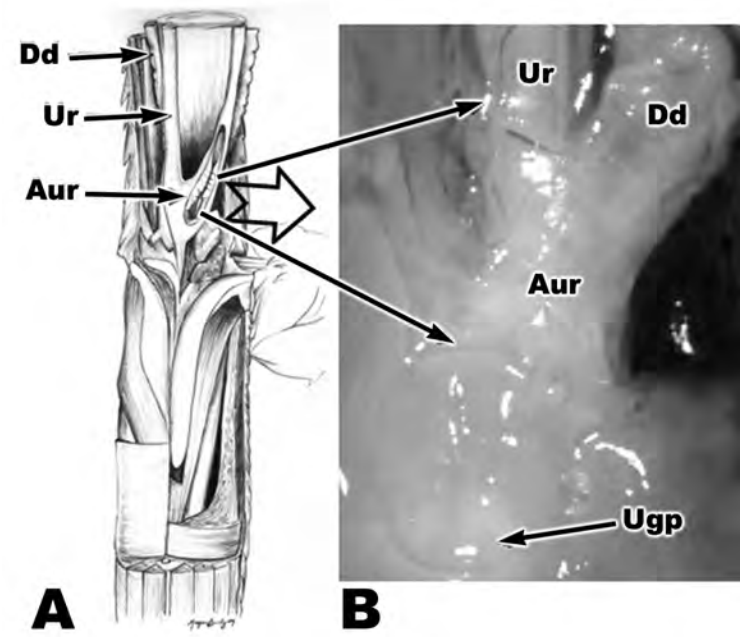

Fig. 10.28 Composite diagram including an illustration of the adult male distal urogenital anatomy of a European viperine snake, *Vipera berus* (**A**; redrawn from Volsøe 1944) matched alongside a North American crotaline snake, *Agkistrodon contortrix* (**B**).The presence of an ampulla ureter (Aur) represents a fundamental anatomical difference between viperine urogenital morphology and the colubrine urogenital morphology as shown in Fig. 10.20. Aur, ampulla ureter; Dd, ductus deferens; Ugp, urogenital papilla; Ur, ureter. **A** is adapted from Volsøe, H. 1944. Spolia Zoologica Musei Hauniensis V. Skrifter, Universitetets Zoologiske Museum, København, Fig. 11.

Color image of this figure appears in the color plate section at the end of the book.

the ureterine muscularis along with a commitment expansion of their lumina. In contrast, the ureterine muscularis of *T. p. proximus* enlarges because of the development and swelling of the ampulla urogenital papilla embedded within its dorsomedial wall (Fig. 10.22E,F). In *S. m. streckeri*, however, no similar development occurs. Instead, the two enlarging ureters move medially and become enveloped within a common muscularis in conjunction with the wall of the newly emerging anterior dorsal recess (Fig. 10.29E,F). At this point, each ureter can now justifiably be called an ampulla ureter. At the same time that this enlargement occurs, each ductus deferens also moves medially to become a small component of a singular medial urogenital complex (Fig. 10.29F). Each ampulla ureter now characteristically exhibits a highly convoluted internal lining. In a more posterior plane, as seen in Fig. 10.29G, the ampullae begin to lengthen dorsoventrally; in Fig. 10.29H, the anterior dorsal recess merges with the cavity of the coprodaeum. The medial urogenital complex has now also incorporated the muscularis of the coprodaeum to become a singular mass,

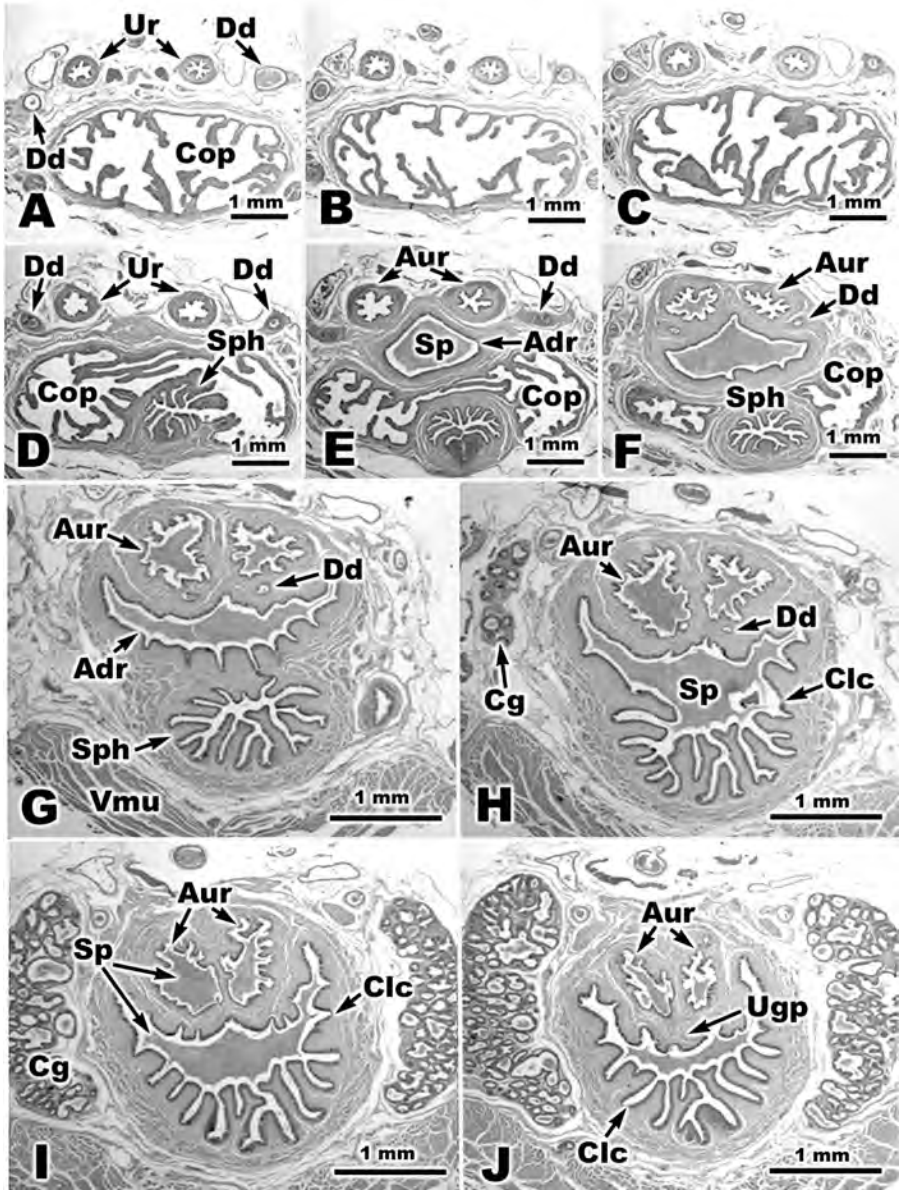

Fig. 10.29 Light micrographs of selected anterior-to-posterior serial histosections of approximately 7.0 mm of urogenital tissue revealing distal urogenital ducts and the anterior cloacal chamber of *Sistrurus miliarius streckeri*, a North American crotaline snake, stained with hematoxylin and eosin. **A.** Anteriormost section of series showing the relationship between each ureter (Ur), ductus deferens (Dd), each lying lateral to its respective ureter, and the first coprodaeal chamber (Cop). **B.** Section posterior to A showing gradual decrease in diameter of the right ductus deferens. **C.** Section revealing a gradual enlargement of the ureters; each

Fig. 10.29 Contd. ...

the cloacal complex. Cloacal glands begin to appear within this histological plane and reside lateral to the cloacal complex. At this point, each ductus deferens has lost most of its muscularis and has become a minute ventral duct lying beneath the ampullae. They soon merge with the ampullary cavities (Fig. 10.29H). The ventral surfaces of each ampulla protrude in the form of individual folds into the cloacal cavity and are referred to as the external ampullary folds of the urogenital papilla (Fig. 10.29I). Finally, the ampullae narrow as they near the urogenital orifice (in this species a single orifice; Fig. 10.29J).

For an evaluation of the secretory activity of the ampulla ureter, we examined this structure in a reproductively active individual of the crotaline species, *Agkistrodon contortrix* (Figs. 10.30, 10.31). The internal walls of the ampullae of *A. contortrix* lack the characteristic folding seen in *Sistrurus miliarius streckeri*. The epithelial lining of the ampullae exhibits a highly secretory, tall, thick pseudostratified columnar epithelium. Spherical cytoplasmic blebs (Fig. 10.30B) form a distinctive layer along the apical surfaces of the epithelial cells. These cytoplasmic blebs show little affinity for histological stains. Under transmission electron microscopy (Fig. 10.31), the apical blebs appear to contain amorphous materials released as an apocrine-packaged unit housed within a compartment created by a growing free cytoplasmic membrane, hence, the term apocrine blebs is appropriate as in more anterior efferent ducts. The epithelial cells appear to accumulate materials within numerous secretory vesicles in a region just below the apical bleb (Fig. 10.31A). These membrane-bound secretory vesicles appear to swell, lose their integrity, and disintegrate along a well-defined linear boundary line. In general, secretory vesicles remain on the nuclear side of the boundary line, whereas secretory materials occupy the luminal side. As the membrane coats of the secretory vesicles are lost, an expansion of the

... Fig. 10.29 Contd.

ductus deferens remains situated lateral to its respective ureter. **D.** The muscularis and the lumen of both ureters have continued their enlargement; the coprodaeal sphincter (Sph) appears along the floor of the coprodaeum. **E.** Each enlarged ureter, now nearly twice the diameter as seen in A, is becoming medially displaced and is also transitioning into an ampulla ureter (see text for explanation); the anterior dorsal recess (Adr) appears medial and dorsal to the coprodaeal chamber. **F.** The ampullae ureters are now encompassed by a common muscularis envelope and are continuing their medial displacement and enlargement; sperm fill the lumen of the dorsal recess. Blind pouches of the coprodaeal cavity now lie on either side of the coprodaeal sphincter. **G.** Each ductus deferens now resides ventral to its respective ipsilateral ampulla ureter; the dorsal recess has expanded laterally. **H.** The left ductus deferens nears merging with its ipsilateral ampulla ureter; the lumen of the coprodaeal sphincter has merged with the dorsal recess creating an expansive anterior cloacal chamber (Clc). **I.** The ampullae reach maximum volume; spermatozoa fill the anterior cloacal chamber. **J.** Each lumen of the individual ampulla ureter elongates as both descend into the tip of the urogenital papilla. Adr, anterior dorsal recess; Aur, ampulla ureter; Cg, cloacal gland; Clc, cloacal chamber; Cop, coprodaeal chamber; Dd, ductus deferens; Sp, sperm; Sph, sphincter; Ugp, urogenital papilla; Ur, ureter; Vmu, ventral musculature.

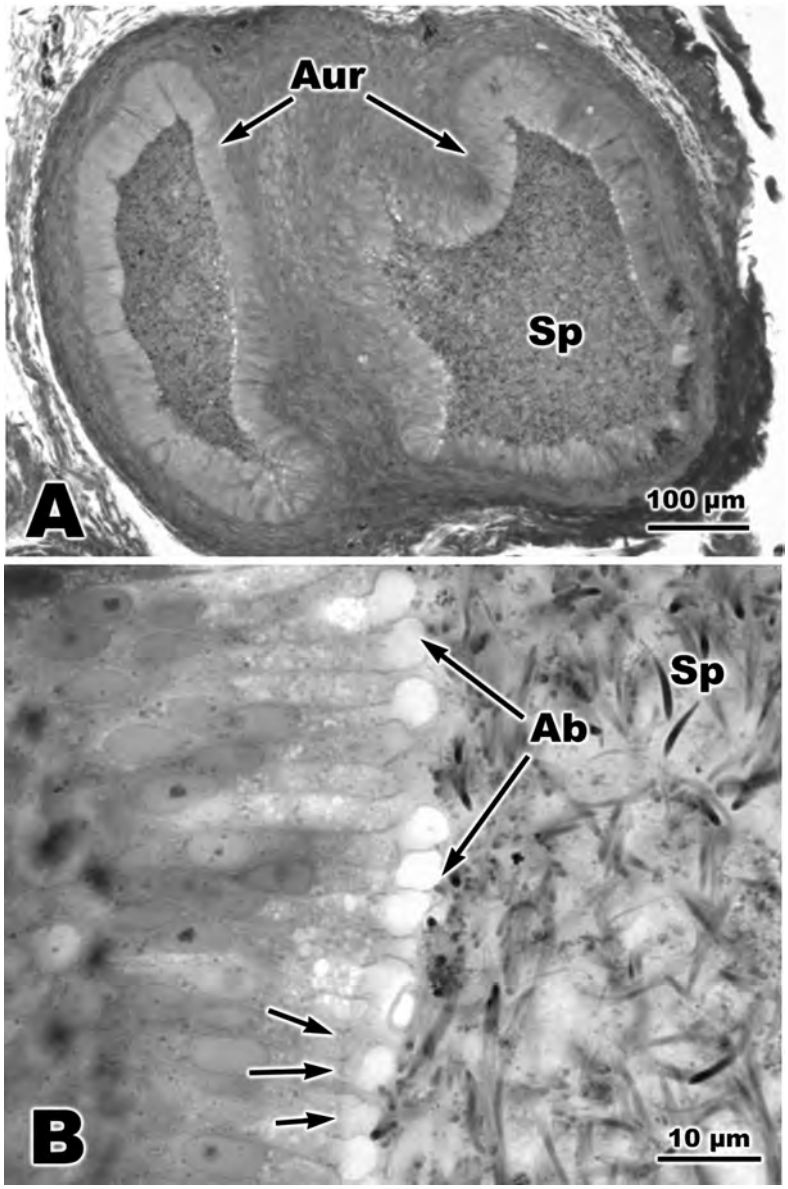

Fig. 10.30 Light micrographs of the ampulla ureter and its secretory epithelium of an adult male *Agkistrodon contortrix*, a North American crotaline snake, stained with Ladd multiple stain. **A.** Section from plastic embedded tissue (ca. 1 mm in thickness) showing the tall pseudostratified columnar epithelium (pale band) lining the lumina of the ampullae. Spermatozoa completely fill luminal cavities. **B.** Portion of secretory epithelium from A exhibiting the presence of apocrine blebs (Ab) being liberated from numerous principal cells. A series of arrows (lower left) follow a faint, but distinctive cytoplasmic demarcation line, which lies at the base of these cytoplasmic blebs. Ab, apocrine blebs; Aur, ampulla ureter; Sp, sperm.

Color image of this figure appears in the color plate section at the end of the book.

plasma membrane accommodates the festooning accumulation of cellular products along the free surface. Apocrine blebs appear to be squeezed away from the parent cell to become a luminal bleb (Fig. 10.31C,D). Thus, the eccrine process is similar to that described for the ductus epididymis and ductus deferens. Sperm lie in close proximity to the margins of these cellular and luminal blebs.

10.4. UROGENITAL PAPILLA AND CLOACA

Review. In male snakes, spermatozoa transversing through the ductus deferens and urine transversing through the ureter exit directly into the cloacal urodaeum via a common pore at the terminal end of a distinctive anatomical structure known as the urogenital papilla (Fig. 10.32). Snakes either possess a single, medial urogenital papilla or paired, bilateral urogenital papillae. In either case, the urogenital papilla projects ventrally from the dorsal wall of the anterior cloacal chamber (Seshadri 1959; Bellairs 1970; Fox 1977; Lombardi 1998). Little anatomical information is available regarding this structure. No authors have incorporated species-specific illustrations, descriptions, and details of the urogenital papilla when discussing the distal urogenital tracts of individual snake species in conjunction with its urogenital anatomy (e.g., W. Fox 1952; H. Fox 1977). Instead, some authors have redrawn the basic anatomical sketches provided by Volsøe (1944) for *Vipera berus* and by Gabe and Saint Girons (1965) for *Vipera aspis*. Surprisingly, contemporary illustrations featuring male snake gross internal anatomy often omit the region occupied by the urogenital papilla entirely (e.g., Shine 1991; Vitt and Caldwell 2009). Gabe and Saint Girons (1965) provided a histological cross section of the urogenital papilla in a male Banded Krait (*Bungarus fasciatus*), making this drawing the only micro-anatomical depiction of the male urogenital papilla in the snake literature until the present study.

Illustrated descriptions of the co-joining of the ureter and the ductus deferens appear as infrequently as do depictions of the urogenital papilla in snake anatomical literature. The only exceptions include an illustration by Martin Saint Ange (1854) for a European natricine (*Natrix natrix*) and the aforementioned viperid species drawn by Volsøe (1944) and by Gabe and Saint Girons (1965).

New observations. Below, we provide descriptive coverage of the urogenital papilla by revealing its macroscopic, microscopic, and ultrastructural anatomy from a diverse group of male North American colubroid snakes. We utilized 39 species and subspecies from four subfamilies (Crotalinae, Xenodontinae, Natricinae, Colubrinae) and follow the classification provided by Vitt and Caldwell (2009); these representative species include the following: *Agkistrodon cortortrix*, *A. piscivorus*, *Crotalus atrox*, Timber Rattlesnake (*C. horridus*), Prairie Rattlesnake (*C. viridis*), *Sistrurus miliarius streckeri*, *Carphophis vermis*, *Cemophora coccinea copei*, Eastern Yellow-bellied Racer (*Coluber constrictor flaviventris*), *C. c. priapus*,

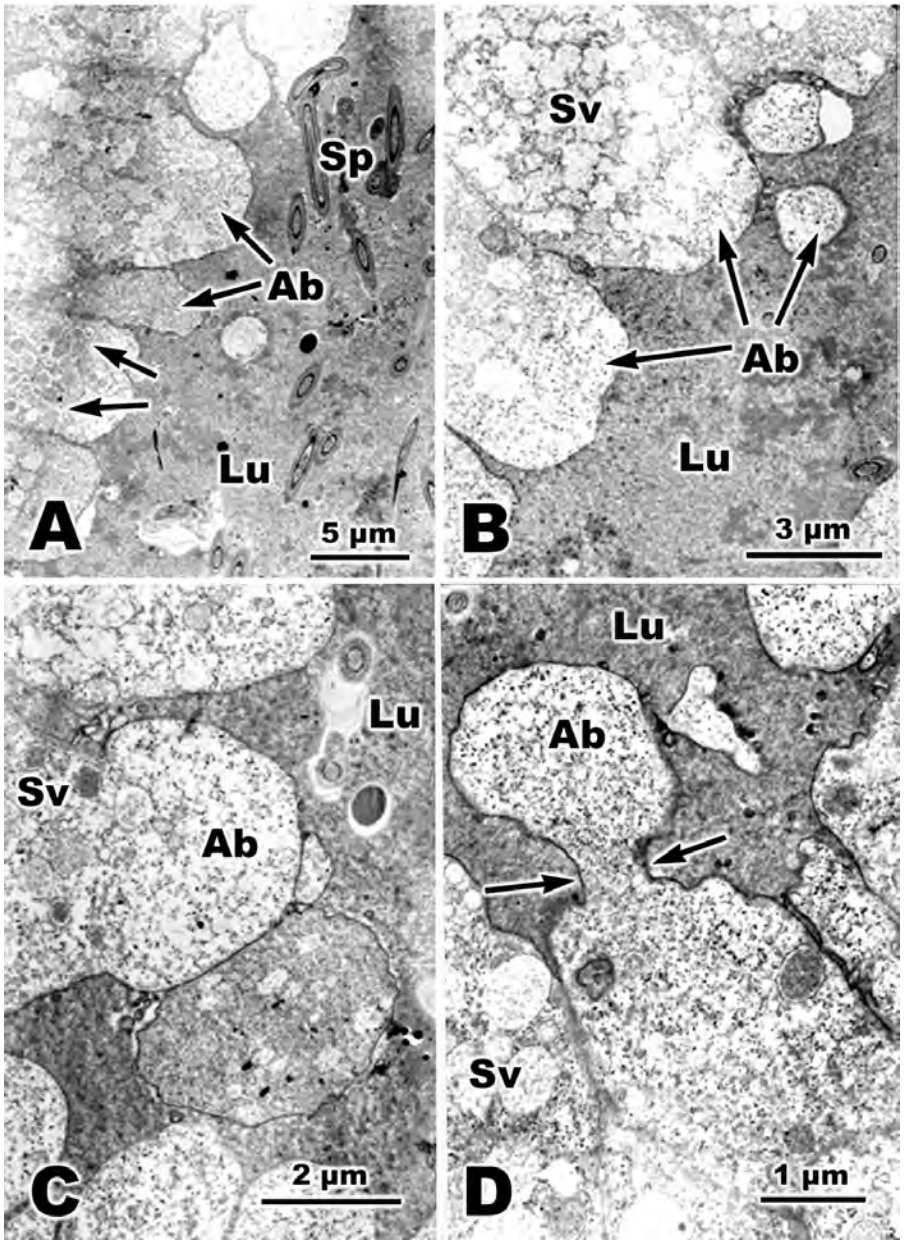

Fig. 10.31 Transmission electron micrographs of the apocrine bleb region of the secretory epithelium of *Agkistrodon contortrix* illustrated in Fig. 10.30. **A.** Arrows point to interface region between cytoplasmic secretory vacuoles and their dissociation to become secretory material of apocrine blebs (Ab). **B,C.** Higher magnification of region of apocrine blebs showing transition from circular secretory vesicles to mostly amorphous material of apocrine blebs and breakdown of vesicular membranes. **D.** Opposing arrows show neck of an apocrine bleb just prior to release into lumen. Ab, apocrine blebs; Lu, lumen; Sp, sperm.

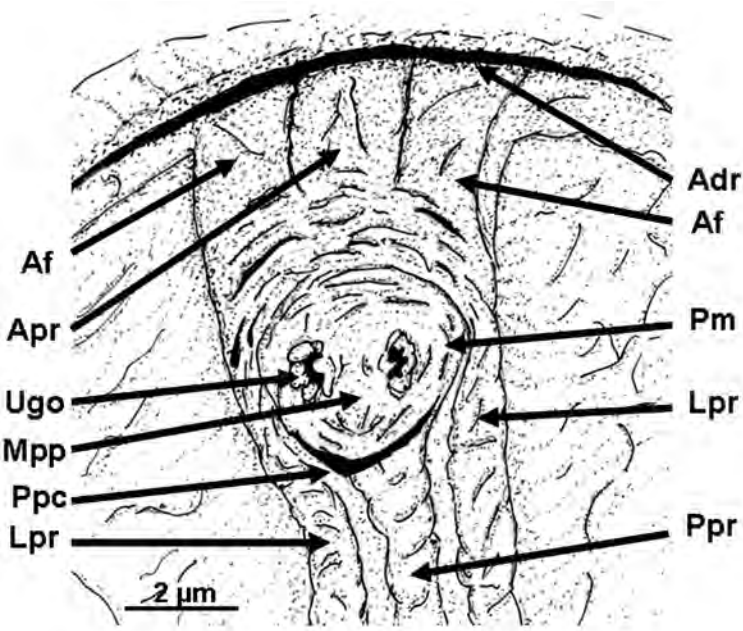

Fig. 10.32 Generalized illustration of a composite urogenital papilla (posterioventral view) including its surrounding tissues of a male North American colubrine snake. Abbreviations: Adr, anterior dorsal recess; Af, ampullary folds (paired); Apr, anterior papillary ridge; Lpr, lateral papillary ridge (paired); Mpp, medial papillary prominence; Pm, papillary mound; Ppc, posterior papillary recess; Ppr, posterior papillary ridge; Ugo, fleshy lips surround the paired urogenital orifices. Drawing by S. E. Trauth.

Black-masked Racer (*C. c. latrunculus*), *C. flagellum flagellum*, Desert Striped Whipsnake (*C. taeniatus taeniatus*), *Diadophis punctatus arnyi*, *Pantherophis obsoletus*, *Farancia abacura reinwardtii*, *Heterodon platirhinos*, Prairie Kingsnake (*Lampropeltis calligaster calligaster*), *L. holbrooki*, *L. triangulum syspila*, Yellow-bellied Watersnake (*Nerodia erythrogaster flavigaster*), Broad Banded Watersnake (*N. fasciata confluens*), Northern Diamond-backed Watersnake (*N. rhombifer rhombifer*), Midland Watersnake (*N. sipedon pleuralis*), *N. cyclopion*, *Opheodrys aestivus*, Bullsnake (*Pituophis catenifer sayi*), Long-nosed Snake (*Rhinocheilus lecontei*), Queensnake (*Regina septemvittata*), *Regina grahamii*, Texas Patch-nosed Snake (*Salvadora grahamiae lineata*), Variable Groundsnake (*Sonora semiannulata semiannulata*), *Storeria dekayi wrightorum*, Northern Red-bellied Snake (*Storeria occipitomaculata occipitomaculata*), *Tantilla gracilis*, *Thamnophis proximus proximus*, *T. sirtalis sirtalis*, *Virginia striatula*, and Western Smooth Earthsnake (*Virginia valeriae elegans*).

A variety of micro-anatomies exists for the urogenital papilla within our sample of crotaline species. For example, two closely-related species of *Agkistrodon* (Fig. 10.33A-D) possess sharply contrasting morphologies. In *A. contortrix*, the urogenital orifices open individually, project posteriorly,

and are narrowly separated on two small, but distinct, papillary mounds (Fig. 10.33A,B). This bilobate condition is reinforced by the structure of the ampullary folds, as they extend anteriorly and diagonally away from the individual papillary mounds. In *A. piscivorus*, however, the urogenital orifices lie atop a single well-defined, papillary mound, and the ampullary folds lie side by side anteriorly (Fig. 10.33C). This particular bi-lobate morphology was not observed in any other snake species in our sample.

Within the genus *Crotalus*, congruent morphologies exist between *C. atrox* and *C. horridus* (Fig. 10.33E,F), but neither morphology is similar to that of *C. viridis* (Fig. 10.34A-C). One striking feature of the urogenital papilla in *C. atrox* and *C. horridus* is the flat, platform-like, papillary mound. The urogenital orifices project in a postereolateral direction. The papillary mound is supported by a posterior papillary ridge as well as the two anterior ampullary folds. In *C. viridis*, a round papillary mound has no posterior papillary ridge (Fig. 10.34A,B). Two urogenital orifices, which open ventrally, are grooved, chevron shaped pits with mostly non-fleshy lips (Fig. 10.34C).

The urogenital papilla of another crotaline species, *Sistrurus miliarius streckeri*, is distinctly different from the other viperids described above as well as from all other species examined. It is the only species that exhibits co-joined urogenital orifices (Fig. 10.34D,E). The papillary mound in this species is conical and possesses circular grooves. The mound summit terminates into a pinnacle, and a large anterior papillary ridge exists. No posterior and lateral papillary ridges occur in this species.

In *Carphophis vermis*, the urogenital papilla possesses fleshly-lipped and relatively large, thinly separated orifices (Fig. 10.35A). The ampullary folds can be viewed between two, pin-hole artifacts in the cloacal wall. The lateral papillary ridges support the papillary mound, and a narrow posterior papillary recess is seen beneath the urogenital orifices.

The papillary mound in *Cemophora coccinea* is shaped in the form of a tugboat (Fig. 10.35B,C) and lies atop an oblong papillary base. The mound possesses several concentric grooves near its basal region. Posteriorly, the mound exhibits two large, cup-shaped orifices (right orifice occluded by sperm mass). A distinct posterior papillary ridge supports the papillary base, which lacks supportive lateral papillary ridges.

Three subspecies of racers and a coachwhip (genus *Coluber;* i.e., *C. constrictor flaviventris*, *C. c. priapus*, and *C. c. latrunculus*, Figs. 10.35D-F; 10.36A and *C. flagellum flagellum*, Fig. 10.36B) exhibit very similar papillary morphologies. These similarities include tall, circular, papillary mounds with fleshy-lipped, grooved orifices spaced widely apart atop a smooth papillary summit. The lips appear slightly raised and protrude away from the summit, yielding a bulging appearance in *C. constrictor priapus* (Fig. 10.35F). Within *C. taeniatus* a very different morphology exists (Fig. 10.36C). This species possesses a distinctive, blunt spear-shaped, papillary mound, posteriolaterally projecting orifices, and a deep posterior papillary recess. The recess is flanked by a moderately sized lateral papillary

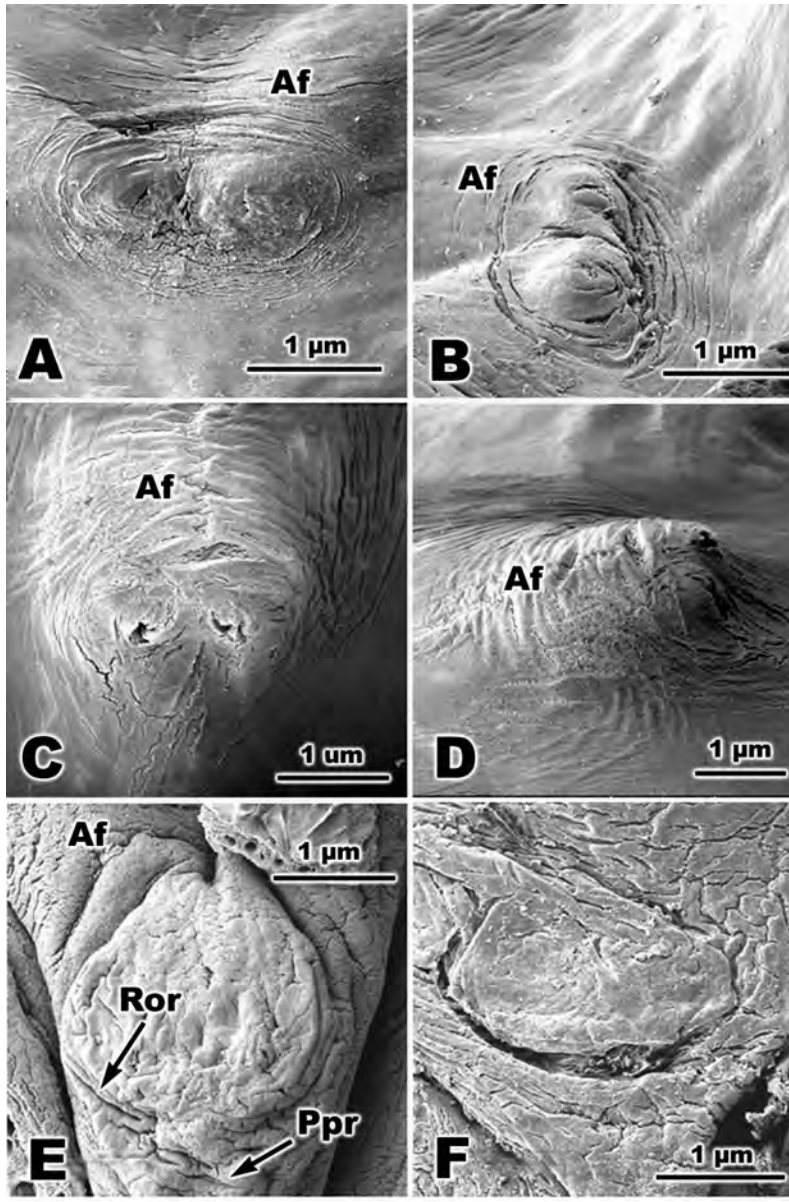

Fig. 10.33 Scanning electron micrographs of the urogenital papilla of representative North American male crotaline snakes. **A.** *Agkistrodon contortrix*, posterioventral view of bi-lobate papillae. **B.** *A. contortrix*, right ventrolateral view of A. **C.** *Agkistrodon piscivorus*, ventral view; urogenital orifices clearly visible. **D.** *A. piscivorus*, right ventrolateral view. An elevated, anterior papillary ridge (Af) leads to the urogenital orifices. **E.** *Crotalus atrox*, ventral view; urogenital orifices project posteriolaterally away from a depressed spatulate-like, urogenital papilla, which lies atop a posterior papillary ridge (Ppr); Right orifice is indicated (Ror). **F.** *Crotalus horridus*, ventral view and anatomical parts similar to E. Af, ampullary fold; Ppr, posterior papillary ridge; Ror, right orifice.

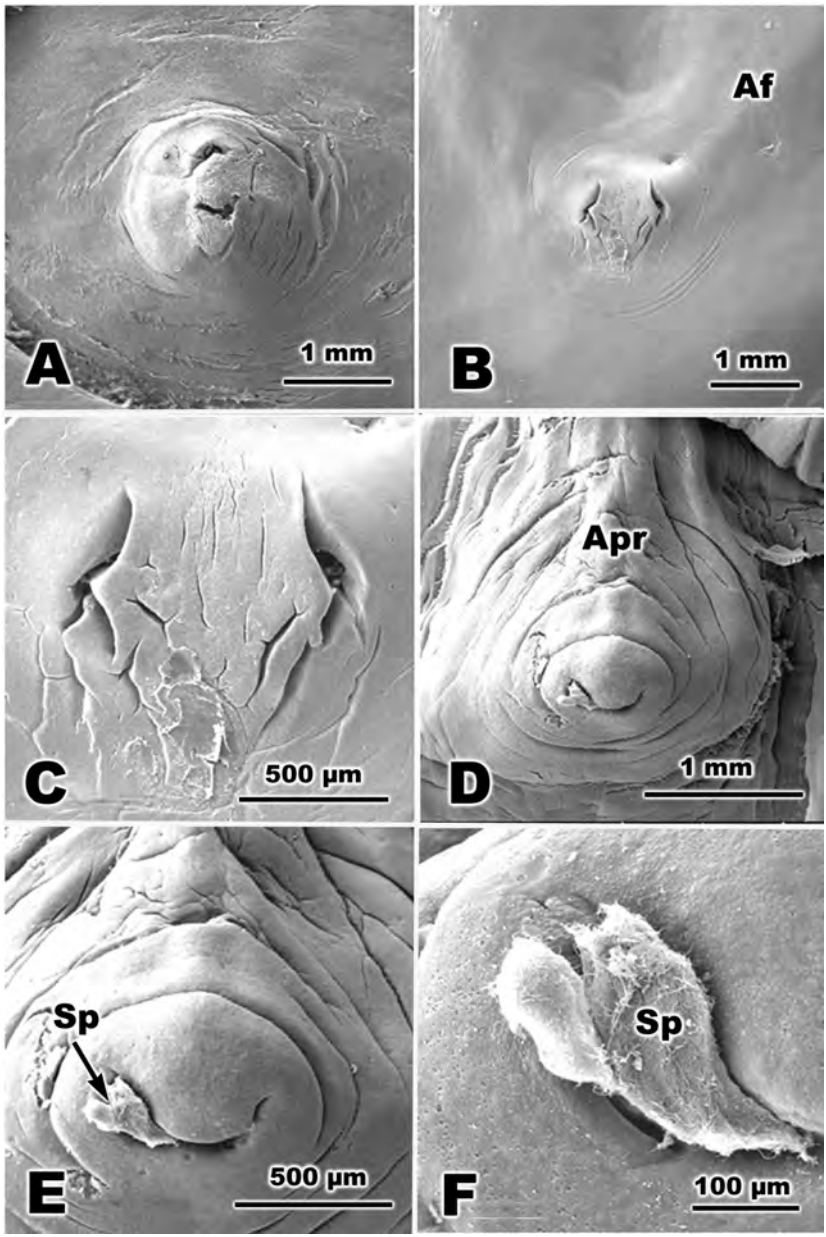

Fig. 10.34 Scanning electron micrographs of the urogenital papilla of representative North American male crotaline snakes. **A.** *Crotalus viridis*, right ventrolateral view. **B-C.** Same species as A, but showing ventral view of opposing, chevron-shaped urogenital orifices (B) and higher magnification (C). **D-F**. *Sistrurus miliarius streckeri*, ventral view of pinnacle-like papillary mound (Apr) and a single urogenital orifice exuding sperm. **E.** Higher magnification of D showing concentric grooves circumscribing pinnacle. **F.** Higher magnification of E showing C-shape urogenital orifice and sperm aggregation. Af, ampullary fold; Apr, anterior papillary ridge; Sp, sperm.

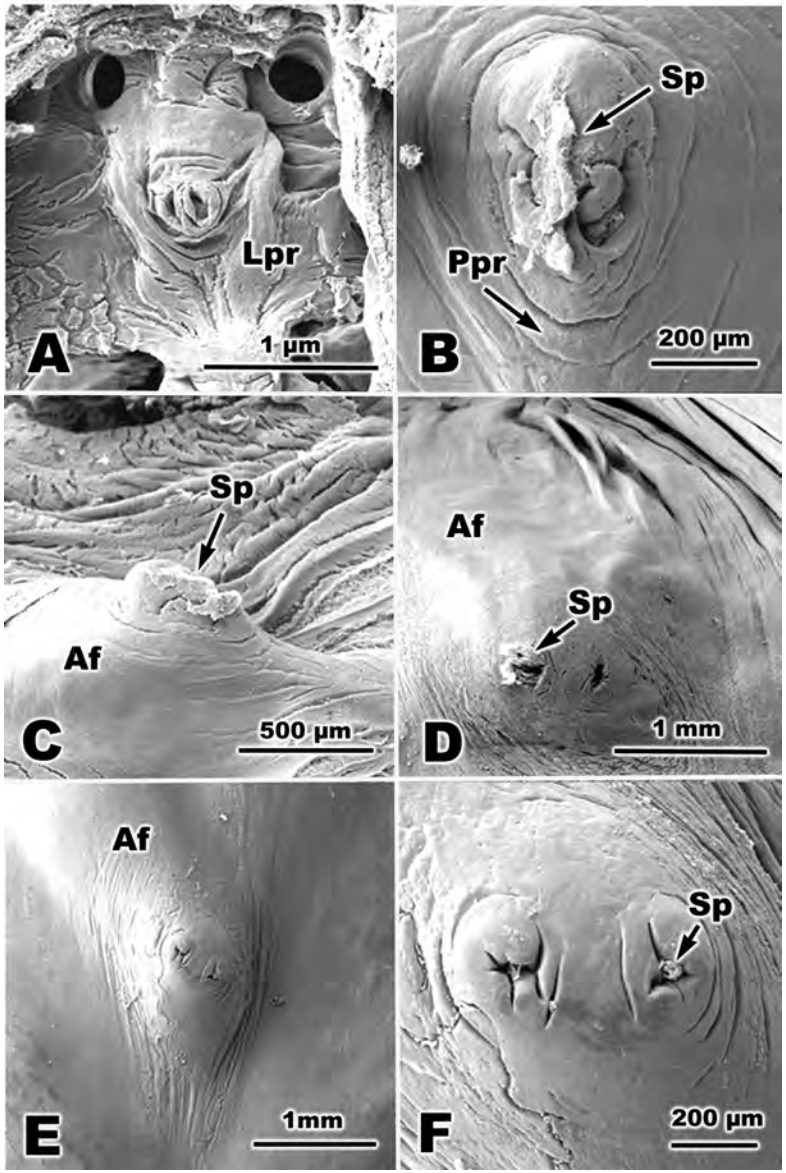

Fig. 10.35 Scanning electron micrographs of the urogenital papilla of representative North American male colubrine colubroid snakes. **A.** *Carphophis vermis*, ventral view showing paired half-moon shaped orifices, a small posterior papillary recess, and lateral papillary ridges (Lpr). **B-C.** *Cemophora coccinea copei*, ventral and right ventrolateral views, respectively, showing elevated tugboat-shaped papillary mound with sperm masses exuding from right orifice. **D.** *Coluber constrictor flaviventris*, ventral view of round papillary stalk with widely spaced orifices; sperm are aggregated at right orifice. **E-F.** *Coluber constrictor priapus*, ventral view of contorted papillary mound (E) not supported by well-defined anterior and posterior papillary ridges; orifices possess fleshy grooved lips (F) with left orifice exuding sperm. Af, ampullary fold; Lpr, lateral papillary ridge; Ppr, posterior papillary ridge; Sp, sperm.

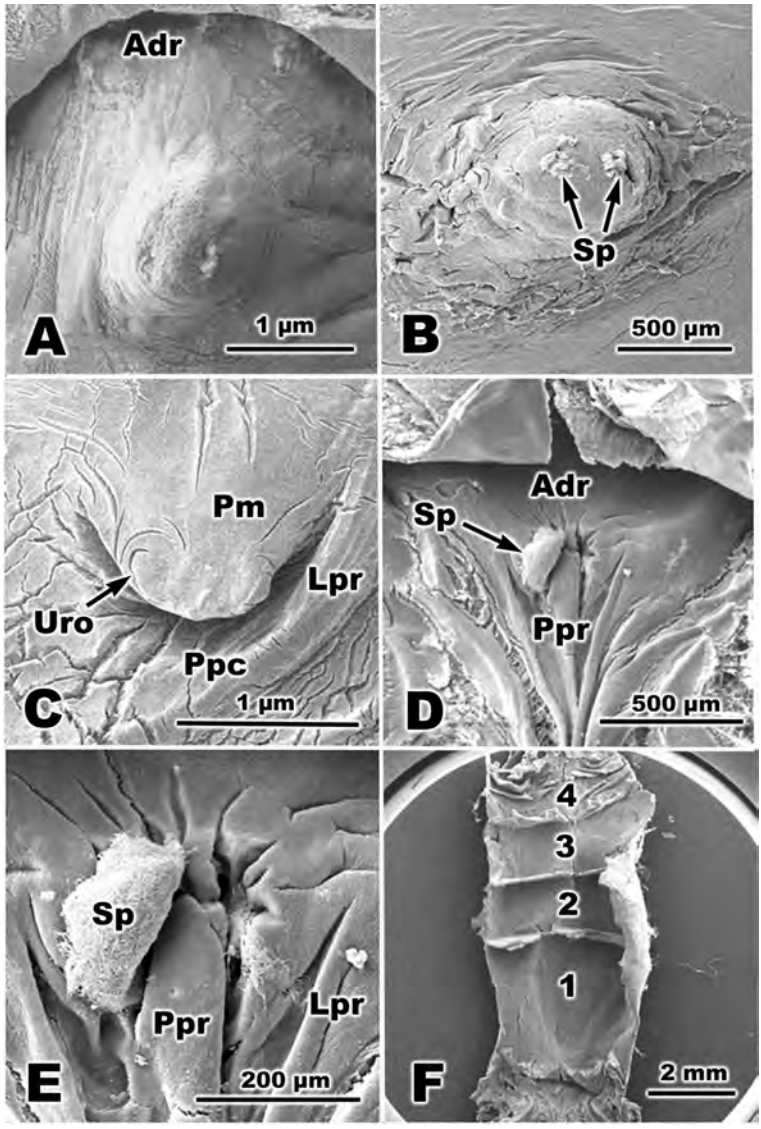

Fig. 10.36 Scanning electron micrographs of the urogenital papilla of representative North American male colubrine colubroid snakes. **A.** *Coluber constrictor latrunculus*, ventral view of circular papillary mound with orifices inconspicuous due to occlusion by sperm; anterior dorsal recess in background. **B.** *Coluber flagellum flagellum*, ventral view of papillary mound similar to A with sperm aggregates occluding orifices. **C.** *Coluber taeniatus*, ventral view of tongue-like papilla with posteriolateral orifices and deep posterior papillary recess. Left urogenital orifice (Uro) is indicated. **D-F.** *Diadophis punctatus arnyi*, ventral view of mostly flat, highly grooved papillary mound with large sperm aggregate occluding right orifice (E). An expansive anterior dorsal recess is evident in D. Coprodaeal chambers (see Fig. 10.20) in F, numbered 1-4, extend anteriorly from cloacal region (as viewed in D). Adr, anterior dorsal recess; Lpr, lateral papillary ridge; Pm, papillary mound; Ppc, posterior papillary recess; Ppr, posterior papillary ridge; Sp, sperm; Uro, urogenital orifice.

ridge on the left size. Recent taxonomic changes removed both *C. flagellum* and *C. taeniatus* from their former genus *Masticophis* (Utiger *et al.* 2005). The inclusion, however, of *M. taeniatus* into *Coluber* could be disputed based upon morphological homologies pertaining to the urogenital papilla among these similar species.

We found the simplest papillary mound in the urogenital papilla of *Diadophis punctatus arnyi* (Fig. 10.36D-F). The mound is not raised above a basal level. Several grooves radiate from the papillary orifices (Fig. 10.36E); these non-fleshy grooves, therefore, preclude the presence of well-defined circular or cup-shaped papillary lips as is the cases with many species in our sample. This species does, however, possess a relatively, large posterior papillary ridge that extends anteriorly through the midline of the mound to a point between the orifices and two lateral papillary ridges. We show the anatomical relationship among coprodaeal chambers and the urogenital papilla in this species (Fig. 10.36F; see also Fig. 10.20D,E).

In *Pantherophis obsoletus* (Fig. 10.37A-C), the urogenital papilla is a robust structure containing well-seated pits and grooves in the papillary summit, well-developed anterior and posterior papillary ridges, a posterior papillary recess, and two cup-shaped urogenital orifices. Anterior lateral ridges, which support the papillary mount, also occur; these prominent ridges are unique to this species.

Among the two xenodontine snakes examined (*Farancia abacura reinwardtii* and *Heterodon platirhinos*), we observed two distinct morphologies. For example, *F. abacura reinwardtii* is the only species among all snakes examined that possesses two distinct urogenital papillae and two distinct posterior papillary recesses (Fig. 10.37D-F). Reproductive and non-reproductive specimens provide contrasting, but congruent, micro-anatomies in this species. In the reproductive individual (Fig. 10.37D,E), no distinct papillary mound exists, but rather bulbous distal segments of the ampullary folds take the place of what should be typical papillary mounds. The folds are highly rugose and closely aligned beside one another. Grooved, fleshy lips bulge around distinctly separate orifices, and spermatozoa can be seen exuding from the left orifice (Fig. 10.37D). In the non-reproductive individual (Fig. 10.37F) the ampullary folds are not rugose, and the bulb-like expansions of the ampullary folds are regressed. In both specimens, the posterior papillary ridge can be seen penetrating far anteriorly and, thus, separating the ampullary folds into two distinct entities. In *H. platirhinos* (Fig. 10.38A), a single urogenital papilla exists. The ampullary folds merge into a single unit and provide support to the papillary mound. The papillary summit and its pair of orifices are not well differentiated in the micrograph.

Marked differences occur between two of the three *Lampropeltis* species (*L. calligaster* and *L. holbrooki*) with the third species (*L. triangulum*) examined (Fig. 10.38B-F). First, both *L. calligaster* and *L. holbrooki* exhibit highly grooved and oblong urogenital orifices, although individually distinct lips are not recognizable in *L. holbrooki*. The species differ from

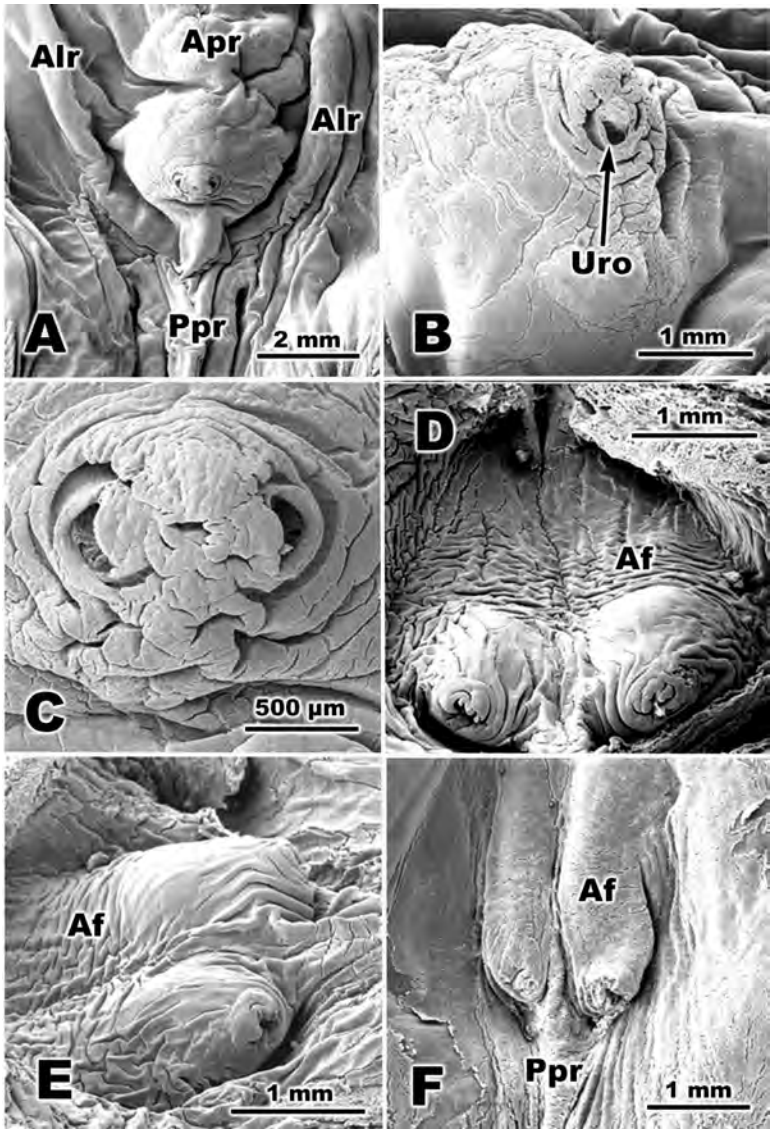

Fig. 10.37 Scanning electron micrographs of the urogenital papilla of representative North American male colubrine colubroid snakes. **A-C.** *Pantherophis obsoletus*, ventral view of pyramidal-shaped papilla with paired (cup-shaped) lateral orifices, well-developed anterior (Apr) and posterior papillary ridges (Ppr), and a small posterior papillary recess. Anterior lateral ridges (Alr) are well developed. Crescent-shaped grooves surround the urogenital orifices. **D-F.** *Farancia abacura reinwardtii*, ventral view of paired urogenital papillae exhibiting bulbous distal segments of the ampullary folds. Fleshy lips surround orifices which project posteriorly, and left orifice in D contains sperm. **E.** Right lateral view of distinct bulbous distal segments seen in D. **F.** Non-reproductive male shows deflated distal segments of papillary mounds (E), and the posterior papillary ridge extends anteriorly between individual papillae. Left and right ampullary folds are distinct. Af, ampullary fold; Alr, anterior lateral ridges; Apr, anterior papillary ridge; Ppc, posterior papillary recess; Ppr, posterior papillary ridge, Uro, urogenital orifice.

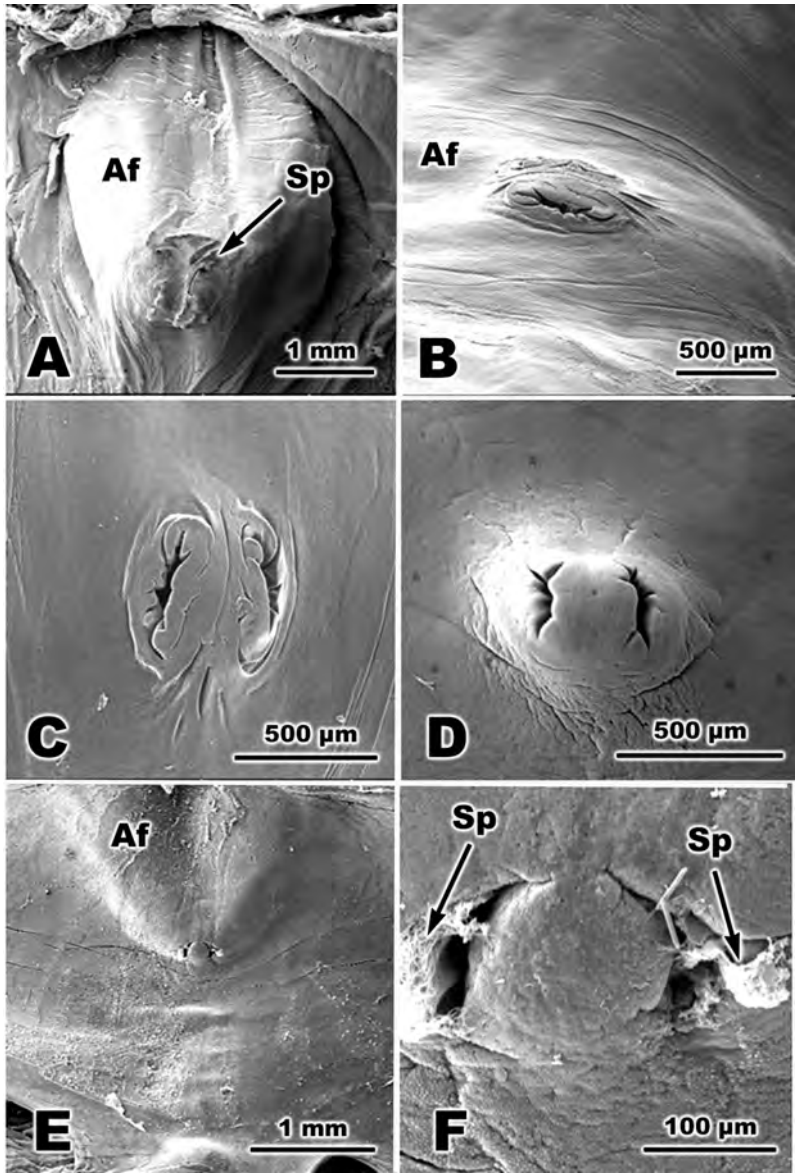

Fig. 10.38 Scanning electron micrographs of the urogenital papilla of representative North American male colubrine colubroid snakes. **A.** *Heterodon platirhinos*, ventral view showing greatly expanded anterior ampullary folds; urogenital orifices mostly obscured and/or occluded by sperm masses. **B-C.** *Lampropeltis calligaster*, right ventrolateral view (B) and ventral view (C) of papillary mound (possibly in a regressed condition?) showing pair of large, grooved, fleshy-lipped orifices. **D.** *Lampropeltis holbrooki*, ventral view of small, nipple-like papilla with pair of large, highly grooved orifices. **E-F.** *Lampropeltis triangulum syspila*, ventral view of papillary region showing no individual papillary mound (E); elevated ampullary folds are evident; F shows crescent-shaped orifices (filled with sperm) separated by a small tissue partition. Af, ampullary fold; Sp, sperm.

one another, however, by the presence of a well-defined, circular papillary mound, which *L. holbrooki* possesses (Fig. 10.38D) and *L. calligaster* generally lacks (Fig. 10.38B,C). The major difference between these two species and *L. triangulum* is the lack of grooved lips within the latter. In *L. triangulum*, the urogenital orifices are also roughly C-shaped slits, and they possess a prominent spherical partition between them (Fig. 10.38F). This microstructure is not a papillary mound nor is it papilla-like in configuration. Broad ampullary folds are distinctive in *L. triangulum*, but are generally absent in the other two species. All three species lack ridge attachments to the papillary mound (or just the papillary lips) as well as any vestige of a posterior papillary recess.

The natricine watersnakes (Figs 10.39; 10.40A,B) exhibit an array of synapomorphic character states that they share with conspecifics, but at the same time, they also possess distinctive features of their urogenital papillae that are found in other snakes. For instance, four of five species of *Nerodia* (*N. erythrogaster, N. fasciata, N. rhombifer,* and *N. sipedon*) examined possess the following morphologies: 1) the presence of a papillary mound with concentric papillary grooves; 2), the presence of grooved, fleshy papillary lips, and 3) the presence of conspicuous posterior and/or lateral papillary ridges. One synapomorphic character, the presence of a distinctive medial papillary prominence consisting of minute tissue spheres (best observed in Fig. 10.39D, F), is shared by at least *N. rhombifer* and *N. sipedon*. Otherwise, all features mentioned above, except for number 2, are absent from the urogenital papilla of a fifth species of watersnake, *N. cyclopion* (Fig. 10.40B). Alfaro and Arnold (2001) placed *N. cyclopion* and the closely related Florida Green Watersnake (*N. floridana*) in paraphyly with all other *Nerodia.* Our micro-anatomical data, therefore, lends support to their phylogeny of thamnophiine snakes.

Several snake species represent a morphological assortment of character states previously mentioned, and some add unique features of their own to the urogenital papilla micro-anatomy. For example, the urogenital papilla of *Opheodrys aestivus* (Fig. 10.40C,D) exhibits circular urogenital orifices along with smooth, enlarged and elevated, non-grooved lips. The circular orifices are unique to this species. In addition, the lateral papillary ridges are enlarged in this species and, apparently, exclude the development of a posterior papillary ridge. In *Pituophis catenifer sayi*, however, all three posterior ridges are approximately of equal width as they lead away from the papillary mound (Fig. 10.40E). *Pituophis c. sayi* also has a pronounced medial papillary prominence between fleshy, grooved orifices, although the prominence lacks the tissue configuration described earlier for the two *Nerodia* species. Finally, the anterior ampullary folds in *O. aestivus* are somewhat similar to the condition found in *Rhinocheilus lecontei* (Fig. 10.40F).

A morphological disparity exists between the urogenital papillae of two species of *Regina* (Fig. 10.41A,B). In *R. septemvittata*, the orifices are grooved, half-moon shaped openings that lie to the side of the papillary mound.

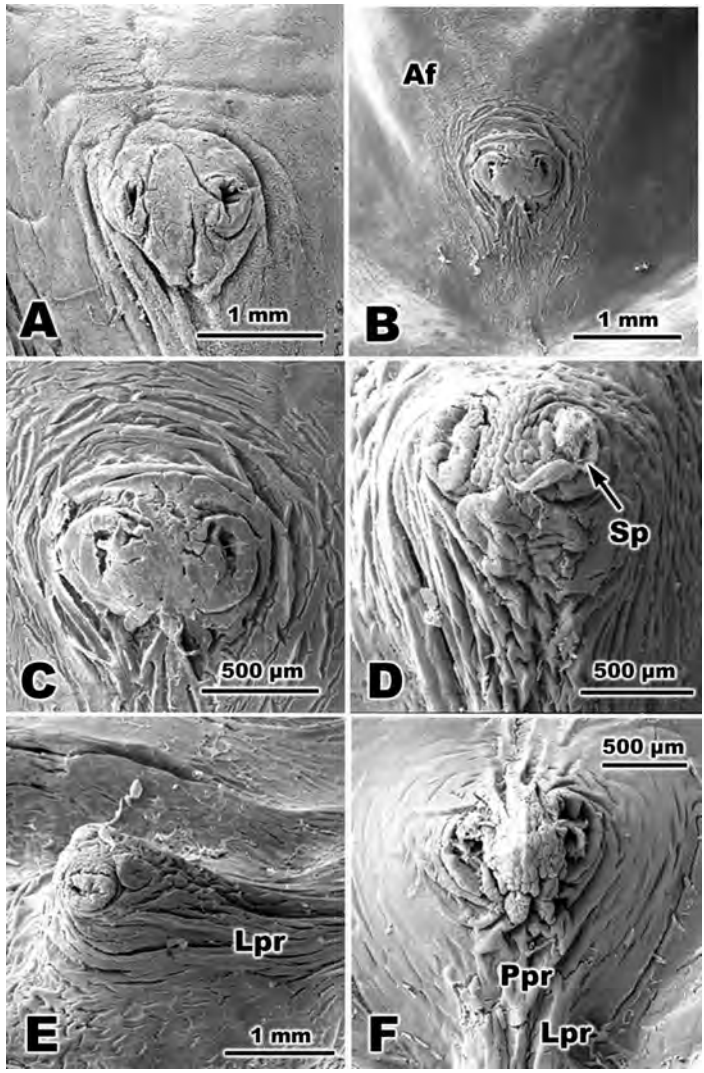

Fig. 10.39 Scanning electron micrographs of the urogenital papilla of representative North American male natricine colubroid snakes**. A.** *Nerodia erythrogaster flavigaster*, ventral view of oblong, smooth papillary mound revealing widely spaced, grooved, fleshy-lipped orifices; a shallow posterior papillary recess is present. **B-C.** *Nerodia fasciata confluens,* ventral view similar to A, but showing instead a circular papillary mound. Ventally directed, paired orifices possess robust lips separated by midventral tissue tuffs (C). Circular grooves surround entire mound, with the exception of the region occupied by the posterior papillary ridge. **D-E.** *Nerodia rhombifer rhombifer*, ventral view of papillary mound characterized by a midventral longitudinal series of 6-8 rows of minute tissue tuffs; fleshy-lipped orifices point ventrally. Sperm mass occludes left orifice (D); right ventrolateral view of D showing lateral papillary ridges extending posteriorly; no posterior papillary ridge present. **F.** *Nerodia sipedon pleuralis* (see also Fig. 10.30A), ventral view showing very similar micro-anatomy as found in D, except that a posterior papillary ridge is present and flanked by lateral papillary ridges. Af, ampullary fold; Lpr, lateral papillary ridge; Ppr, posterior papillary ridge; Sp, sperm.

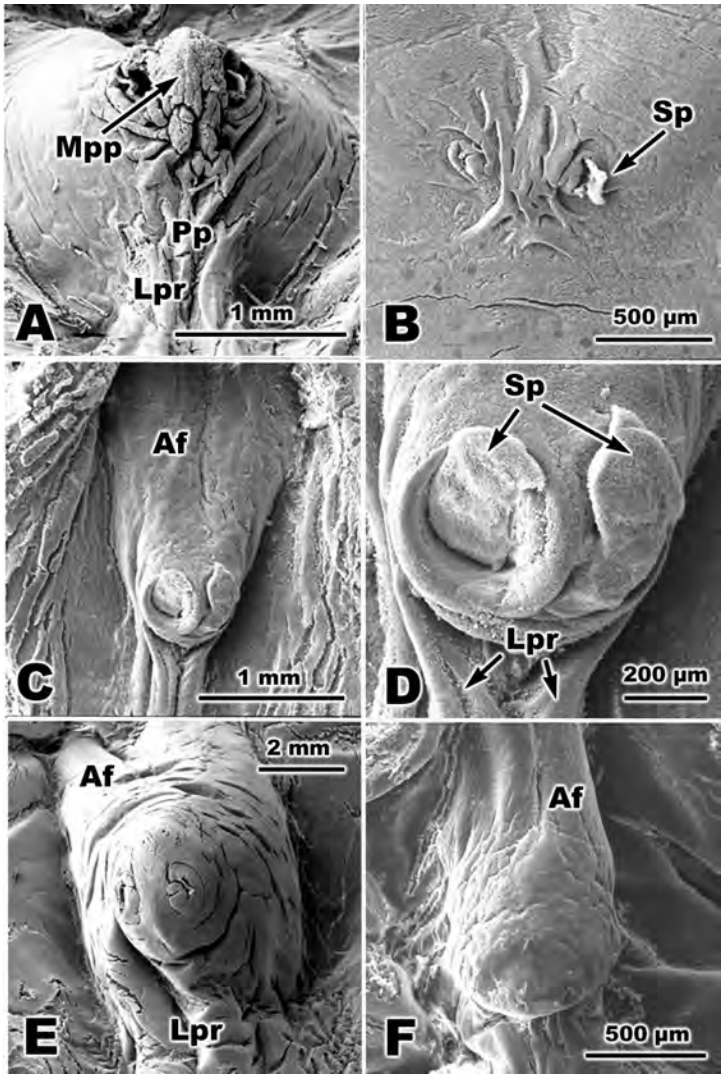

Fig. 10.40 Scanning electron micrographs of the urogenital papilla of representative North American male natricine and colubrine colubroid snakes. **A.** *Nerodia sipedon* (same specimen as Fig. 10.29F), postereoventral view showing elevated position of the midventral rows of papillary tissue tuffs extending beyond the papillary mound; posterior papillary ridge reduced in size and flanked by lateral papillary ridges. Medial papillary prominence (Mpp) exhibiting minute tissue spheres. **B.** *Nerodia cyclopion*, ventral view of flattened mound with no anterior or posterior papillary ridges; midventral tissue tuffs absent; sperm mass resides at mouth of left orifice. **C-D.** *Opheodrys aestivus*, ventral view of papilla (C) showing circular orifices occluded with sperm and fleshy, non-grooved lips; posterior papillary ridge well developed; a small posterior papillary recess present. **E.** *Pituophis catenifer sayi*, ventral view of papillary mound exhibiting fleshy-lipped, crescent-shaped orifices; a small posterior papillary recess present. A well-developed posterior papillary ridge is flanked by lateral papillary ridges. **F.** *Rhinocheilus lecontei*, ventral view of papillary mound with occluded orifices. Af, ampullary fold; Lpr, lateral papillary ridge; Mpp, medial papillary prominence; Pp, papillary prominence; Sp, sperm.

The papillary mound is well supported by all three posterior papillary ridges. In addition, this species has a deep posterior papillary recess and a broad medial papillary prominence. In contrast, *R. grahamii* exhibits posterior-projecting orifices, a narrow medial papillary prominence, and lacks a papillary mound and posterior ridge components. The two species share other features such as grooved ampullary folds, a deep posterior papillary recess, and fleshy lips. Alfaro and Arnold (2001) found these two species to be closely related, whereas the differing papillary morphologies we found in these two species remain equivocal and require further study.

Two colubrine species possessed strikingly different papillary micro-anatomies compared to all other species examined. The papillary mound of *Salvadora grahamiae* (Fig. 10.41C) appears as a tall, laterally compressed pyramid with minute urogenital orifices residing atop a narrow papillary summit. The papillary mound lacks grooves. The ampullary folds project ventrally in the form of distinct ridges. The posterior papillary ridge is absent; instead, the two lateral papillary ridges stand as tall, narrow sheets of tissue. *Sonora semiannulata* (Fig. 10.41D-F) exhibits a conical, slightly grooved, papillary mound that projects posterioventrally. A smooth, pointed, knob-like medial papillary prominence characterizes the papillary summit. The orifices open laterally as distinctive slit-like configurations located at the base of the prominence. No conspicuous posterior ridges and no posterior papillary recess are evident. Well-developed ampullary folds are present in this individual, which was in active reproductive condition.

Two small, closely related, thamnophiine species, *Storeria dekayi wrightorum* and *S. o. occipitomaculata*, share several papillary traits, and, at the same time have features conspicuously different from one another (Fig. 10.42A-D). The grooved, oblong, fleshy-lipped urogenital orifices of both species are clearly similar to the lips of natricine species (Figs. 10.39; 10.40), their allied thamnophiines (Alfaro and Arnold 2001). Both species also exhibit grooved walls in their papillary mounds. Circular grooves exist in *S. d. wrightorum*, whereas mostly diagonal ones are found in *S. o. occipitomaculata*. Both species also exhibit small posterior papillary recesses as well as posterior papillary ridges, although *S. o. occipitomaculata* appears to lack lateral papillary ridges or all three posterior ridges are fused into one structure. The two species differ, however, in the construction of their papillary mounds. *Storeria d. wrightorum* exhibits a somewhat laterally compressed mound base that appears linear in relation to the ampullary folds and the posterior papillary ridges. On the other hand, *S. o. occipitomaculata* possesses a widened, flaring papillary base, which is particularly evident in Fig. 10.42C.

The smallest colubrine species examined, *Tantilla gracilis*, exhibits a disproportionally large urogenital papilla in comparison to its anterior dorsal recess (Fig. 10.42E,F). This species also exhibits a slightly enlarged medial papillary prominence which separates two slit-like orifices on its papillary summit. The base of the papillary mound is circular; lateral papillary ridges provide support to the papillary mound.

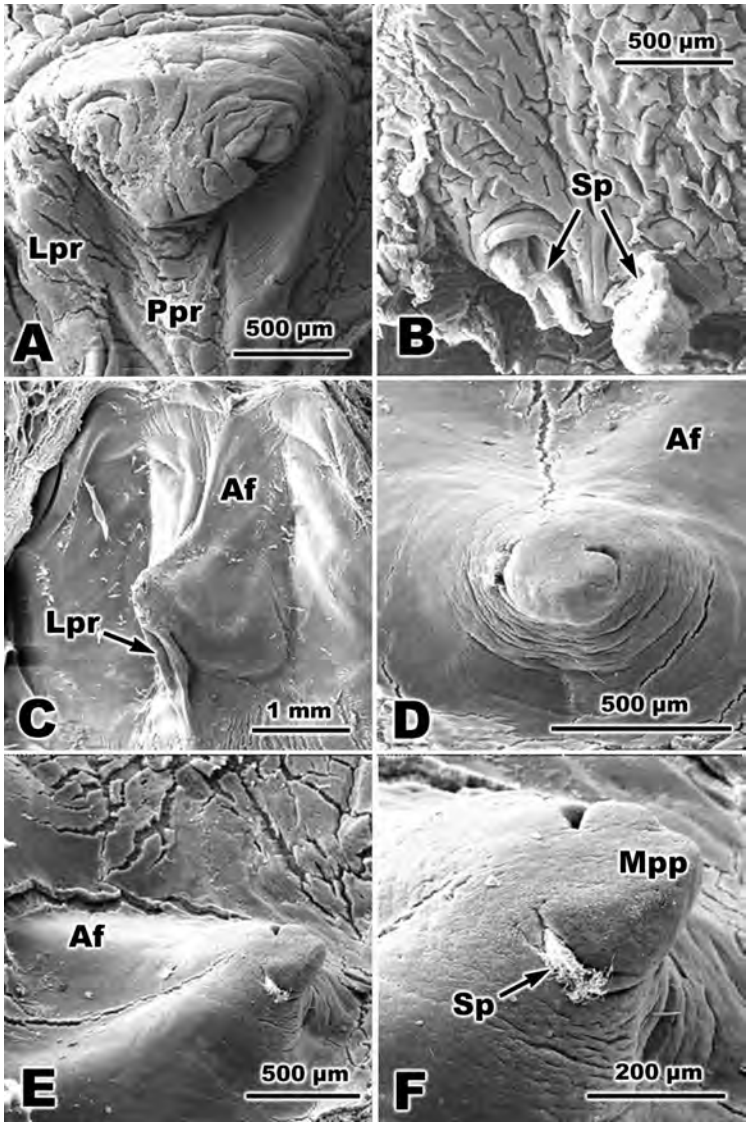

Fig. 10.41 Scanning electron micrographs of the urogenital papilla of representative North American male colubrine colubroid snakes. **A.** *Regina septemvittata*, ventral view of papillary mound characterized by several surface grooves and indentations between posteriolaterally directed orifices. A well-developed posterior papillary recess, posterior papillary ridge, and paired lateral papillary ridges are present. **B.** *Regina grahamii*, ventral view of paired, fleshy-lipped orifices full of sperm; papillary mound flat with highly grooved and pleated surface. C. *Salvadora grahamiae,* left ventrolateral view of tall laterally compressed papilla well supported by anterior and posterior papillary ridges. **D-F**. *Sonora semiannulata*, ventral view of conical papilla containing a fleshy medial papillary prominence; laterally directed, paired orifices with non-fleshy lips are present; sperm are existing right orifice; no anterior or posterior papillary ridges present. Af, ampullary fold; Lpr, lateral papillary ridge; Mpp, medial papillary prominence; Ppr, posterior papillary ridge; Sp, sperm.

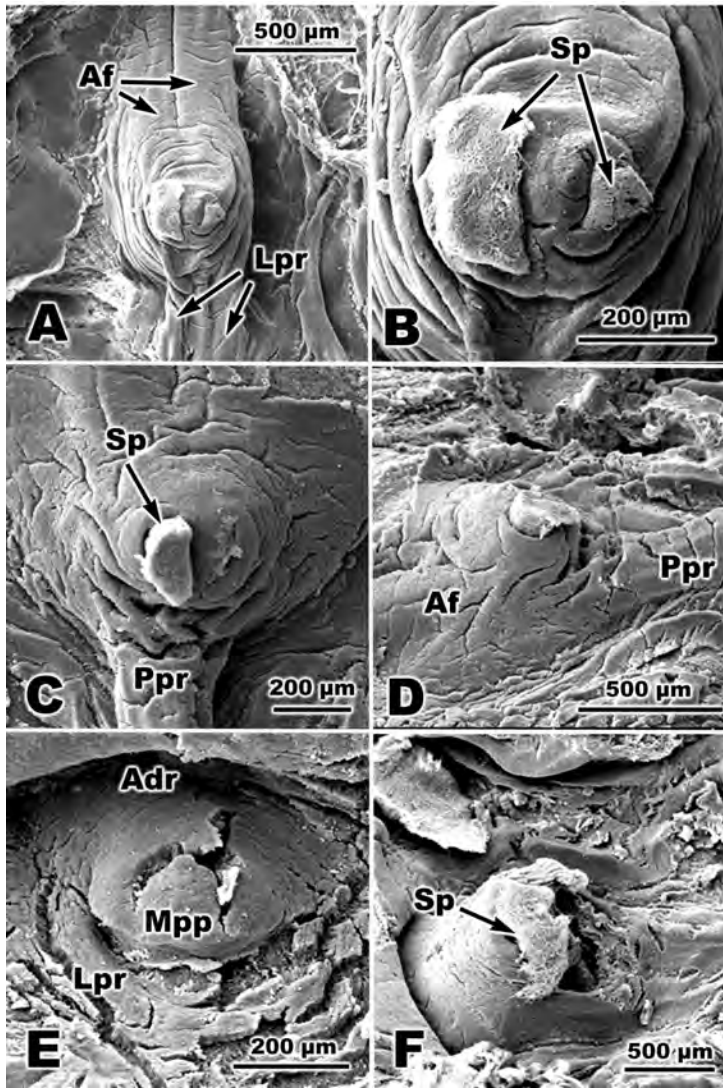

Fig. 10.42 Scanning electron micrographs of the urogenital papilla of representative North American male colubrine colubroid snakes. **A-B.** *Storeria dekayi wrightorum*, ventral view of papilla featuring a laterally compressed papillary mound with large, fleshy-lipped, cup-shaped orifices occluded by sperm masses; posterior papillary recess small; posterior and lateral papillary ridges present. Several circular grooves surround papillary summit. **C-D.** *Storeria occipitomaculata occipitomaculata*, ventral view of papillary summit (C); mound conical with orifices similar to anatomy found in A-B. Right ventrolateral view (D) of single, large posterior papillary ridge; posterior papillary recess small. **E-F.** *Tantilla gracilis*, posteriolateral view of small conical, papillary mound with two slit-like orifices with no fleshy lips (E). Right ventrolateral view (F) of different individual from one shown in E revealing papilla in close proximity to anterior dorsal recess (Adr). Sperm fill the orifices. Papillae of both E and F lack circular grooves. Adr, anterior dorsal recess; Af, ampullary fold; Lpr, lateral papillary ridge; Mpp, medial papillary prominence; Ppr, posterior papillary ridge; Sp, sperm.

Four thamnophiine species (two large-bodied: *Thamnophis proximus proximus* and *T. sirtalis sirtalis* and two diminutive species: *Virginia striatula* and *V. valeriae*) provide additional papillary peculiarities. Although both *T. p. proximus* and *T. s. sirtalis* (Fig. 10.43A,B) exhibit fleshy-lipped orifices as is found among other related species mentioned above, the papillary mound is prominent in *T. p. proximus* and it is nearly non-existent in *T. s. sirtalis*. Both species also exhibit numerous grooves and depressions within their papillary structures, but *T. s. sirtalis* has the most furrowed ampullary folds of all species examined. In addition, this species has dramatically shortened lateral papillary ridges, a very narrow posterior papillary ridge, and a posterior papillary recess.

Distinctive papillary morphologies are found in the two species of *Virginia*. A most peculiar inverted bowl-like papillary base supports a small, circular, recessed papillary mound in *V. striatula* (Fig. 10.43C,D). Extremely large, irregular, cup-shaped and fleshy-lipped orifices dominate the surface of its papillary summit. On either side of the mound are tall posterior papillary ridges that attach firmly to the oval papillary base and not to the papillary mound, *per se*. In addition, two short anterior papillary ridges attach directly to the papillary summit and extend anteriorly for a short distance (Fig. 10.43D). The oval papillary base, indeed, represents an extreme morphology for the paired ampullary folds, which in this specimen, are undoubtedly filled with sperm. Finally, the micro-structure of the urogenital papilla in *V. valeriae* is similar to that of *V. striatula*, except for the lack of well-developed fleshy lips surrounding the orifices. Both species exhibit posterior papillary recesses, although this region is regressed in *V. valeriae* even though both are reproductive individuals. These two species exhibit the most extreme variation in papillary micro-anatomy compared to the basic urogenital papilla morphology shown in Fig. 10.32.

10.5 CONCLUSIONS AND DIRECTIONS FOR FUTURE RESEARCH

The only reproductive tract characters that have been coded for use in recent phylogenetic analyses concern morphology of sperm, hemipenes, and/or cloacal glands (Jamieson 1995; Oliver *et al.* 1996; Young *et al.* 1999; Lee 2000; Sánchez-Martínez 2007). The only broadly based comparative study of the accessory duct system of squamates is that of Dufaure and Saint Girons (1984) who examined histology of the epididymides of 89 species of squamates, representing 72 genera and 18 families, including 25 species of snakes. They found 5 types of secretory activity in the main duct of the epididymis. Type 1 consists of large secretory granules with a chromophilic central core surrounded by a chromophobic vacuole, and this type characterizes the Lacertidae. Types 2-4 show decreasing size and density of secretory products, and Type 5 demonstrates no secretory activity (Table 10.2). Interestingly, type 5 characterizes all snakes that were examined. Dufaure and Saint Girons (1984) noted that differences especially between types 3 and 4 are not considerable, and that electron

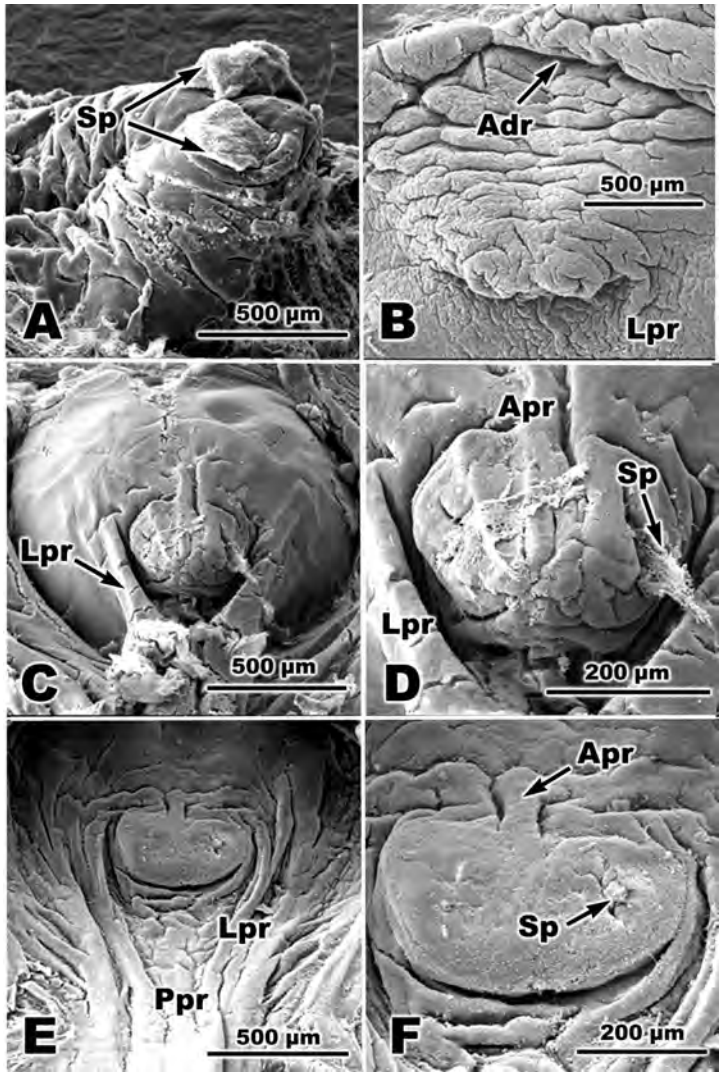

Fig. 10.43 Scanning electron micrographs of the urogenital papilla of representative North American male thamnophiine colubroid snakes. **A.** *Thamnophis proximus proximus*, right ventrolateral view of papillary mound with smooth, fleshy-lipped orifices filled with sperm. Numerous circular papillary grooves surround papilla. **B.** *Thamnophis sirtalis sirtalis*, ventral view of papillary mound exhibiting numerous transverse folds and ridges; anterior dorsal recess conspicuous. Orifices with fleshy lips and are cup-shaped in appearance. **C-D.** *Virginia striatula*, ventral view of papillary mound which is recessed into a cavity between the large lateral papillary ridges and resides atop bulbous basilar region. Two small, anterior papillary ridges are attached to papillary mound (C). Higher magnification of C in D reveals fleshy-lipped and grooved orifices exuding sperm. **E-F.** *Virginia valeriae*, ventral view of papillary mound similar to that found in C, but no bulbous basilar region. Flat, hemispheric papillary summit with two groove-lipped orifices. Large lateral papillary ridges present; single anterior papillary ridge; posterior papillary recess large. Sperm are exiting left orifice. Adr, anterior dorsal recess; Apr, anterior papillary ridge; Lpr, lateral papillary ridge; Ppr, posterior papillary ridge; Sp, sperm.

Table 10.2 States of secretory activity in the epididymides of squamates as described by Dufaure and Saint Girons (1984). They described 5 "Types" and an intermediate stage, which are coded as 6 different character states.

Character State	*Families*	*Description*
1 (Type 1)	Lacertidae	numerous large vacuoles 10-12 μm dia with a central dense core
2 (Type 2)	Agamidae	clusters of apical dense granules 1 μm dia
3 (Type 3)	Iguanidae, some Gekkonidae	finer granules than Type 2 and not clustered
4 (Intermediate)	Anguidae, Amphisbaenidae	in between Types 3 and 4, granulation apparent in dense cytoplasm
5 (Type 4)	Chameleonidae, Iguanidae, Teiidae, Polychrotidae, Scincidae, some Gekkonidae	granules not distinct but cytoplasm dense and heterogeneous; secretory product in lumen
6 (Type 5)	Serpentes	secretory activity completely absent

microscopy is needed to fully resolve the differences in secretory activity in the epididymis among squamates.

When mapped upon a phylogeny from Lee (2005) based upon morphology and a phylogeny from Vidal and Hedges (2005) inferred from nine nuclear protein-coding genes, the results are shown on the cladograms illustrated in Fig. 10.44. Relationships shown among taxa are limited to those groups examined by Dufaure and Saint Girons (1984). Despite the differences in the morphological and molecular phyletic hypotheses, the mapping results are consistent in the two cladograms. The ancestral state is 5 (Type 4), a state in which secretory granules are not present but the cytoplasm appears active as it is dense and heterogenous. Dufaure and Saint Girons (1984) also indicate that even when secretory granules are not present, some secretory product appears associated with sperm in the lumen of the epididymis, and this may have come from the epididymal epithelium. The most interesting conclusion, however, is that snakes lost all secretory activity whereas lizards either retained the ancestral condition or evolved increased secretory activity. Thus, basal snakes went in a different evolutionary direction from lizards.

The interesting question that follows is why this variation in secretory activity exists. The occurrence of an epididymis as a sperm conduit between the testis and ductus deferens is most parsimoniously considered an ancestral character for amniotes (or else it independently evolved numerous times). Thus, the epididymis is a very ancient character that has been evolving separately in major clades for hundreds of millions of years. We know that some functional differences occur in the epididymides of these groups (for example, in mammals the epididymis is the site for sperm storage and maturation whereas in squamates the ductus deferens is the major sperm storage area), but much of the basic anatomy seems to

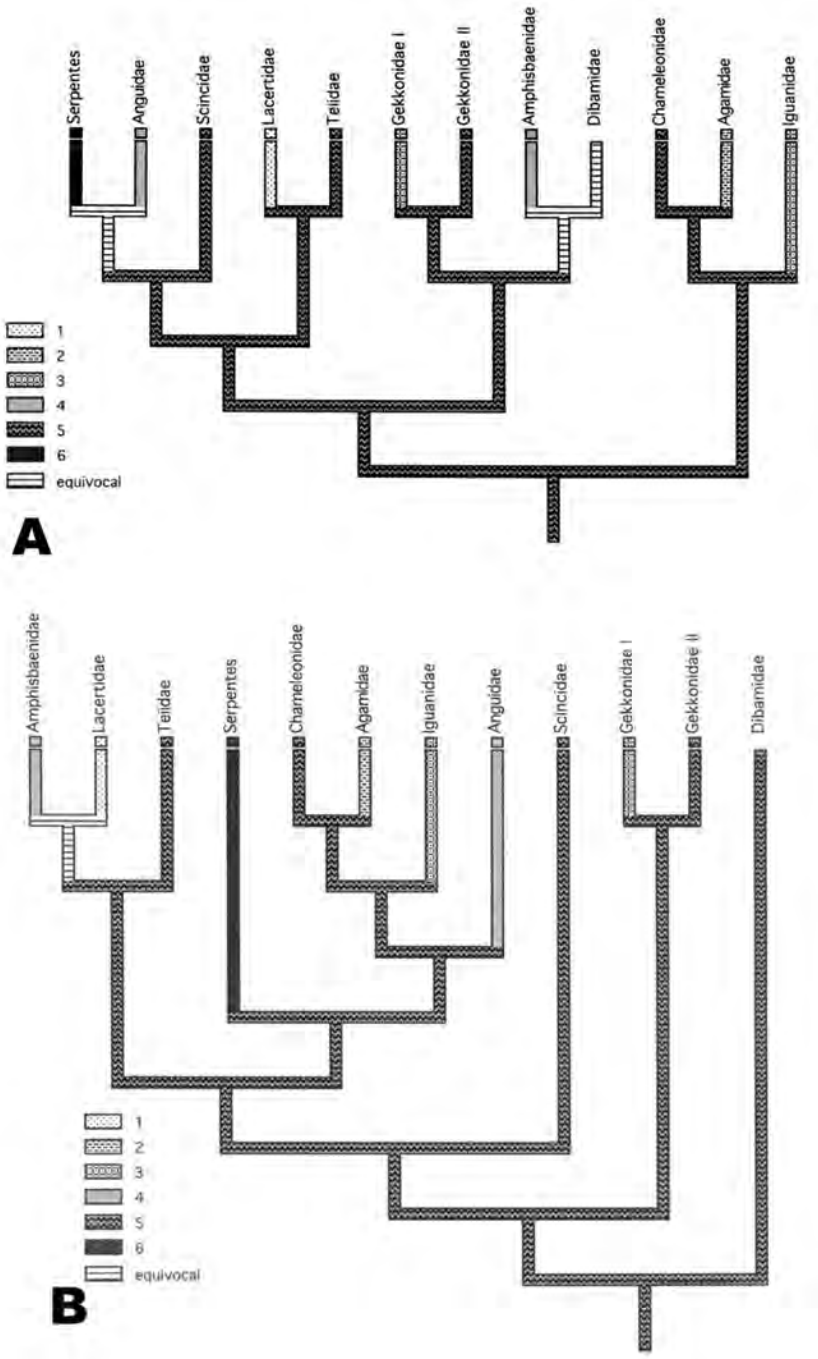

Fig. 10.44 Epididymal secretions from most copious (1) to none (6) based upon data from Dufaure and Saint Girons (1984) and mapped on phyletic hypotheses using McClade version 4.1. **A.** A phyletic hypothesis based upon morphological characters from Lee (2005). **B.** A phyletic hypothesis based upon molecular characters by Vidal and Hedges (2005).

be conserved. If the epididymal secretions in some lizards play a role in formation of the seminal fluid, capacitation of sperm, etc., those functions must occur elsewhere in snakes.

As noted here and by Sever (2010), however, secretory activity is apparent in the two snakes, *Seminatrix pygaea* and *Agkistrodon piscivorus*, in which the ductus epididymis has been examined by electron microscopy. *Seminatrix pygaea* and *A. piscivorus* possess a constitutive secretory pathway, similar to that of the proximal efferent ducts of mammals (Hoffer *et al.* 1973), in which the product is transported to the surface in small vesicles that Dufaure and Saint Girons (1984) would not have observed with light microscopy. Thus, the product is not concentrated or stored in granules while waiting for a neural or hormonal stimulus, but released as it is produced. In the case of *S. pygaea*, production seems to be year-around, although somewhat reduced in the summer. The product is both PAS positive and bromphenol blue positive, and therefore contains glycoprotein.

Studies on lizards demonstrate that secretions of the epididymis may contain lipid (Haider 1987), proteins (Depeiges and Dufaure 1980), and/or glycoproteins (Manimekalai and Akbarsha 1992). Labate *et al.* (1997) found a variety of glycoconjugates using lectin histochemistry in the ductuli efferentes of the European Wall Lizard (*Podarcis sicula*), and the binding pattern varied seasonally. In the same species, Desantis *et al.* (2002) found that secretory cells along the length of the epididymis have 12 lectins binding to the secretions, with some regionalization. Although the function of the glycoconjugates in the epididymal secretory granules was not determined, perhaps they produce an environment for sperm storage and/or maturation, as known in mammals (Acott and Hoskins 1981).

We have examined the male urogenital ducts and cloacae of only a small subset of the 2800+ extant species of snakes. We do not currently have enough comparative material to enable hypotheses of ancestral and derived traits of the squamate reproductive tract and the use of such data in phylogenetic analyses. The primary direction for future research is obvious: examine more species from a wide range of taxa with special attention to cytological variation and secretory activity of the reproductive ducts. Then, the challenge is to place these data in a phylogenetic context.

Our conclusions, therefore, at this time are modest. (1) The proximal testicular ducts in snakes are probably similar in structure and function to those of other amniotes. We need to look for regionalization of cell types and functions in the ductus epididymis, as well known in mammals and reported in some lizards. (2) The ductus deferens stores sperm in snakes, but how long sperm can remain viable is unknown. Also, secretory activity of the ductus deferens varies among the species examined so far, and the significance of this variation needs resolution. (3) Colubrines examined so far possess an ampulla urogenital papilla, whereas viperids have an ampulla ureter. We need to discover whether these differences are consistent in other taxa in these groups and discern the ancestral condition

for Serpentes, including the examination of non-colubroid snakes. (4) The urogenital papilla shows wide variation among the taxa examined so far. Some of this variation is concordant with phylogenetic hypotheses for these groups, but again, snakes from more basal taxa require examination.

10.6 ACKNOWLEDGMENTS

DMS acknowledges with much appreciation support from National Science Foundation grant DEB-0809831. We also thank Layla Freeborn and Justin Rheubert for their input into this manuscript. SET sincerely thanks the many snake collectors, especially Richard Baxter, Matt Connior, Richard F. Hoyer, Phillip Jordan, Chris T. McAllister, Jonathan Stanley, and Benjamin Wheeler, who provided live specimens. Megan Bundy is thanked for the line drawings in Figs. 10.20 and 10.28. Kevin Gribbins is appreciated for his insightful advice during the early preparation of this manuscript. Finally, we thank Barrie G. M. Jamieson and Dustin S. Siegel for their critical reviews of the chapter.

10.7 LITERATURE CITED

Acott, T. S. and Hoskins, D. D. 1981. Bovine sperm forward motility protein: binding to epididymal spermatozoa. Biology of Reproduction 24: 234-240.

Aire, T. A. 2007. Anatomy of the testis and male reproductive tract. Pp. 37-113. In Jamieson, B. G. M. (ed.), *Reproductive Biology and Phylogeny of Birds*, Vol. 6A. Science Publishers, Enfield, New Hampshire.

Akbarsha, M. A. and Meeran, M. M. 1995. Occurrence of ampulla in the ductus deferens of the Indian garden lizard *Calotes versicolor* Daudin. Journal of Morphology 225: 261-268.

Akbarsha, M. A., Kadalmani, B. and Tamilarasan, V. 2007. Efferent ductules of the fan-throated lizard *Sitana ponticeriana* Cuvier; light and transmission electron microscopy study. Acta Zoologica (Stockholm) 88: 265-274.

Akbarsha, M. A., Tamilarasan, V., Kadalmani, B. and Daisy, P. 2005. Ultrastructural evidence for secretion the epithelium of ampulla ductus deferentis of the Fan-Throated Lizard, *Sitana ponticeriana* Cuvier. Journal of Morphology 266: 94-111.

Alfaro, M. E. and Arnold, S. J. 2001. Molecular systematics and evolution of *Regina* and the thamnophiine snakes. Molecular Phylogenetics and Evolution 21: 408-423.

Bellairs, A. 1970. *The Life of Reptiles*. Volumes 1 and 2. Universe Books, New York. Pp. 590.

Bergerson, W., Amselgruber, W., Sinowatz, F. and Bergerson, M. 1994. Morphological evidence of sperm maturation in the ampulla ductus deferentis of the bull. Cell and Tissue Research 275: 537-541.

Cooper, T. G. and Hamilton, D. W. 1977. Phagocytosis of spermatozoa in the terminal region and gland of the vas deferens of the rat. American Journal of Anatomy 150: 247-268.

Depeiges, A. and Dufaure, J. P. 1980. Major proteins secreted by the epididymis of *Lacerta vivipara*. Isolation and characterization by electrophoresis of the central core. Biochimica et Biophysica Acta 628: 109-115.

Desantis, S., Labate, M., Labate, G. M. and Cirillo, F. 2002. Evidence of regional differences in the lectin histochemistry along the ductus epididymis of the lizard, *Podarcis sicula* Raf. Histochemical Journal 34: 123-130.

Dufaure, J. and Saint Girons, H. 1984. Histologie compare de l'epididyme et de ses secretions chez les reptiles (lezards et serpents). Archives d'anatomie microscopique et de morphologie expérimentale 73 : 15-26.

Fox, H. 1977. The urinogenital system of reptiles. Pp. 1-157. In Gans, C. and Parsons, T. S. (eds), *Biology of the Reptilia*, Vol. 6. Academic Press, New York.

Fox, W. 1952. Seasonal variation in the male reproductive system of Pacific coast garter snakes. Journal of Morphology 90: 481-553.

Fox, W. 1965. A comparison of the male urogenital systems of blind snakes, Leptotyphlopidae and Typhlopidae. Herpetologica 21: 241-256.

Gabe, M. and Saint Girons, H. 1965. Contribution à la morphologie comparée du cloaque et des glandes épidermoïdes de la region cloacale chez les lépidosauriens. Mémoires du Muséum National d'Histoire Naturelle. Séries A Zoologie 33: 149-292.

Gribbins, K. M., Happ, C. S. and Sever, D. M. 2005. Ultrastructure of the reproductive system of the black swamp snake (*Seminatrix pygaea*). V. The temporal germ cell development of the testis. Acta Zoologica (Stockholm) 86: 223-230.

Guerrero, S. M., Calderón, M. L., Pérez, G. R. and Pinilla, M. P. R. 2004. Morphology of the male reproductive duct system of *Caiman crocodiles* (Crocodylia, Alligatoridae). Annals of Anatomy 186: 235-245.

Haider, S. and Rai, U. 1987. Epididymis of the Indian wall lizard (*Hemidactylus flaviviridis*) during the sexual cycle and in response to mammalian pituitary gonadotropins and testosterone. Journal of Morphology 191: 151-160.

Hess, R. A. 2002. The efferent ductules: structure and functions. Pp. 49-80. In Robaire, B. and Hinton, B. T. (eds), *The Epididymis: From Molecules to Clinical Practice*. Kluwer Academic/Plenum Press, New York.

Hoffer, A. P., Hamilton, D. W. and Fawcett, D. W. 1973. The ultrastructure of the principal cells and intraepithelial leuckocytes in the initial segment of the rat epididymis. Anatomical Record 175: 169-202.

Holmes, H. J. and Gist, D. H. 2004. Excurrent duct system of the male turtle *Chrysemys picta*. Journal of Morphology 261: 312-322.

Jamieson, B. G. M. 1995. The ultrastructure of spermatozoa of the Squamata (Reptilia) with phylogenetic considerations. Pp. 359-383. In Jamieson, B. G. M., Ausio, J. and Justin, J.-L. (eds), *Advances in Spermatozoal Phylogeny and Taxonomy.* Mémoires du Muséum national d'Histoire Naturelle 166, Paris.

Jones, R. C. 1998. Evolution of the vertebrate epididymis. Journal of Reproduction and Fertilization Supplement 53: 163-181.

Labate, M., Desantis, S. and Corriero, A. 1997. Glycoconjugates during the annual sexual cycle in lizard epididymal ductuli efferentes: a histochemical study. European Journal of Histochemistry 41: 47-56.

Lee, M. S. 2000. Soft anatomy, diffuse homoplasy, and the relationships of lizards and snakes. Zoologica Scripta 29: 101-130.

Lee, M. S. Y. 2005. Squamate phylogeny, taxon sampling, and data congruence. Organisms, Diversity & Evolution 5: 25-45.

Lombardi, J. 1998. *Comparative Vertebrate Reproduction*. Kluwer Academic Publishers, Boston, Massachusetts. Pp. 469.

Manimekalai, M. and Akbarsha, M. A. 1992. Secretion of glycoprotein granules in the epididymis of the agamid lizard *Calotes versicolor* (Daudin) is region-specific. Biology of Structural Morphogenesis 4: 96-101.

Martin Saint Ange, G.-J. 1854. Étude de l'appariel reproducteur dans les cinq classes d'animaux vertébrés, au point de vue anatomique, physiolgique et zoologique. J.-B. Balliére, Libraire de l'Académe Impériale de Médecine, Paris. Pp. 234.

Oliver, S. C., Jamieson, B. G. M. and Scheltinga, D. M. 1966. The ultrastructure of spermatozoa of Squamata. II. Agamidae, Varanidae, Colubridae, Elapidae, and Boidae (Reptilia). Herpetologica 52: 216-241.

Riva, A., Testa-Riva, F., Usai, E. and Cossu, M. 1982. The ampulla ductus deferentis in man, as viewed by SEM and TEM. Archives of Andrology 8: 157-164.

Sánchez-Martínez, P. M., Ramirez-Pinilla, M. P. and Miranda-Esquivel, D. R. 2007. Comparative histology of the vaginal-cloacal region in Squamata and its phylogenetic implications. Acta Zoologica (Stockholm) 88: 289-307.

Seshardi, C. 1959. Structural modification of the cloaca of *Lycodon aulicus aulicus,* Linn., in relation to urine excretion and the presence of sexual segment in the kidney of male. Proceedings of the National Institute of Science of India B 25: B: 271-278.

Setchell, B. P., Maddocks, S. and Brooks, D. E. 1994. Anatomy, vasculature, innervation, and fluids of the male reproductive tract. Pp. 1063-1175. In Knobil, E. and Neill, J. D. (eds), *The Physiology of Reproduction,* 2nd ed., Raven Press, New York.

Sever, D. M. 2004. Ultrastructure of the reproductive system of the black swamp snake (*Seminatrix pygaea*). IV. Occurrence of an ampulla ductus deferentis. Journal of Morphology 262: 714-730.

Sever, D. M. 2010. Ultrastructure of the reproductive system of the black swamp snake (*Seminatrix pygaea*). IV. The proximal testicular ducts. Journal of Morphology 271: 104-115.

Shine, R. 1991. *Australian Snakes: A Natural History*. Cornell University Press, Ithaca, New York. Pp. 223.

Siegel, D. S., Sever, D. M., Rheubert, J. L. and Gribbins, K. M. 2009. Reproductive biology of *Agkistrodon piscivorus* Lacépède (Squamata, Serpentes, Viperidae, Crotalinae). Herpetological Monographs 23: 74-107.

Vidal, N. and Hedges, S. B. 2005. The phylogeny of squamate reptiles (lizards, snakes, and amphisbaenians) inferred from nine nuclear protein-coding genes. Comptes Rendus Biologies 328: 1000-1008.

Vitt, L. J. and J. P. Caldwell. 2009. *Herpetology,* 3rd ed., Elsevier Inc., Burlington, Massachusetts. Pp. 697.

Volsøe, H. 1944. Structure and seasonal variation of the male reproductive organs of *Vipera berus* (L.). Spolia Zoologica Musei Hauniensis 5: 1-157.

Young, B. A., Marsit, C. and Meltzer, K. 1999. Comparative morphology of the cloacal scent gland in snakes (Serpentes: Reptilia). Anatomical Record 256: 127-138.